NASA/TP-2003-212131

Buckling Behavior of Long Anisotropic Plates Subjected to Fully Restrained Thermal Expansion

Michael P. Nemeth
Langley Research Center, Hampton, Virginia

February 2003

The NASA STI Program Office . . . in Profile

Since its founding, NASA has been dedicated to the advancement of aeronautics and space science. The NASA Scientific and Technical Information (STI) Program Office plays a key part in helping NASA maintain this important role.

The NASA STI Program Office is operated by Langley Research Center, the lead center for NASA's scientific and technical information. The NASA STI Program Office provides access to the NASA STI Database, the largest collection of aeronautical and space science STI in the world. The Program Office is also NASA's institutional mechanism for disseminating the results of its research and development activities. These results are published by NASA in the NASA STI Report Series, which includes the following report types:

- TECHNICAL PUBLICATION. Reports of completed research or a major significant phase of research that present the results of NASA programs and include extensive data or theoretical analysis. Includes compilations of significant scientific and technical data and information deemed to be of continuing reference value. NASA counterpart of peer-reviewed formal professional papers, but having less stringent limitations on manuscript length and extent of graphic presentations.

- TECHNICAL MEMORANDUM. Scientific and technical findings that are preliminary or of specialized interest, e.g., quick release reports, working papers, and bibliographies that contain minimal annotation. Does not contain extensive analysis.

- CONTRACTOR REPORT. Scientific and technical findings by NASA-sponsored contractors and grantees.

- CONFERENCE PUBLICATION. Collected papers from scientific and technical conferences, symposia, seminars, or other meetings sponsored or co-sponsored by NASA.

- SPECIAL PUBLICATION. Scientific, technical, or historical information from NASA programs, projects, and missions, often concerned with subjects having substantial public interest.

TECHNICAL TRANSLATION. English-language translations of foreign scientific and technical material pertinent to NASA's mission.

Specialized services that complement the STI Program Office's diverse offerings include creating custom thesauri, building customized databases, organizing and publishing research results . . . even providing videos.

For more information about the NASA STI Program Office, see the following:

- Access the NASA STI Program Home Page at ***http://www.sti.nasa.gov***

- Email your question via the Internet to help@sti.nasa.gov

- Fax your question to the NASA STI Help Desk at (301) 621-0134

- Telephone the NASA STI Help Desk at (301) 621-0390

- Write to:
  NASA STI Help Desk
  NASA Center for AeroSpace Information
  7121 Standard Drive
  Hanover, MD 21076-1320

NASA/TP-2003-212131

Buckling Behavior of Long Anisotropic Plates Subjected to Fully Restrained Thermal Expansion

Michael P. Nemeth
Langley Research Center, Hampton, Virginia

National Aeronautics and
Space Administration

Langley Research Center
Hampton, Virginia 23681-2199

February 2003

Available from:

NASA Center for AeroSpace Information (CASI)
7121 Standard Drive
Hanover, MD 21076-1320
(301) 621-0390

National Technical Information Service (NTIS)
5285 Port Royal Road
Springfield, VA 22161-2171
(703) 605-6000

Summary

An approach for synthesizing buckling results and behavior for long, balanced and unbalanced symmetric laminates that are subjected to uniform heating or cooling and that are fully restrained against thermal expansion or contraction is presented. This approach uses a nondimensional analysis for infinitely long, flexurally anisotropic plates that are subjected to combined mechanical loads and is based on useful nondimensional parameters. In addition, stiffness-weighted laminate thermal-expansion parameters are derived that are used to determine critical temperature changes in terms of physically intuitive mechanical buckling coefficients, and the effects of membrane orthotropy and membrane anisotropy are included. Many results are presented for some common laminates that are intended to facilitate a structural designer's transition to the use of the generic buckling design curves that are presented in the paper. Several generic buckling design curves are presented that provide physical insight into the buckling response in addition to providing useful design data. Examples are presented that demonstrate the use of the generic design curves. The analysis approach and generic results indicate the effects and characteristics of laminate thermal expansion, membrane orthotropy and anisotropy, and flexural orthotropy and anisotropy in a very general and unifying manner.

Symbols

a	plate length (see fig. 2), in.
$A_{11}, A_{12}, A_{22}, A_{66}$	orthotropic-plate membrane stiffnesses, lb/in.
A_{16}, A_{26}	anisotropic-plate membrane stiffnesses, lb/in.
$a_{11}, a_{12}, a_{22}, a_{66}, a_{16}, a_{26}$	plate membrane compliances (see eq. (25)), in/lb
A_m, B_m	displacement amplitudes (see eq. (22)), in.
b	plate width (see fig. 1), in.
D	isotropic-plate bending stiffness (see eq. (61)), in-lb
$D_{11}, D_{12}, D_{22}, D_{66}$	orthotropic plate-bending stiffnesses, in-lb
D_{16}, D_{26}	anisotropic plate-bending stiffnesses, in-lb
E	Young's modulus (see table 1), psi
E_L, E_T, G_{LT}	lamina moduli (see table 2), psi
$K_b \equiv \left(n_{b1}\right)_{\mathrm{cr}}$	nondimensional buckling coefficient associated with the critical value of an eccentric inplane bending load (see eq. (21) and fig. 1(a))
$K_s \equiv \left(n_{xy1}\right)_{\mathrm{cr}}$	nondimensional buckling coefficient associated with the critical value of a uniform shear load (see eq. (20) and fig. 1(a))
$K_x\big\vert_{\gamma=\delta=0}$	axial-compression buckling coefficient, defined by equation (18) in which anisotropy is neglected in the analysis

$K_x \equiv \left(n_{x1}^c \right)_{\text{cr}}$	nondimensional buckling coefficient associated with the critical value of a uniform axial compression load (see eq. (18) and fig. 1(a))
$K_y \equiv \left(n_{y1} \right)_{\text{cr}}$	nondimensional buckling coefficient associated with the critical value of a uniform transverse compression load (see eq. (19) and fig. 1(a))
L_1, L_2, L_3, L_4	nondimensional load factors defined by equations (14) through (17), respectively
N	number of terms in the series representation of the out-of-plane displacement field at buckling (see eq. (22))
N_b	intensity of the eccentric inplane bending load distribution defined by equation (5), lb/in.
N_{xc}	intensity of the constant-valued tension or compression load distribution defined by equation (5), lb/in.
N_x, N_y, N_{xy}	longitudinal, transverse, and shear membrane stress resultants, respectively (see eqs. (5), (7), and (8)), lb/in.
$N_{x1}^c,\ N_{y1}, N_{xy1}, N_{b1}$	membrane stress resultants of the system of destabilizing loads (see eqs. (6) through (9) and fig. 1(a)), lb/in.
$N_{x2}^c,\ N_{y2}, N_{xy2}, N_{b2}$	membrane stress resultants of the system of subcritical loads (see eqs. (6) through (9) and fig. 1(b)), lb/in.
$n_{x1}^c,\ n_{y1}, n_{xy1}, n_{b1}$	nondimensional membrane stress resultants of the system of destabilizing loads defined by equations (10) through (13), respectively
$n_{x2}^c,\ n_{y2}, n_{xy2}, n_{b2}$	nondimensional membrane stress resultants of the system of subcritical loads defined by equations (10) through (13), respectively
$\tilde{p}, \tilde{p}_{\text{cr}}$	nondimensional loading parameter (see eqs. (14) through (17)) and corresponding value at buckling (see eqs. (18) through (21)), respectively
t	plate thickness, in.
u,v	plate inplane displacements (see fig. 2(a)), in.
$w_N(\xi, \eta)$	out-of-plane displacement field at buckling defined by equation (22), in.
x, y	plate rectangular coordinate system (see fig. 1), in.
α	coefficient of thermal expansion for an isotropic material, 1/°F
$\alpha_x, \alpha_y, \alpha_{xy}$	overall laminate coefficients of thermal expansion (see eq. (25)), 1/°F
$\hat{\alpha}_1, \hat{\alpha}_2, \hat{\alpha}_3$	stiffness-weighted laminate coefficients of thermal expansion (see eqs. (41) through (43), respectively), 1/°F

α_∞, β, γ, δ	nondimensional parameters defined by equations (1), (2), (3), and (4), respectively
ε_0, ε_1	symbols that define the distribution of the inplane bending load (see fig. 1 and eq. (5))
$\eta = y/b$, $\xi = x/\lambda$	nondimensional plate coordinates
θ	fiber angle (see fig. 9), deg
Θ_0	temperature change (see eq. (25)), °F
Θ_0^{cr}	critical value of temperature change, °F
λ	half-wavelength of buckling mode (see fig. 1), in.
λ/b	buckle aspect ratio (see fig. 1)
λ_{cr}	critical value of buckling mode half-wavelength, in.
λ_{cr}/b	critical value of buckle aspect ratio
ν	Poisson's ratio for an isotropic material (see table 1)
ν_{LT}	lamina major Poisson's ratio (see table 2)
$\Phi_m(\eta)$	basis functions (see eqs. (22) through (24))

Introduction

Buckling behavior of laminated-composite plates that are subjected to combined mechanical and thermal loads is an important consideration in the preliminary design of contemporary, high-performance aerospace vehicles. The sizing of many structural subcomponents of these vehicles is often determined by buckling constraints. One subcomponent that is of practical importance in structural design is the long rectangular plate. These plates commonly appear as elements of stiffened panels that are used for wing structures and as semimonocoque shell segments that are used for fuselage structures. Buckling results for infinitely long plates are important because they often provide a practical estimate of the behavior of finite-length rectangular plates, and they also provide information that is useful in explaining the behavior of these finite-length plates. Moreover, knowledge of the behavior of infinitely long plates can provide insight into the buckling behavior of more complex structures such as stiffened panels.

An important type of long plate that appears as a component of contemporary composite structures is the symmetrically laminated plate. In the present paper, the term "symmetrically laminated" refers to composite plates in which every lamina above the plate midplane has a corresponding lamina located at the same distance below the plate midplane, with the same thickness, material properties, and fiber orientation. Symmetrically laminated plates are essentially flat after the manufacturing process and exhibit flat prebuckling deformation states, which is desirable for many applications. More importantly, the amenability of these plates to structural tailoring provides symmetrically laminated plates with a significant potential for reducing the weight of aerospace vehicles or for meeting special

performance requirements. Thus, understanding the buckling behavior of symmetrically laminated plates in a very broad manner is an important part of the search for ways to exploit plate orthotropy and anisotropy to reduce structural weight or to fulfill a special design requirement.

For many practical cases, symmetrically laminated plates exhibit specially orthotropic behavior. However, in some cases, such as thin-walled $[\pm 45]_s$ laminates that are candidates for spacecraft applications, these plates exhibit anisotropy in the form of material-induced coupling between pure bending and twisting deformations. This coupling is referred to herein as flexural anisotropy, and it generally yields buckling modes that are skewed in appearance (see fig. 1), even when inplane shear loads are absent. Symmetrically laminated plates that are unbalanced are also being investigated for special-purpose uses in aerospace structures. These laminated plates exhibit anisotropy in the form of material-induced coupling between pure inplane dilatation and inplane shear deformations, in addition to flexural anisotropy. This coupling is referred to herein as membrane anisotropy, and it generally yields combined inplane stress states for simple loadings like uniform edge compression when inplane displacement constraints are imposed on one or more edges of a plate. For example, when the edges of an unbalanced, symmetrically laminated plate, such as a $[+45_2/0/90]_s$ laminate, are totally restrained against thermal expansion and contraction that is caused by uniform heating or cooling, inplane shear stresses are developed in addition to the usual tensile or compressive stresses that are often present in balanced laminates. These kinematically induced shear stresses may be relatively large in magnitude, compared to the direct compressive stresses, and as a result, may greatly affect the buckling behavior of the plate and amplify the skewed appearance of the buckling modes that is caused by flexural anisotropy.

The effects of flexural orthotropy and flexural anisotropy on the buckling behavior of long rectangular plates that are subjected to single and combined mechanical loading conditions are becoming better understood. For example, recent in-depth parametric studies that show the effects of flexural orthotropy and flexural anisotropy on the buckling behavior of long plates that are subjected to compression, shear, pure inplane bending, and various combinations of these loads have been presented in references 1–3. The results presented in these references indicate that the importance of flexural anisotropy on the buckling resistance of long plates varies with the magnitude and character of the combined loading condition. Similar results for plates loaded by uniform shear and a general linear distribution of axial load across the plate width have also been presented in reference 4. In a similar manner, the effects of membrane orthotropy and membrane anisotropy on the buckling behavior of long rectangular plates that are restrained against axial thermal expansion and contraction and subjected to uniform heating or cooling and mechanical loads have been presented in reference 5. This extensive work has provided a better understanding of the load interaction effects of balanced and unbalanced, symmetrically laminated plates that are subjected to mechanical loads and restrained against axial thermal expansion and contraction.

Although an extensive body of work exists that addresses the thermal-buckling behavior of plates (see ref. 5 for a literature review), a broad understanding of the effects of orthotropy and anisotropy on their response has not yet been obtained. In particular, the effects of membrane orthotropy and membrane anisotropy on the buckling behavior of long rectangular plates that are fully restrained against thermal expansion and contraction and subjected to uniform heating or cooling are not well understood for the large variety of laminated plates that exist and the variety of support conditions that are possible. One objective of the present paper is to present a more intuitive buckling analysis for balanced and unbalanced, symmetrically laminated plates that are fully restrained against thermal expansion and contraction and subjected to uniform heating or cooling. To achieve this goal, the buckling analysis is formulated in terms of buckling coefficients for the known, mechanically equivalent loads and stiffness-weighted laminate thermal-expansion parameters instead of in terms of a less intuitive thermal buckling

coefficient. Thus, the present study is a continuation or extension of the work that is presented in reference 5. The analysis procedure is based on classical laminated-plate theory, which neglects transverse-shear flexibility and is applied to long plates herein. However, the analysis procedure is applicable to finite-length plates and to more sophisticated plate buckling theories that include effects like transverse-shear flexibility.

Two other objectives of the present paper are to present a wide range of buckling results in terms of useful nondimensional design parameters and to provide a means for comparing the buckling-response characteristics of seemingly dissimilar laminated plates. Other objectives are to identify the effects of orthotropy and anisotropy on the buckling behavior of long symmetrically laminated plates that are subjected to the same loading conditions, and to present some previously unknown results. In particular, new results are presented for plates with the two long edges clamped or simply supported and with all edges fully restrained against inplane movement. Several generic buckling-design curves that are applicable to a wide range of laminate constructions are presented that use the nondimensional parameters described in references 1–6, along with some other parameters that are derived subsequently. Finally, examples are presented that demonstrate the use of the generic buckling-design curves and the analysis procedure.

Analysis Description

In preparing generic design charts for buckling of a single flat, thin plate, a special-purpose analysis is often preferred over a general-purpose analysis code, such as a finite-element code, because of the cost and effort that is usually involved in generating a large number of results with a general-purpose code. The results presented in the present paper were obtained by using such a special-purpose buckling analysis that is based on classical laminated-plate theory. The analysis details are lengthy; hence, only a brief description of the buckling analysis is presented herein. First, the buckling analysis for long plates that are subjected to a general set of mechanical loads is described. Next, the mechanical loads that are induced by fully restrained thermal expansion and contraction and that are used in the buckling analysis are derived, and an expression for the critical temperature change is presented in terms of the corresponding critical loading parameter and mechanical-buckling coefficients.

Buckling Analysis

Symmetrically laminated plates can have many different constructions because of the wide variety of material systems, fiber orientations, and stacking sequences that can be selected to construct a laminate. A convenient way of coping with the large number of choices for laminate constructions is to use nondimensional parameters to understand overall behavioral trends and sensitivities of the structural behavior to variations in laminate construction. The buckling analysis used in the present paper is based on classical laminated-plate theory and the classical Rayleigh-Ritz method and is derived explicitly in terms of the nondimensional parameters defined in references 1–6. This approach was motivated by the need for generic (independent of a specific laminate construction) parametric results for composite-plate buckling behavior that are expressed in terms of the minimum number of independent parameters needed to fully define the behavior and that indicates the overall trends and sensitivity of the results to changes in the parameters. The nondimensional parameters that were used to formulate the buckling analysis are given by

$$\alpha_{\infty} = \frac{b}{\lambda}\left(\frac{D_{11}}{D_{22}}\right)^{1/4} \tag{1}$$

$$\beta = \frac{D_{12} + 2D_{66}}{(D_{11}\, D_{22})^{1/2}} \tag{2}$$

$$\gamma = \frac{D_{16}}{(D_{11}^3\, D_{22})^{1/4}} \tag{3}$$

$$\delta = \frac{D_{26}}{(D_{11}\, D_{22}^3)^{1/4}} \tag{4}$$

where b is the plate width and λ is the half-wavelength of the buckle pattern of an infinitely long plate (see fig. 1). The subscripted D-terms are the bending stiffnesses of classical laminated-plate theory (see ref. 7 or 8). The parameters α_∞ and β characterize the flexural orthotropy, and the parameters γ and δ characterize the flexural anisotropy.

The mechanical loading conditions that are included in the buckling analysis are uniform transverse tension or compression, uniform shear, and a general linear distribution of axial load across the plate width, as depicted in figure 1. Typically, an axial stress resultant distribution is partitioned into a uniform part and a pure bending part; however, this representation is not unique. The longitudinal stress resultant N_x is partitioned in the analysis into a uniform tension or compression part and a linearly varying part that corresponds to eccentric inplane bending loads. This partitioning is given by

$$N_x = N_{xc} - N_b[\varepsilon_0 + (\varepsilon_1 - \varepsilon_0)\eta] \tag{5}$$

where N_{xc} denotes the intensity of the constant-valued tension or compression part of the load, and the term containing N_b defines the intensity of the eccentric inplane bending load distribution. The symbols ε_0 and ε_1 define the distribution of the inplane bending load, and the symbol η is the nondimensional coordinate given by $\eta = y/b$. This particular way of partitioning the longitudinal stress resultant was used for convenience by eliminating the need to calculate the uniform and pure bending parts of an axial stress resultant distribution prior to performing a buckling analysis.

The analysis is based on a general formulation that includes combined destabilizing loads that are proportional to a positive-valued loading parameter $\tilde{p}$ that is increased until buckling occurs and independent subcritical combined loads that remain fixed at a specified load level for which buckling does not occur. Herein, the term "subcritical load" is defined as any load that does not cause buckling to occur. In practice, the subcritical loads are applied to a plate prior to and independent of the destabilizing loads, with an intensity below that which will cause the plate to buckle. Then, with the subcritical loads fixed, the active, destabilizing loads are applied by increasing the magnitude of the loading parameter until buckling occurs. This approach permits certain types of combined-load interaction to be investigated in a direct and convenient manner. For example, in analyzing the stability of an aircraft fuselage, the nondestabilizing transverse tension load in a fuselage panel that is caused by cabin pressurization can be considered to remain constant and, as a result, can be represented as a passive, subcritical load. The combined shear, compression, and inplane bending loads that are caused by flight maneuvers can vary and cause buckling and, as a result, can be represented as active, destabilizing loads.

The distinction between the active, destabilizing and passive, subcritical loading systems is implemented in the buckling analysis by partitioning the prebuckling stress resultants as follows:

$$N_{xc} = -N_{x1}^{c} + N_{x2}^{c} \tag{6}$$

$$N_{y} = -N_{y1} + N_{y2} \tag{7}$$

$$N_{xy} = N_{xy1} + N_{xy2} \tag{8}$$

$$N_{b} = N_{b1} + N_{b2} \tag{9}$$

where the stress resultants with the subscript 1 are the destabilizing loads and those with the subscript 2 are the subcritical loads. The sign convention used herein for positive values of these stress resultants is shown in figure 1. In particular, positive values of the general linear edge stress distribution parameters N_{b1}, N_{b2}, ε_0, and ε_1 correspond to compression loads. Negative values of N_{b1} and N_{b2} or negative values of either ε_0 or ε_1 yield linearly varying stress distributions that include tension. Depictions of a variety of inplane bending load distributions are given in reference 4. The two normal stress resultants of the system of destabilizing loads, N_{x1}^{c} and N_{y1}, are defined to be positive-valued for compression loads. This convention results in positive eigenvalues being used to indicate instability due to uniform compression loads.

The buckling analysis includes several nondimensional stress resultants associated with equations (6) through (9). These dimensionless stress resultants are given by

$$n_{xj}^{c} = \frac{N_{xj}^{c} b^2}{\pi^2 (D_{11} D_{22})^{1/2}} \tag{10}$$

$$n_{yj} = \frac{N_{yj} b^2}{\pi^2 D_{22}} \tag{11}$$

$$n_{xyj} = \frac{N_{xyj} b^2}{\pi^2 (D_{11} D_{22}^3)^{1/4}} \tag{12}$$

$$n_{bj} = \frac{N_{bj} b^2}{\pi^2 (D_{11} D_{22})^{1/2}} \tag{13}$$

where the subscript j takes on the values of 1 and 2. In addition, the destabilizing loads are expressed in terms of the loading parameter $\tilde{p}$ in the analysis by

$$n_{x1}^{c} = L_1 \tilde{p} \tag{14}$$

$$n_{y1} = L_2 \tilde{p} \tag{15}$$

$$n_{xy1} = L_3\,\tilde{p} \tag{16}$$

$$n_{b1} = L_4\,\tilde{p} \tag{17}$$

where L_1 through L_4 are load factors that determine the specific form (relative contributions of the load components) of a given system of destabilizing loads. Typically, the dominant load factor is assigned a value of 1 and all others are given as positive or negative fractions.

Nondimensional buckling coefficients that are used herein are given by the values of the dimensionless stress resultants of the system of destabilizing loads at the onset of buckling; that is,

$$K_x \equiv \left(n^c_{x1} \right)_{\mathrm{cr}} = \frac{\left(N^c_{x1} \right)_{\mathrm{cr}} b^2}{\pi^2 (D_{11}\, D_{22})^{1/2}} = L_1\,\tilde{p}_{\mathrm{cr}} \tag{18}$$

$$K_y \equiv \left(n_{y1} \right)_{\mathrm{cr}} = \frac{\left(N_{y1} \right)_{\mathrm{cr}} b^2}{\pi^2 D_{22}} = L_2\,\tilde{p}_{\mathrm{cr}} \tag{19}$$

$$K_s \equiv \left(n_{xy1} \right)_{\mathrm{cr}} = \frac{\left(N_{xy1} \right)_{\mathrm{cr}} b^2}{\pi^2 (D_{11}\, D_{22}^3)^{1/4}} = L_3\,\tilde{p}_{\mathrm{cr}} \tag{20}$$

$$K_b \equiv \left(n_{b1} \right)_{\mathrm{cr}} = \frac{\left(N_{b1} \right)_{\mathrm{cr}} b^2}{\pi^2 (D_{11}\, D_{22})^{1/2}} = L_4\,\tilde{p}_{\mathrm{cr}} \tag{21}$$

where quantities enclosed in the parentheses with the subscript "cr" are critical values that correspond to buckling, and $\tilde{p}_{\mathrm{cr}}$ is the magnitude of the loading parameter at buckling. Positive values of the coefficients K_x and K_y correspond to uniform compression loads, and the coefficient K_s corresponds to uniform positive shear. The direction of a positive shear stress resultant that acts on a plate is shown in figure 1. The coefficient K_b corresponds to the specific inplane bending load distribution defined by the selected values of the parameters ε_0 and ε_1 (see fig. 1).

The mathematical expression used in the variational analysis to represent the general off-center and skewed buckle pattern is given by

$$w_N(\xi,\eta) = \sum_{m=1}^{N} \left(A_m \sin \pi\xi + B_m \cos \pi\xi \right) \Phi_m(\eta) \tag{22}$$

where $\xi = x/\lambda$ and $\eta = y/b$ are nondimensional coordinates, w_N is the out-of-plane displacement field, and A_m and B_m are the unknown displacement amplitudes. In accordance with the Rayleigh-Ritz method, the basis functions $\Phi_m(\eta)$ are required to satisfy the kinematic boundary conditions on the plate edges at $\eta = 0$ and $\eta = 1$. For the simply supported plates, the basis functions used in the analysis are given by

$$\Phi_m(\eta) = \sin m\pi\eta \tag{23}$$

for values of $m = 1, 2, 3, ..., N$. Similarly, for the clamped plates, the basis functions are given by

$$\Phi_m(\eta) = \cos(m-1)\pi\eta - \cos(m+1)\pi\eta \tag{24}$$

For both boundary conditions, the two long edges of a plate are free to move inplane.

Algebraic equations that govern the buckling behavior of infinitely long plates are obtained by substituting the series expansion for the buckling mode given by equation (22) into a nondimensionalized form of the second variation of the total potential energy and then by computing the integrals appearing in the nondimensional second variation in closed form. The resulting equations constitute a generalized eigenvalue problem that depends on the aspect ratio of the buckle pattern λ/b (see fig. 1) and the nondimensional parameters and nondimensional stress resultants defined herein. The smallest eigenvalue of the problem corresponds to buckling and is found by specifying a value of λ/b and solving the corresponding generalized eigenvalue problem for its smallest eigenvalue. This process is repeated for successive values of λ/b until the overall smallest eigenvalue is found. The value of λ/b that corresponds to the overall smallest eigenvalue is denoted herein by λ_{cr}/b.

Results that were obtained from the analysis described herein for uniform compression, uniform shear, pure inplane bending (given by $\varepsilon_0 = -1$ and $\varepsilon_1 = 1$), and various combinations of these mechanical loads have been compared with other results for isotropic, orthotropic, and anisotropic plates that were obtained by using other analysis methods. These comparisons are discussed in references 1–3, and in every case the results described herein were found to be in good agreement with those obtained from other analyses. Likewise, results were obtained for isotropic and specially orthotropic plates that are subjected to a general linear distribution of axial load across the plate width and compared with results that were obtained by seven different authors (see ref. 4). In every case, the agreement was good; that is, all had less than a 5 percent difference and most less than a 2 percent difference. More recently, results obtained for symmetrically laminated, balanced anisotropic angle-ply plates with the buckling analysis described herein (given in ref. 4) were compared to experiments in reference 9. The analytical results in reference 4 show a set of complex, nonintuitive buckling interaction curves, for plates loaded by inplane bending and shear, that are skewed substantially because of the presence of flexural anisotropy. The experimental results verify the unusual trends of the highly skewed buckling interaction curves, and the agreement between analysis and test appears to be very good.

Prebuckling Stresses and Critical Temperature Change

Uniformly heated or cooled plates that are symmetrically laminated and restrained against thermal expansion and contraction may develop internal mechanical loads that can cause buckling. These induced mechanical loads enter the analysis through the membrane constitutive equations. The standard form of these membrane constitutive equations for thin plates, which is based on classical laminated-plate theory, is found in references 7 and 8 and is expressed in terms of membrane stiffness coefficients and fictitious thermal stress resultants. In the present study, the membrane constitutive equations are used in an inverted form that uses the overall laminate coefficients of thermal expansion and the membrane compliance coefficients (see ref. 8). This form of the membrane constitutive equations for symmetrically laminated plates is given by

$$\begin{Bmatrix} u_{,x} \\ v_{,y} \\ u_{,y} + v_{,x} \end{Bmatrix} = \begin{bmatrix} a_{11} & a_{12} & a_{16} \\ a_{12} & a_{22} & a_{26} \\ a_{16} & a_{26} & a_{66} \end{bmatrix} \begin{Bmatrix} N_x \\ N_y \\ N_{xy} \end{Bmatrix} + \begin{Bmatrix} \alpha_x \\ \alpha_y \\ \alpha_{xy} \end{Bmatrix} \Theta_0 \tag{25}$$

where $u(x,y)$ and $v(x,y)$ are the prebuckling, inplane displacements in the x- and y-coordinate directions, respectively (see fig. 2); α_x, α_y, and α_{xy} are the overall laminate coefficients of thermal expansion; the subscripted a-terms are the plate membrane compliance coefficients; Θ_0 is the magnitude of the uniform temperature change from a predetermined stress- and strain-free reference state; and commas followed by a subscript denote partial differentiation with respect to the coordinate associated with the subscript. For restrained thermal expansion and contraction problems, the plates are assumed to be supported and loaded such that the prebuckling stress field is uniform. With this assumption, a compatible displacement field is obtained directly by integrating equations (25). This integration yields

$$u(x,y) = \left(a_{11}\,\mathcal{N}_x + a_{12}\,\mathcal{N}_y + a_{16}\,\mathcal{N}_{xy} + \alpha_x\,\Theta_0\right)x + g_1 y + g_2 \tag{26}$$

$$v(x,y) = \left(a_{12}\,\mathcal{N}_x + a_{22}\,\mathcal{N}_y + a_{26}\,\mathcal{N}_{xy} + \alpha_y\,\Theta_0\right)y + g_3 x + g_4 \tag{27}$$

and

$$g_1 + g_3 = a_{16}\,\mathcal{N}_x + a_{26}\,\mathcal{N}_y + a_{66}\,\mathcal{N}_{xy} + \alpha_{xy}\,\Theta_0 \tag{28}$$

where g_1 through g_4 are constants that are determined from the boundary conditions.

Equations (26)–(28) can be used to determine the thermally induced mechanical loadings for several problems of practical interest. The problems consist of plates restrained against axial thermal expansion or contraction (see ref. 5), plates restrained against transverse thermal expansion or contraction (y-coordinate direction), and plates restrained against axial and transverse thermal expansion and contraction. In the present paper, however, only plates that are fully restrained against axial and transverse thermal expansion and contraction are considered. For this case, all the subcritical loads are zero-valued and $N_x(x,y) = -N_{x1}^c$, $N_y(x,y) = -N_{y1}$, and $N_{xy}(x,y) = N_{xy1}$ (see fig. 2). All the stress resultants are induced by the fully restrained thermal expansion and, when considered together, are destabilizing. Upon substitution of these relationships, the displacements given by equations (26) and (27) become

$$u(x,y) = \left(-a_{11}\,\mathcal{N}_{x1}^c - a_{12}\,\mathcal{N}_{y1} + a_{16}\,\mathcal{N}_{xy1} + \alpha_x\,\Theta_0\right)x + g_1 y + g_2 \tag{29}$$

$$v(x,y) = \left(-a_{12}\,\mathcal{N}_{x1}^c - a_{22}\,\mathcal{N}_{y1} + a_{26}\,\mathcal{N}_{xy1} + \alpha_y\,\Theta_0\right)y + g_3 x + g_4 \tag{30}$$

and equation (28) becomes

$$g_1 + g_3 = -a_{16}\,\mathcal{N}_{x1}^c - a_{26}\,\mathcal{N}_{y1} + a_{66}\,\mathcal{N}_{xy1} + \alpha_{xy}\,\Theta_0 \tag{31}$$

Enforcing the restraint condition (displacement boundary condition) $u(0,y) = 0$ gives $g_1 = g_2 = 0$. Similarly, enforcing the restraint condition $v(x,0) = 0$ gives $g_3 = g_4 = 0$. Enforcing $u(a,y) = 0$ gives

$$-a_{11}\,\mathcal{N}_{x1}^c - a_{12}\,\mathcal{N}_{y1} + a_{16}\,\mathcal{N}_{xy1} + \alpha_x\,\Theta_0 = 0 \tag{32}$$

which yields $u(x,y) = 0$. Similarly, enforcing $v(x,b) = 0$ gives

$$-a_{12}\,N_{x1}^{c} - a_{22}\,N_{y1} + a_{26}\,N_{xy1} + \alpha_{y}\,\Theta_0 = 0 \tag{33}$$

which yields $v(x,y) = 0$. Substituting $g_1 = g_3 = 0$ into equation (31) gives

$$-a_{16}\,N_{x1}^{c} - a_{26}\,N_{y1} + a_{66}\,N_{xy1} + \alpha_{xy}\,\Theta_0 = 0 \tag{34}$$

The thermally induced stress resultants for this problem are obtained by solving equations (32)–(34) for N_{x1}^{c}, N_{y1}, and N_{xy1}. The solution is given by

$$N_{x1}^{c} = \left(A_{11}\alpha_{x} + A_{12}\alpha_{y} + A_{16}\alpha_{xy}\right)\Theta_0 \tag{35}$$

$$N_{y1} = \left(A_{12}\alpha_{x} + A_{22}\alpha_{y} + A_{26}\alpha_{xy}\right)\Theta_0 \tag{36}$$

$$N_{xy1} = -\left(A_{16}\alpha_{x} + A_{26}\alpha_{y} + A_{66}\alpha_{xy}\right)\Theta_0 \tag{37}$$

where the subscripted A-terms are the membrane stiffnesses of classical laminated-plate theory. Equations (35)–(37) define a combined loading state that is induced by restrained thermal expansion and contraction. These equations show that each of the thermally induced mechanical loads depends on all three laminate coefficients of thermal expansion and that positive values for the compressive stress resultants are possible even for negative values of Θ_0 (uniform cooling) and vice versa. For example, a laminate could have a negative value of α_x and still have a positive value of N_{x1}^{c} (axial compression). Thus, the signs of Θ_0 and the parenthetical quantities in equations (35)–(37) must be considered in formulating the buckling problem.

The buckling problem is posed by first substituting equations (35)–(37) into equations (10)–(12), respectively, to obtain expressions for the nondimensional stress resultants that can be used to characterize the thermally induced mechanical loads. In particular, the nondimensional stress resultants are expressed in terms of stiffness-weighted laminate thermal-expansion parameters denoted by $\hat{\alpha}_1$, $\hat{\alpha}_2$, and $\hat{\alpha}_3$. These expressions, with the use of equations (14)–(16), are given by

$$n_{x1}^{c} = \frac{12b^2}{\pi^2 t^2}\hat{\alpha}_1\Theta_0 = L_1\,\tilde{p} \tag{38}$$

$$n_{y1} = \frac{12b^2}{\pi^2 t^2}\hat{\alpha}_2\Theta_0 = L_2\,\tilde{p} \tag{39}$$

$$n_{xy1} = \frac{12b^2}{\pi^2 t^2}\hat{\alpha}_3\Theta_0 = L_3\,\tilde{p} \tag{40}$$

where

$$\hat{\alpha}_1 = \frac{t^2(A_{11}\alpha_x + A_{12}\alpha_y + A_{16}\alpha_{xy})}{12\sqrt{D_{11}D_{22}}} \tag{41}$$

$$\hat{\alpha}_2 = \frac{t^2(A_{12}\alpha_x + A_{22}\alpha_y + A_{26}\alpha_{xy})}{12D_{22}} \tag{42}$$

$$\hat{\alpha}_3 = -\frac{t^2(A_{16}\alpha_x + A_{26}\alpha_y + A_{66}\alpha_{xy})}{12(D_{11}\,D_{22}^3)^{1/4}} \tag{43}$$

where t is the plate thickness. Note that the stiffness-weighted coefficients of thermal expansion have the same units as the laminate and lamina coefficients of thermal expansion.

Equations (10)–(12) and (38)–(40) indicate that $\mathcal{N}_{x1}^c$, $\mathcal{N}_{y1}$, and N_{xy1} are positive-valued when $\hat{\alpha}_1$, $\hat{\alpha}_2$, and $\hat{\alpha}_3$ are positive-valued, respectively, and when Θ_0 is positive-valued. Similarly, $\mathcal{N}_{x1}^c$, $\mathcal{N}_{y1}$, and N_{xy1} are negative-valued when $\hat{\alpha}_1$, $\hat{\alpha}_2$, and $\hat{\alpha}_3$ are positive-valued, respectively, and Θ_0 is negative-valued, or when $\hat{\alpha}_1$, $\hat{\alpha}_2$, and $\hat{\alpha}_3$ are negative-valued, respectively, and Θ_0 is positive-valued. Next, equations (38)–(40) are substituted into equations (18)–(20) to obtain the relationships between the mechanical-buckling coefficients, the load factors, and the critical temperature Θ_0^{cr}; that is,

$$K_x \equiv \left(n_{x1}^c \right)_{\mathrm{cr}} = \frac{12b^2}{\pi^2 t^2}\hat{\alpha}_1\Theta_0^{\mathrm{cr}} = L_1\,\tilde{p}_{\mathrm{cr}} \tag{44}$$

$$K_y \equiv \left(n_{y1} \right)_{\mathrm{cr}} = \frac{12b^2}{\pi^2 t^2}\hat{\alpha}_2\Theta_0^{\mathrm{cr}} = L_2\,\tilde{p}_{\mathrm{cr}} \tag{45}$$

$$K_s \equiv \left(n_{xy1} \right)_{\mathrm{cr}} = \frac{12b^2}{\pi^2 t^2}\hat{\alpha}_3\Theta_0^{\mathrm{cr}} = L_3\,\tilde{p}_{\mathrm{cr}} \tag{46}$$

where the critical eigenvalue $\tilde{p}_{\mathrm{cr}} = \tilde{p}_{\mathrm{cr}}\left(\beta, \gamma, \delta, L_1, L_2, L_3\right)$ for a given set of flexural boundary conditions.

The next step in posing the buckling problem is to define the load factors L_1, L_2, and L_3 that appear in equations (38)–(40) and (44)–(46). These load factors define the relative proportions of the thermally induced mechanical loads. It is important to reiterate that positive, negative, and zero values for $\hat{\alpha}_1\Theta_0$ correspond to positive, negative, and zero values for $\mathcal{N}_{x1}^c$, respectively (see fig. 2(b)). Similarly, positive, negative, and zero values for $\hat{\alpha}_2\Theta_0$ correspond to positive, negative, and zero values for $\mathcal{N}_{y1}$, respectively; and positive, negative, and zero values for $\hat{\alpha}_3\Theta_0$ correspond to positive, negative, and zero values for N_{xy1}, respectively. To define the load factors properly, the signs of $\mathcal{N}_{x1}^c$, $\mathcal{N}_{y1}$, and N_{xy1} must be considered. Specifically, the load factors must be defined such that positive values of L_1, L_2, and L_3 correspond to positive values of $\mathcal{N}_{x1}^c$, $\mathcal{N}_{y1}$, and N_{xy1}, respectively (see fig. 1(a)). Moreover, both positive and negative values of Θ_0 must be considered. These requirements lead to six cases that must be considered in formulating the buckling analysis; that is, the cases for which $\hat{\alpha}_1\Theta_0 > 0$, $\hat{\alpha}_1\Theta_0 < 0$, $\hat{\alpha}_1 = 0$ with $\hat{\alpha}_2\Theta_0 > 0$, $\hat{\alpha}_1 = 0$ with $\hat{\alpha}_2\Theta_0 < 0$, $\hat{\alpha}_1 = \hat{\alpha}_2 = 0$ with $\hat{\alpha}_3\Theta_0 > 0$, and $\hat{\alpha}_1 = \hat{\alpha}_2 = 0$ with $\hat{\alpha}_3\Theta_0 < 0$. The buckling analysis for each of these cases is presented subsequently.

Case 1. For the case in which $\hat{\alpha}_1\Theta_0 > 0$, the stress resultant $N_{x1}^c > 0$ and $L_1 = 1$ is appropriate (induced axial compression). The values for the other two load factors that are needed to completely define the prebuckling stress state are obtained by dividing equations (19) and (20) by equation (18), with $L_1 = 1$, or by dividing equations (39) and (40) by equation (38). This step yields

$$L_2 = \frac{N_{y1}}{N_{x1}^c}\left(\frac{D_{11}}{D_{22}}\right)^{1/2} = \frac{\hat{\alpha}_2}{\hat{\alpha}_1} = \frac{A_{12}\alpha_x + A_{22}\alpha_y + A_{26}\alpha_{xy}}{A_{11}\alpha_x + A_{12}\alpha_y + A_{16}\alpha_{xy}}\left(\frac{D_{11}}{D_{22}}\right)^{1/2} \tag{47}$$

$$L_3 = \frac{N_{xy1}}{N_{x1}^c}\left(\frac{D_{11}}{D_{22}}\right)^{1/4} = \frac{\hat{\alpha}_3}{\hat{\alpha}_1} = -\frac{A_{16}\alpha_x + A_{26}\alpha_y + A_{66}\alpha_{xy}}{A_{11}\alpha_x + A_{12}\alpha_y + A_{16}\alpha_{xy}}\left(\frac{D_{11}}{D_{22}}\right)^{1/4} \tag{48}$$

For an isotropic material, $A_{11} = A_{22}$, $A_{16} = A_{26} = 0$, $D_{11} = D_{22}$, $\alpha_x = \alpha_y$, $\alpha_{xy} = 0$, and these expressions reduce to $L_2 = 1$ and $L_3 = 0$. With $L_1 = 1$ and L_2 and L_3 defined by equations (47) and (48), the relationship between the critical value of the mechanical loading parameter $\tilde{p}_{\text{cr}}$ and the critical temperature Θ_0^{cr} is determined by equation (44); that is,

$$K_x = \frac{12b^2}{\pi^2 t^2}\hat{\alpha}_1\Theta_0^{\text{cr}} = \tilde{p}_{\text{cr}} \tag{49}$$

where $\tilde{p}_{\text{cr}} = \tilde{p}_{\text{cr}}\left(\beta, \gamma, \delta, L_1, L_2, L_3\right)$ for a given set of flexural boundary conditions. It is important to point out that equation (49) yields positive and negative values for Θ_0^{cr} for positive and negative values of $\hat{\alpha}_1$, respectively. Moreover, it is important to reiterate that the relationship between $\tilde{p}_{\text{cr}}$ and the corresponding mechanical buckling coefficients K_x, K_y, and K_s is given by equations (49), (45), and (46), respectively.

Case 2. For the case when $\hat{\alpha}_1\Theta_0 < 0$, the stress resultant $N_{x1}^c < 0$ and $L_1 = -1$ is appropriate (induced axial tension). As for the previous case, the values for the other two load factors that are needed to completely define the prebuckling stress state are obtained by dividing equations (19) and (20) by equation (18), but with $L_1 = -1$, or by dividing equations (39) and (40) by equations (38). This step yields

$$L_2 = -\frac{N_{y1}}{N_{x1}^c}\left(\frac{D_{11}}{D_{22}}\right)^{1/2} = -\frac{\hat{\alpha}_2}{\hat{\alpha}_1} = -\frac{A_{12}\alpha_x + A_{22}\alpha_y + A_{26}\alpha_{xy}}{A_{11}\alpha_x + A_{12}\alpha_y + A_{16}\alpha_{xy}}\left(\frac{D_{11}}{D_{22}}\right)^{1/2} \tag{50}$$

$$L_3 = -\frac{N_{xy1}}{N_{x1}^c}\left(\frac{D_{11}}{D_{22}}\right)^{1/4} = -\frac{\hat{\alpha}_3}{\hat{\alpha}_1} = \frac{A_{16}\alpha_x + A_{26}\alpha_y + A_{66}\alpha_{xy}}{A_{11}\alpha_x + A_{12}\alpha_y + A_{16}\alpha_{xy}}\left(\frac{D_{11}}{D_{22}}\right)^{1/4} \tag{51}$$

With $L_1 = -1$ and L_2 and L_3 defined by equations (50) and (51), the relationship between the critical value of the mechanical loading parameter $\tilde{p}_{\text{cr}}$ and the critical temperature Θ_0^{cr} is again determined by equation (44); that is,

$$K_x = \frac{12b^2}{\pi^2 t^2}\hat{\alpha}_1\Theta_0^{\text{cr}} = -\tilde{p}_{\text{cr}} \tag{52a}$$

In contrast to the previous case, equation (52a) yields positive values for Θ_0^{cr} for negative values of $\hat{\alpha}_1$, and vice versa. For laminates with $L_3 = 0$ (balanced laminates) and $L_2 \leq 0$ (no induced transverse load or transverse tension), no destabilizing compression or shear loads are present, and buckling cannot occur because the plate is in a state of uniaxial or biaxial tension. In contrast, when $L_3 = 0$ and $L_2 > 0$, a plate is subjected to axial tension and transverse compression. Figures 29–31 of reference 1 indicate that an infinitely long plate buckles as a wide column for this type of loading and that the buckling coefficients $K_y = 1$ and $K_y = 4$ for simply supported and clamped plates, respectively. With K_y known, equations (45) and (52a) give

$$K_x = \frac{12b^2}{\pi^2 t^2}\hat{\alpha}_1\Theta_0^{cr} = -\frac{K_y}{L_2} \tag{52b}$$

Case 3. For a general symmetric laminate, the possibility exists that $\hat{\alpha}_1 = 0$, which implies that the stress resultant $N_{x1}^c = 0$; that is, there is no axial expansion or contraction. For this case, $L_1 = 0$ is appropriate and the sign of $\hat{\alpha}_2\Theta_0$ must be considered in defining the nonzero load factors. In particular, for $\hat{\alpha}_2\Theta_0 > 0$, $N_{y1} > 0$ and $L_1 = 0$ and $L_2 = 1$ are appropriate (induced transverse compression). The value for the load factor L_3 that is needed to completely define the prebuckling stress state is obtained by dividing equation (20) by equation (19), with $L_2 = 1$, or by dividing equation (40) by equation (39). This step yields

$$L_3 = \frac{N_{xy1}}{N_{y1}}\left(\frac{D_{22}}{D_{11}}\right)^{1/4} = \frac{\hat{\alpha}_3}{\hat{\alpha}_2} = -\frac{A_{16}\alpha_x + A_{26}\alpha_y + A_{66}\alpha_{xy}}{A_{12}\alpha_x + A_{22}\alpha_y + A_{26}\alpha_{xy}}\left(\frac{D_{22}}{D_{11}}\right)^{1/4} \tag{53}$$

The relationship between L_3 and the mechanical-buckling coefficients K_y and K_s is shown in figures 24–27 of reference 1. With $L_1 = 0$, $L_2 = 1$, and L_3 defined by equation (53), the relationship between the critical value of the mechanical loading parameter $\tilde{p}_{cr}$ and the critical temperature Θ_0^{cr} is determined by equation (45); that is,

$$K_y = \frac{12b^2}{\pi^2 t^2}\hat{\alpha}_2\Theta_0^{cr} = \tilde{p}_{cr} \tag{54a}$$

It is important to point out that equation (54a) yields positive and negative values for Θ_0^{cr} for positive and negative values of $\hat{\alpha}_2$, respectively. For laminates with $L_3 = 0$ (balanced laminates) a plate is subjected to only transverse compression. Thus, an infinitely long plate buckles as a wide column for this type of loading, and the buckling coefficients $K_y = 1$ and $K_y = 4$ for simply supported and clamped plates, respectively. With K_y known, equation (45) gives

$$\frac{12b^2}{\pi^2 t^2}\hat{\alpha}_2\Theta_0^{cr} = K_y \tag{54b}$$

Case 4. For the case when $\hat{\alpha}_1 = 0$ and $\hat{\alpha}_2\Theta_0 < 0$, the stress resultant $N_{y1} < 0$, $L_1 = 0$, and $L_2 = -1$ are appropriate (transverse tension). As for the previous case, the value for the load factor L_3 that is needed to completely define the prebuckling stress state is obtained by dividing equation (20) by equation (19), with $L_2 = -1$, or by dividing equation (40) by equation (39). This step yields

$$L_3 = -\frac{N_{xy1}}{N_{y1}}\left(\frac{D_{22}}{D_{11}}\right)^{1/4} = -\frac{\hat{\alpha}_3}{\hat{\alpha}_2} = \frac{A_{16}\alpha_x + A_{26}\alpha_y + A_{66}\alpha_{xy}}{A_{12}\alpha_x + A_{22}\alpha_y + A_{26}\alpha_{xy}}\left(\frac{D_{22}}{D_{11}}\right)^{1/4} \tag{55}$$

Like the previous case, the relationship between L_3 and the mechanical-buckling coefficients K_y and K_s is shown in figures 24–27 of reference 1. With $L_1 = 0$, $L_2 = -1$, and L_3 defined by equation (55), the relationship between the critical value of the mechanical loading parameter $\tilde{p}_{cr}$ and the critical temperature Θ_0^{cr} is determined by equation (45); that is,

$$K_y = \frac{12b^2}{\pi^2 t^2}\hat{\alpha}_2\Theta_0^{cr} = -\tilde{p}_{cr} \tag{56}$$

For this case, equation (56) yields positive values for Θ_0^{cr} for negative values of $\hat{\alpha}_2$ and vice versa. For laminates with $L_3 = 0$ (balanced laminates), no destabilizing compression or shear loads are present, and buckling cannot occur because the plate is loaded by transverse tension only.

Case 5. For the case with $\hat{\alpha}_1 = \hat{\alpha}_2 = 0$ and $\hat{\alpha}_3\Theta_0 > 0$, the stress resultants $N_{x1}^c = N_{y1} = 0$ and $N_{xy1} > 0$, which implies that $L_1 = L_2 = 0$, and that $L_3 = 1$ is appropriate (positive shear loading as in fig. 1(a)). With $L_1 = 0$, $L_2 = 0$, and $L_3 = 1$, the relationship between the critical value of the mechanical loading parameter $\tilde{p}_{cr}$ and the critical temperature Θ_0^{cr} is determined by equation (46); that is,

$$K_s = \frac{12b^2}{\pi^2 t^2}\hat{\alpha}_3\Theta_0^{cr} = \tilde{p}_{cr} \tag{57}$$

Again, it is important to point out that equation (57) yields positive and negative values for Θ_0^{cr} for positive and negative values of $\hat{\alpha}_3$, respectively. In addition, values of the mechanical-buckling coefficient K_s for several laminates are given in reference 1.

Case 6. The final case to consider is when $\hat{\alpha}_1 = \hat{\alpha}_2 = 0$ and $\hat{\alpha}_3\Theta_0 < 0$. For this case, the stress resultants $N_{x1}^c = N_{y1} = 0$ and $N_{xy1} < 0$, which implies that $L_1 = L_2 = 0$, and that $L_3 = -1$ is appropriate (negative shear loading). With $L_1 = 0$, $L_2 = 0$, and $L_3 = -1$, the relationship between the critical value of the mechanical loading parameter $\tilde{p}_{cr}$ and the critical temperature Θ_0^{cr} is again determined by equation (46); that is,

$$K_s = \frac{12b^2}{\pi^2 t^2}\hat{\alpha}_3\Theta_0^{cr} = -\tilde{p}_{cr} \tag{58}$$

In contrast to the previous case, equation (58) yields positive values for Θ_0^{cr} for negative values of $\hat{\alpha}_3$ and vice versa.

It is important to mention that the approach used herein to define the prebuckling stress state and the critical temperature Θ_0^{cr} also applies for a more sophisticated plate theory, such as a first-order transverse-shear deformation theory. For this theory, $\tilde{p}_{cr}$ would depend also upon additional nondimensional parameters that characterize the transverse-shear flexibility. Thus, the only difference in the results for the two plate bending theories is the actual value of $\tilde{p}_{cr}$ that is used in equations (44)–(46), for a given problem. It is also important to point out that $\tilde{p}_{cr}$ for a long plate does not depend on the parameter α_∞. This fact has been shown in references 1–4.

Results for Isotropic Plates and Common Laminates

Results are presented in this section and in figures 3–16 that illustrate behavioral trends for isotropic plates and for several common symmetrically laminated plates that are fully restrained against thermal expansion and contraction and subjected to uniform heating or cooling. In particular, results are

presented first for plates made of typical aluminum, steel, titanium, brass, and copper (see table 1 for properties). Then, results are presented for several common balanced, symmetric laminates that are made of IM7/5260 graphite-bismaleimide material (see table 2 for properties); that is, $[(\pm 45/0/90)_m]_s$ quasi-isotropic laminates, $[(\pm 45/0_2)_m]_s$ and $[(\pm 45/90_2)_m]_s$ quasiorthotropic laminates, and $[(\pm\theta)_m]_s$ angle-ply laminates, where a positive value of the lamina fiber angle θ is shown in figure 9. The $[(\pm 45/0_2)_m]_s$ and $[(\pm 45/90_2)_m]_s$ laminates are described as quasiorthotropic because of the presence of a relatively small amount of flexural anisotropy. Results are also presented for $[\pm\theta/0/90]_s$ laminates with angle plies and for a quasi-isotropic laminate whose principal material coordinate frame is rotated by an angle θ; that is, $[(\pm 45/0/90) + \theta]_s$. In addition, results are presented for similar unbalanced, symmetric laminates; primarily, $[(+45_2/0/90)_m]_s$, $[(+45_2/0_2)_m]_s$, $[(+45_2/90_2)_m]_s$, $[(+\theta)_{2m}]_s$, and $[+\theta_2/0/90]_s$ laminates that exhibit a significant degree of membrane anisotropy in addition to flexural anisotropy. All of the results are based on classical laminated-plate theory, and the nominal ply thickness used in the calculations was 0.005 in.

Results for Isotropic Plates

Results for homogeneous, isotropic plates are obtained from the analysis presented herein by first noting that for an isotropic material, the stiffness-weighted laminate thermal expansion parameters reduce to $\tilde{\alpha}_3 = 0$ and $\tilde{\alpha}_1 = \tilde{\alpha}_2 = \alpha(1 + \nu)$, where α is the coefficient of thermal expansion and ν is Poisson's ratio. Because $\tilde{\alpha}_1$ and $\tilde{\alpha}_2$ are positive valued for isotropic materials, it follows that the isotropic plates that are subjected to fully restrained thermal expansion or contraction can buckle only when subjected to uniform heating; that is, $\Theta_0^{cr} > 0$. The buckling equations for this case are obtained by noting that $\tilde{\alpha}_1\Theta_0 > 0$ and by using equations (47)–(49). These equations and considerations give $L_1 = 1$, $L_2 = 1$, $L_3 = 0$, and

$$\Theta_0^{cr} = \frac{\pi^2 \tilde{p}_{cr}}{12\left(b/t\right)^2 \alpha(1 + \nu)} \tag{59}$$

The condition $L_1 = L_2 = 1$ means that $\mathcal{N}_{x1}^c = \mathcal{N}_{y1}$. Moreover, the corresponding mechanical buckling coefficients are given by

$$K_x = \frac{\left(\mathcal{N}_{x1}^c\right)_{cr} b^2}{\pi^2 D} = K_y = \frac{\left(\mathcal{N}_{y1}\right)_{cr} b^2}{\pi^2 D} = \tilde{p}_{cr} \tag{60}$$

where D denotes the bending stiffness for isotropic plates given by

$$D = \frac{Et^3}{12\left(1 - \nu^2\right)} \tag{61}$$

Equations (59)–(61) are combined to give the relationship between that critical temperature change and the mechanically equivalent critical loading; that is,

$$\left(\mathcal{N}_{x1}^c\right)_{cr} = \left(\mathcal{N}_{y1}\right)_{cr} = \frac{E\alpha t}{1 - \nu}\,\Theta_0^{cr} \tag{62}$$

For long simply supported plates, $\tilde{p}_{cr} = 1$, and for long clamped plates $\tilde{p}_{cr} = 3.76$. These results are illustrated by the well-known K_x-K_y buckling interaction curves for isotropic plates that are shown in

figure 3 (e.g., see ref. 10). The solid line in this figure represents plates with simply supported edges, and the dashed line is for plates with clamped edges. The load factor L_2 generally appears implicitly as the slope of a line emanating from the origin of the graph. The buckling coefficients that correspond to a given value of L_2 are determined by the point of intersection of the line and the appropriate buckling interaction curve. Points of intersection that occur on the horizontal portion of the curves, given by $K_y = 1$ and $K_y = 4$ for the simply supported and clamped plates, respectively, correspond to wide-column-like buckling modes. The points of intersection that correspond specifically to $L_2 = 1$ are depicted in figure 3 for the simply supported and clamped plates by the open and filled circular symbols, respectively.

Results are presented in figure 4 that show the critical temperature change Θ_0^{cr} for uniform heating of steel and aluminum plates, as a function of the plate width-to-thickness ratio b/t. The solid lines in this figure are for plates with simply supported edges and the dashed lines are for plates with clamped edges. Moreover, the gray and black lines correspond to results for aluminum and steel plates, respectively. As expected, the plates with clamped edges are more buckling resistant than the corresponding plates with simply supported edges. As indicated by equation (59), the magnitude of Θ_0^{cr} shown in the figure decreases proportionally to the inverse square of b/t.

Additional results that are applicable to the entire class of isotropic materials and the full range of b/t are presented in figure 5. Several curves are shown in this figure that give the critical temperature change $\frac{12b^2}{\pi^2 t^2}\Theta_0^{cr}$ as a function of the coefficient of thermal expansion α for values of Poisson's ratio ν given by $0.1 \le \nu \le 0.4$. The solid lines in this figure are for plates with simply supported edges and the dashed lines are for plates with clamped edges. Also shown on the figure by the circular, square, and diamond-shaped symbols are values of $\frac{12b^2}{\pi^2 t^2}\Theta_0^{cr}$ for typical aluminum, steel, titanium, magnesium, copper, and brass engineering metals (see table 1 for properties). These curves indicate that Θ_0^{cr} decreases with increasing values for α and increasing values for ν, with the decrease being more pronounced for the clamped plates than for the simply supported plates, as expected.

Results for Common Laminates

Results are presented in figures 6–7 and tables 3–8 that give the stiffness-weighted laminate thermal expansion parameter $\hat{\alpha}_1 \times 10^6$ and the load factor ratio $\hat{\alpha}_2/\hat{\alpha}_1$ as a function of the number of laminate plies for several balanced and unbalanced, symmetric laminates. In particular, the black solid lines in the figures are for the $[(\pm 45/0/90)_m]_s$, $[(\pm 45/0_2)_m]_s$, and $[(\pm 45/90_2)_m]_s$ balanced, symmetric laminates, and three of the gray dashed lines are for the $[(+45_2/0/90)_m]_s$, $[(+45_2/0_2)_m]_s$, and $[(+45_2/90_2)_m]_s$ unbalanced, symmetric laminates. The symbols shown in the figures correspond to the actual values for a given number of laminate plies. A major difference between these two groups of laminates is the presence of membrane anisotropy in the laminates of the second group that is caused by orienting all the 45° plies in the same direction. In addition, the flexural anisotropy is much greater in the unbalanced laminates than in the corresponding balanced laminates. Results are also presented for $[(\pm 45/10_2)_m]_s$ and $[(\pm 45/30_2)_m]_s$ unbalanced, symmetric laminates in tables 9 and 10, respectively, and with two additional gray dashed lines in figures 6 and 7. Similarly, results are presented in figure 8 and tables 4, 6, 8, 9, and 10 that show the shear-load-factor ratio $\hat{\alpha}_3/\hat{\alpha}_1$ as a function of the number of laminate plies for the same unbalanced, symmetric laminates. The solid black lines in figure 8 are for the $[(+45_2/0/90)_m]_s$, $[(+45_2/0_2)_m]_s$, and $[(+45_2/90_2)_m]_s$ laminates, and the dashed gray lines are for the $[(\pm 45/10_2)_m]_s$ and $[(\pm 45/30_2)_m]_s$ laminates. The reason for presenting $\hat{\alpha}_2/\hat{\alpha}_1$ and $\hat{\alpha}_3/\hat{\alpha}_1$ in

figures 7 and 8, respectively, is that these quantities determine the mechanical-buckling load factors L_2 (see eqs. (47) and (50)) and L_3 (see eqs. (48) and (51)), respectively, that are used to determine the critical temperature change when $\hat{\alpha}_1$ is nonzero. Recall that these buckling load factors are nondimensional measures of the relative proportions of the thermally induced destabilizing loads.

The results in figure 6 and tables 3–10 indicate that the values of $\hat{\alpha}_1$ are all positive. Thus, these laminates are loaded by axial compression when uniformly heated and by axial tension when uniformly cooled (see eqs. (38) and (10)). The results also show equal values of $\hat{\alpha}_1$ for the $[(\pm 45/0_2)_m]_s$ and $[(+45_2/0_2)_m]_s$ laminates, for the $[(\pm 45/0/90)_m]_s$ and $[(+45_2/0/90)_m]_s$ laminates, and for the $[(\pm 45/90_2)_m]_s$ and $[(+45_2/90_2)_m]_s$ laminates, respectively. The largest values of $\hat{\alpha}_1$ are exhibited by the $[(\pm 45/90_2)_m]_s$ and $[(+45_2/90_2)_m]_s$ laminates and the smallest by the $[(\pm 45/0_2)_m]_s$ and $[(+45_2/0_2)_m]_s$ laminates. The results also show, for the most part, relatively small variations in $\hat{\alpha}_1$ with the number of laminate plies, with the largest variations exhibited by the $[(\pm 45/0/90)_m]_s$ and $[(+45_2/0/90)_m]_s$ laminates.

The results in figure 7 and tables 3–10 indicate that the values of $\hat{\alpha}_2/\hat{\alpha}_1$ are all positive, which means that the values for $\hat{\alpha}_2$ are positive because the values of $\hat{\alpha}_1$ are all positive. Thus, the restrained thermal expansion or contraction induces a uniform compressive stress in the y-coordinate direction for uniform heating and a uniform tension stress for uniform cooling (see eqs. (39) and (11)). The results also show equal values of $\hat{\alpha}_2/\hat{\alpha}_1$ for the $[(\pm 45/0_2)_m]_s$ and $[(+45_2/0_2)_m]_s$ laminates, for the $[(\pm 45/0/90)_m]_s$ and $[(+45_2/0/90)_m]_s$ laminates, and for the $[(\pm 45/90_2)_m]_s$ and $[(+45_2/90_2)_m]_s$ laminates, respectively. In addition, the values of $\hat{\alpha}_2/\hat{\alpha}_1$ for the $[(\pm 45/0/90)_m]_s$ quasi-isotropic laminates converge to a value of one as the number of plies increases, that is, the result for an isotropic plate.

The largest values of $\hat{\alpha}_2/\hat{\alpha}_1$ are exhibited by the $[(\pm 45/0_2)_m]_s$ and $[(+45_2/0_2)_m]_s$ laminates ($\hat{\alpha}_2/\hat{\alpha}_1 = 3.18$) and the smallest by the $[(\pm 45/90_2)_m]_s$ and $[(+45_2/90_2)_m]_s$ laminates ($\hat{\alpha}_2/\hat{\alpha}_1 = 0.32$). The results also show, to a large extent, relatively small variations in $\hat{\alpha}_2/\hat{\alpha}_1$ with the number of laminate plies. However, the results in figure 7 also show a substantial, monotonically increasing variation in $\hat{\alpha}_2/\hat{\alpha}_1$ with the number of laminate plies for the $[(\pm 45/0_2)_m]_s$, $[(+45_2/0_2)_m]_s$, and $[(\pm 45/10_2)_m]_s$ laminates.

The results in figure 8 and in tables 4, 6, 8, 9, and 10 also indicate that the values of $\hat{\alpha}_3/\hat{\alpha}_1$ are all positive, which means that the values for $\hat{\alpha}_3$ are positive because the values of $\hat{\alpha}_1$ are all positive. Thus, the restrained thermal expansion and contraction induces a uniform positive shear stress (see fig. 2(b)) for uniform heating and a uniform negative shear stress for uniform cooling (see eqs. (40) and (12)). The results also show nearly equal values of $\hat{\alpha}_3/\hat{\alpha}_1$ for the $[(\pm 45/10_2)_m]_s$ and $[(+45_2/90_2)_m]_s$ laminates for $m > 2$. The largest values of $\hat{\alpha}_3/\hat{\alpha}_1$ are exhibited by the $[(+45_2/0_2)_m]_s$ laminates ($\hat{\alpha}_3/\hat{\alpha}_1 = 0.53$) and the smallest by the $[(\pm 45/10_2)_m]_s$ laminates ($\hat{\alpha}_3/\hat{\alpha}_1 = 0.15$). The results in figure 8 also show relatively small variations in $\hat{\alpha}_3/\hat{\alpha}_1$ with the number of laminate plies. The largest variation in $\hat{\alpha}_3/\hat{\alpha}_1$ with the number of laminate plies is exhibited by the $[(+45_2/0_2)_m]_s$ laminates.

Three curves that are presented in figures 9 and 10 and results presented in tables 11–16 show the stiffness-weighted laminate thermal expansion parameter $\hat{\alpha}_1$ and load factor ratio $\hat{\alpha}_2/\hat{\alpha}_1$ as a function of the fiber angle, $0° \le \theta \le 90°$, for $[(\pm\theta)_m]_s$, $[\pm\theta/0/90]_s$, $[(\pm 45/0/90) + \theta]_s$ balanced laminates and for $[(+\theta)_{2m}]_s$ and $[+\theta_2/0/90]_s$ unbalanced laminates. Specifically, the black solid lines in the figures are for the $[(\pm\theta)_m]_s$ and $[(+\theta)_{2m}]_s$ laminates and are independent of the value of the stacking sequence number m. The dashed lines represent the $[\pm\theta/0/90]_s$ and $[+\theta_2/0/90]_s$ laminates, and the solid gray curves represent the $[(\pm 45/0/90) + \theta]_s$ laminates. Likewise, results are presented in figure 11 and tables 13 and 16 that show the shear-load-factor ratio $\hat{\alpha}_3/\hat{\alpha}_1$ as a function of the fiber angle θ for the

$[(+\theta)_{2m}]_s$ and $[+\theta_2/0/90]_s$ unbalanced laminates. In figure 11, the solid and dashed black curves are for the $[(+\theta)_{2m}]_s$ and $[+\theta_2/0/90]_s$ laminates, respectively.

The results in figure 9 and tables 11–16 indicate that all laminates exhibit $\hat{\alpha}_1 > 0$ for all values of θ considered. Thus, these laminates are also loaded by axial compression when uniformly heated and by axial tension when uniformly cooled. The largest and smallest values of $\hat{\alpha}_1$ and the greatest variations are exhibited by the $[(\pm\theta)_m]_s$ and $[(+\theta)_{2m}]_s$ laminates. Both the $[(\pm\theta)_m]_s$ and $[(+\theta)_{2m}]_s$ and the $[\pm\theta/0/90]_s$ and $[+\theta_2/0/90]_s$ laminates exhibit a monotonic increase in $\hat{\alpha}_1$, with increasing values of θ. The values of $\hat{\alpha}_1$ for the $[(\pm45/0/90) + \theta]_s$ laminates decrease monotonically with increasing values of θ up to 45° and then increase monotonically. Moreover, the solid gray curve for these laminates is symmetric about the vertical line $\theta = 45°$.

The results in figure 10 and tables 11–16 indicate that the values of $\hat{\alpha}_2/\hat{\alpha}_1$ are all positive, which means that the values for $\hat{\alpha}_2$ are positive because the values of $\hat{\alpha}_1$ are all positive. Thus, the restrained thermal expansion and contraction induces a uniform transverse compressive stress N_{y1} for uniform heating and a uniform transverse tension stress for uniform cooling. The largest and smallest values of $\hat{\alpha}_2/\hat{\alpha}_1$ and the greatest variations are exhibited by the $[(\pm\theta)_m]_s$ and $[(+\theta)_{2m}]_s$ laminates. Specifically, the largest and smallest values are given by $\hat{\alpha}_2/\hat{\alpha}_1 = 14.39$ and 0.07, respectively. Both the $[(\pm\theta)_m]_s$ and $[(+\theta)_{2m}]_s$ and the $[\pm\theta/0/90]_s$ and $[+\theta_2/0/90]_s$ laminates exhibit a monotonic decrease in $\hat{\alpha}_2/\hat{\alpha}_1$, with increasing values of θ, approaching a value of zero. The variation in the values of $\hat{\alpha}_2/\hat{\alpha}_1$ with fiber angle for the $[(\pm45/0/90) + \theta]_s$ laminates is benign compared to the other laminates.

The results in figure 11 and tables 13 and 16 also indicate that the values of $\hat{\alpha}_3/\hat{\alpha}_1$ are all positive, which means that the values for $\hat{\alpha}_3$ are positive because the values of $\hat{\alpha}_1$ are all positive. Thus, the restrained thermal expansion and contraction induces a uniform positive shear stress for uniform heating and a uniform negative shear stress for uniform cooling. Overall, the results show that the values of $\hat{\alpha}_3/\hat{\alpha}_1$ are greater for the $[(+\theta)_{2m}]_s$ laminates than for the $[+\theta_2/0/90]_s$ laminates with respect to the fiber angle θ. In addition, the results show larger variations in $\hat{\alpha}_3/\hat{\alpha}_1$ for both laminates for values of the fiber angle less than approximately 45^o. The largest value of $\hat{\alpha}_3/\hat{\alpha}_1$ exhibited by the $[(+\theta)_{2m}]_s$ laminates is given approximately by $\hat{\alpha}_3/\hat{\alpha}_1 = 1.16$ at approximately $\theta = 21°$. The largest value of $\hat{\alpha}_3/\hat{\alpha}_1$ exhibited by the $[+\theta_2/0/90]_s$ laminates is given approximately by $\hat{\alpha}_3/\hat{\alpha}_1 = 0.43$ at approximately $\theta = 26^o$.

For all unbalanced laminates considered in figures 6–11, biaxial compression and positive shear loading exist when the laminates are subjected to uniform heating. For uniform cooling, biaxial tension and negative shear loading exist in the laminates. Moreover, a biaxial-compression stress state exists in the balanced laminates subjected to uniform heating, and a biaxial-tension stress state exists in the balanced laminates subjected to uniform cooling, which means that buckling cannot occur. Furthermore, it was determined that elastic buckling does not occur for the unbalanced laminates considered in figures 6–11 that are subjected to uniform cooling. For these plates, when subjected to uniform cooling, biaxial-tension stresses are induced that are substantially greater than the induced shearing stresses.

Results are presented in figures 12 and 13 and in tables 3–10 that show the critical temperature change $\frac{12b^2}{\pi^2 t^2}\Theta_0^{cr}$ for uniform heating as a function of the number of laminate plies for the $[(\pm45/0/90)_m]_s$, $[(\pm45/0_2)_m]_s$, and $[(\pm45/90_2)_m]_s$ balanced laminates and the $[(+45_2/0/90)_m]_s$, $[(+45_2/0_2)_m]_s$, $[(+45_2/90_2)_m]_s$, $[(\pm45/10_2)_m]_s$, and $[(\pm45/30_2)_m]_s$ unbalanced laminates. Similarly, results are presented in figures 14 and 15 and in tables 11–16 that show the critical temperature

change for uniform heating as a function of the fiber angle θ for the $[\pm\theta]_s$, $[(+\theta)_{2m}]_s$, and $[(\pm\theta)_m]_s$ ($m > 5$) laminates and for the $[\pm\theta/0/90]_s$, $[+\theta_2/0/90]_s$, and $[(\pm 45/0/90) + \theta]_s$ laminates, respectively. The results in figures 12 and 13 correspond to results for plates with simply supported and clamped edges, respectively. The results were obtained by computing the ratios $\hat{\alpha}_2/\hat{\alpha}_1$ and $\hat{\alpha}_3/\hat{\alpha}_1$ first. Next, the load factors L_2 and L_3 were determined by using equations (47) and (48), respectively; then, the critical value of the loading parameter $\tilde{p}_{cr}$ was determined for each of the laminates, and the critical temperature change was obtained by using equation (49). Equations (47)–(49) were used because $\hat{\alpha}_1\Theta_0 > 0$ for these laminates when they are subjected to uniform heating. For these laminates, the critical value of the loading parameter depends on the flexural boundary conditions, the plate flexural orthotropy and flexural anisotropy, and the values of the load factors L_2 and L_3, which depend on the stiffness-weighted laminate thermal-expansion parameters. The stiffness-weighted laminate thermal-expansion parameters depend on the plate membrane orthotropy, membrane anisotropy, and the stiffnesses associated with pure bending action.

The results in figures 12 and 13 and in tables 3–10 indicate that the critical temperature $\frac{12b^2}{\pi^2 t^2}\Theta_0^{cr}$ is highly dependent on the arrangement of the 45°, 0°, and 90° plies. Generally, as the number of plies increases, the magnitude of the critical temperature change decreases for about half of the laminates and increases for the other half. Overall, the plates with clamped edges are more buckling resistant than the corresponding plates with simply supported edges, as expected. The clamped and simply supported $[(\pm 45/90_2)_m]_s$ laminates require the most heating to cause buckling, and the simply supported $[(\pm 45/0_2)_m]_s$, $[(+45_2/0_2)_m]_s$, and $[(\pm 45/10_2)_m]_s$ laminates and the clamped $[(+45_2/0_2)_m]_s$ laminates require the least amount of heating.

The results in figure 14 and tables 11–13 indicate that the critical temperature change $\frac{12b^2}{\pi^2 t^2}\Theta_0^{cr}$ for the $[\pm\theta]_s$, $[(+\theta)_{2m}]_s$, and $[(\pm\theta)_m]_s$ ($m > 5$) laminates is highly dependent on the fiber angle θ. In particular, the results for the clamped and simply supported $[\pm\theta]_s$ and $[(\pm\theta)_m]_s$ ($m > 5$) laminates show substantial increase in the critical temperature change with increasing θ for values up to approximately 55° and 62°, respectively, followed by a significant decrease. In addition, the $[(\pm\theta)_m]_s$ ($m > 5$) laminates require more heating to cause buckling than the corresponding $[\pm\theta]_s$ laminates. The results for the $[(+\theta)_{2m}]_s$ laminates show a monotonic increase in the critical temperature change with θ, but the temperature changes are always ≤ those for the corresponding $[\pm\theta]_s$ and $[(\pm\theta)_m]_s$ ($m > 5$) laminates. Thus, the $[(+\theta)_{2m}]_s$ laminates generally require less heating to cause buckling than the other corresponding laminates shown in figure 14. Overall, the plates with clamped edges are much more buckling resistant than the corresponding plates with simply supported edges, as expected.

The results in figure 15 and tables 14–16 indicate that the critical temperature change $\frac{12b^2}{\pi^2 t^2}\Theta_0^{cr}$ for the $[\pm\theta/0/90]_s$, $[+\theta_2/0/90]_s$, and $[(\pm 45/0/90) + \theta]_s$ laminates is also highly dependent on the fiber angle θ. Specifically, the results for the $[\pm\theta/0/90]_s$ laminates exhibit a trend similar to the results for the balanced laminates shown in figure 14; that is, the clamped and simply supported $[\pm\theta/0/90]_s$ laminates

exhibit a substantial increase in the critical temperature change with increasing θ for values up to approximately 57° and 67°, respectively, followed by a significant decrease. Like the unbalanced laminates of figure 14, the results for the $[+\theta_2/0/90]_s$ laminates show a monotonic increase in the critical temperature change with θ, but the temperature changes are always ≤ those for the corresponding $[\pm\theta/0/90]_s$ laminates. Thus, the $[+\theta_2/0/90]_s$ laminates require, for the most part, less heating to cause buckling than the corresponding $[\pm\theta/0/90]_s$ laminates. Generally, the $[(\pm45/0/90) + \theta]_s$ laminates require more uniform heating to cause buckling than the other corresponding laminates shown in figure 15 and exhibit greater values of the critical temperature change over a larger range of θ. Moreover, the critical temperature change for the $[(\pm45/0/90) + \theta]_s$ laminates exhibits the smallest variations with fiber angle for the laminates shown in figure 15. Like the laminates of figure 14, the laminates with clamped edges in figure 15 are much more buckling resistant than the corresponding plates with simply supported edges, as expected.

The data presented in figures 13–15 are given in a compact form and are applicable to an infinite range of plate width-to-thickness ratios b/t. Once the number of laminate plies is selected, the critical temperature change Θ_0^{cr} can be found as a function of the plate width b for a given laminate family. However, it is important to keep in mind the limitations of classical laminated-plate bending theory as the plate width-to-thickness ratio b/t becomes smaller than a value of approximately 20. Results of this type are useful in structural design and are shown for the $[(\pm45/0/90)_m]_s$ quasi-isotropic laminates in figure 16. Two sets of curves are shown for various values of the stacking sequence number m in figure 16. Moreover, the results are shown for a maximum temperature-change magnitude of 300 °F. This maximum temperature-change magnitude was selected to ensure a regime of heating in which the material behavior is linear. The solid lines in these figures are for plates with simply supported edges, and the dashed lines are for plates with clamped edges. As indicated by equation (49), the magnitude of Θ_0^{cr} shown in the figure decreases proportionally to the inverse square of the plate width b.

Generic Results and Examples

The simplicity of the equations presented herein that are like equation (49) in form suggested that generic buckling design charts, similar to those presented in references 1–5, could be obtained for the thermal buckling problem of the present study. Specifically, generic design data can be obtained from charts that show the stiffness-weighted laminate thermal-expansion parameters $\tilde{\alpha}_1$, $\tilde{\alpha}_2$, and $\tilde{\alpha}_3$; the flexural orthotropy parameter β; and the flexural anisotropy parameters γ and δ as a function of material system and laminate stacking sequence and from charts that show the critical value of the loading parameter $\tilde{P}_{cr}$ or buckling interaction curves, as a function of flexural boundary conditions, β, γ, δ, L_1, L_2, and L_3. Results of this type illustrate the key aspects of the behavior and show overall trends and sensitivity of the behavior to changes in the parameters. Several figures that illustrate the utility of this type of design data are presented subsequently.

Values of the Nondimensional Parameters

Values of the nondimensional parameters that are used herein are presented in this section for $[(\pm45/0/90)_m]_s$ quasi-isotropic, $[(\pm\theta)_m]_s$ angle-ply, and $[(+\theta)_{2m}]_s$ unidirectional off-axis laminates. Nine different contemporary material systems are used. These material systems include boron-aluminum, S-glass-epoxy, a typical boron-epoxy, AS4/3501-6 graphite-epoxy, AS4/3502 graphite-epoxy, IM7/5260 graphite-bismaleimide, Kevlar 49-epoxy, IM7/PETI-5, and P-100/3502 pitch-epoxy materials. The mechanical properties of these material systems are presented in table 2 and the nominal ply thickness is 0.005 in.

Parameters for $[\pm 45/0/90)_m]_s$ laminates. Values of $\hat{\alpha}_1$ and $\hat{\alpha}_2/\hat{\alpha}_1$ for $[(\pm 45/0/90)_m]_s$ quasi-isotropic laminates are presented in figures 17 and 18, respectively, and in tables 17–19 for the nine material systems. The results show a wide variation in $\hat{\alpha}_1$ with material system, for the laminate considered. Moreover, $\hat{\alpha}_1$ is positive for all the material systems except the P-100/3502 pitch-epoxy material. Similarly, $\hat{\alpha}_2/\hat{\alpha}_1$ is positive for all the material systems and $1 \le \hat{\alpha}_2/\hat{\alpha}_1 < 1.2$. These values for $\hat{\alpha}_2/\hat{\alpha}_1$ indicate that $\hat{\alpha}_2$ is also positive for all the material systems except the P-100/3502 pitch-epoxy material. Thus, the laminates made from all the material systems except the P-100/3502 pitch-epoxy material are loaded by biaxial compression when uniformly heated and by biaxial tension when uniformly cooled, and as a result can buckle only for uniform heating. The laminates made from the P-100/3502 pitch-epoxy material are loaded by biaxial tension when uniformly heated and by biaxial compression when uniformly cooled. These laminates must be cooled to buckle. The results also show that some material systems yield a slightly larger variation in $\hat{\alpha}_1$ and $\hat{\alpha}_2/\hat{\alpha}_1$ with the number of laminate plies. Overall, the results presented in figures 17 and 18 show that there is a wide range of possibilities available for tailoring the thermal buckling characteristics of a laminate family.

The remaining parameters needed for a buckling analysis of the long $[(\pm 45/0/90)_m]_s$ quasi-isotropic laminates are the nondimensional flexural orthotropy parameter β and the flexural anisotropy parameters γ and δ. Values for these parameters are not presented graphically herein but are given in tables 20–23, along with values for $(D_{11}/D_{22})^{1/4}$. The parameters are presented graphically in reference 5 as a function of the stacking-sequence number m for the nine material systems, along with a discussion of their characteristics. The results in reference 5 and tables 20–22 for these parameters show a series of curves that approach $\beta = 1$, $\gamma = 0$, and $\delta = 0$ from above as the number of plies increases. A homogeneous, isotropic material has values of $\beta = 1$, $\gamma = 0$, and $\delta = 0$. Thus, the results for β, γ, and δ in reference 5 and tables 20–22 give, to some extent, a quantitative measure of quasi-isotropy.

Parameters for $[(\pm\theta)_m]_s$ and $[(+\theta)_{2m}]_s$ laminates. Values of $\hat{\alpha}_1$, $\hat{\alpha}_2$, and $\hat{\alpha}_3$ for $[(\pm\theta)_m]_s$ balanced, angle-ply laminates and $[(+\theta)_{2m}]_s$ unbalanced, unidirectional off-axis laminates composed of the nine material systems are presented in figure 19 and table 24, figure 20 and table 25, and figure 21 and table 26, respectively. The values for $\hat{\alpha}_1$ and $\hat{\alpha}_2$ are identical for both laminate families and are independent of the stacking sequence number m. The results show a very wide variation in $\hat{\alpha}_1$, $\hat{\alpha}_2$, and $\hat{\alpha}_3$ with a material system and with fiber angle θ. The largest variations are exhibited by $\hat{\alpha}_2$, followed by $\hat{\alpha}_1$. Moreover, $\hat{\alpha}_1$ and $\hat{\alpha}_2$ are positive for all the material systems except the P-100/3502 pitch-epoxy and Kevlar 49-epoxy materials, which are negative for several values of the fiber angle θ. Similarly, $\hat{\alpha}_3$ is positive for all the material systems except the S-glass-epoxy and boron-epoxy materials, which are negative for $0° < \theta < 90°$. Thus, depending on the material system and fiber angle, a laminate may be loaded by various combinations of tension, compression, and shear and may buckle when subjected to uniform heating, cooling, or both. This point is illustrated by the results in tables 27 and 28, which show the values of N_{y1}/N_{x1}^c and N_{xy1}/N_{x1}^c, respectively, for selected values of θ. Like the results for the quasi-isotropic laminates, the results in figures 19–21 and in tables 24–26 show that there is a very wide range of possibilities available for tailoring the thermal buckling characteristics of a laminate family.

Values of the nondimensional orthotropy parameter β and the nondimensional anisotropy parameters γ and δ for the $[(\pm\theta)_m]_s$ laminates made of the same nine material systems have also been presented graphically in reference 5. The values of β in reference 5 for the $[(\pm\theta)_m]_s$ laminates are identical to the corresponding results for the $[(+\theta)_{2m}]_s$ unbalanced, unidirectional off-axis laminates and are independent of the stacking-sequence number m. Numerical values of β for these laminates are presented in table 29 for selected values of θ. The results in reference 5 show a series of curves for β that vary dramatically with the fiber angle θ and the material system. The largest values of, and greatest variations

in β are generally exhibited by the laminates made of the P-100/3502 pitch-epoxy material. In contrast, the smallest values of, and least variations in β are generally exhibited by the laminates made of the boron-aluminum material. The values of γ and δ for the $[(\pm\theta)_m]_s$ laminates are strongly dependent on the stacking-sequence number m. The results in reference 5 for the flexural anisotropy parameters γ and δ are for $m = 1$, which corresponds to the highest degree of flexural anisotropy for these laminates. Corresponding numerical values of γ and δ for these laminates are presented in tables 30 and 31, respectively, for selected values of θ. In addition, corresponding numerical values for $(D_{11}/D_{22})^{1/4}$ that are used to compute the load factors L_2 and L_3 are presented in table 32. The graphical results in reference 5 show a large effect of the fiber angle θ and the material system on the degree of flexural anisotropy for the $[\pm\theta]_s$ laminates. Like the parameter β, the largest values of, and greatest variations in γ and δ are generally exhibited by the laminates made of the P-100/3502 pitch-epoxy material, and the smallest values of, and least variations in γ and δ are generally exhibited by the laminates made of the boron-aluminum material.

Values of the nondimensional anisotropy parameters γ and δ for the $[(+\theta)_{2m}]_s$ laminates made of the same nine material systems are presented in figure 22 and table 33 and in figure 23 and table 34, respectively. The results for these laminates are independent of the stacking sequence number m and exhibit practically the same trends as the results for corresponding $[\pm\theta]_s$ laminates that are given in reference 5. The values of γ and δ for the $[(+\theta)_{2m}]_s$ laminates, however, are generally larger than the corresponding values for the $[(\pm\theta)_m]_s$ laminates. This fact is illustrated in figure 24, which shows a comparison of results for $[(\pm\theta)_6]_s$, $[\pm\theta]_s$, and $[(+\theta)_{2m}]_s$ laminates made of IM7/5260 graphite-bismaleimide material. The results in this figure indicate that the $[(+\theta)_{2m}]_s$ unidirectional off-axis and $[\pm\theta]_s$ laminates exhibit similar variations with θ, but the $[(+\theta)_{2m}]_s$ laminates exhibit a substantially higher degree of flexural anisotropy. In addition, the results for the $[(\pm\theta)_6]_s$ laminates indicate that the flexural anisotropy is negligible compared to that of the other laminates.

Buckling Coefficients and Critical Temperature Change

The values of the nondimensional parameters β, γ, and δ, given in reference 5 and presented in the present paper, or from similar figures for other laminates, can be used to determine the buckling coefficients for plates subjected to uniform, combined mechanical loads. More specifically, the critical loading parameter $\tilde{p}_{cr}$ and the buckling coefficients K_x, K_y, and K_s depend on the parameters β, γ, and δ for classical laminated-plate theory (see ref. 1), the load factors L_1, L_2, and L_3 that define the relative proportions of the inplane loads, and the flexural boundary conditions. For plates subjected to restrained thermal expansion and contraction and uniform heating or cooling, the relative proportions of the inplane loads that are induced by the restrained deformation are defined by the stiffness-weighted laminate thermal-expansion parameters $\hat{\alpha}_1$, $\hat{\alpha}_2$, and $\hat{\alpha}_3$ (e.g., see eqs. (47) and (48)). Thus, generic buckling design charts for plates subjected to mechanical loads can be used directly to obtain critical temperature changes for the thermal buckling problem considered herein and can be applied to a vast range of laminate constructions that include hybrid laminates made of several materials. Several of these generic buckling design charts that are applicable to balanced and unbalanced, symmetric laminates are presented subsequently.

Charts for balanced laminates. Balanced laminates that are subjected to uniform heating or cooling and that are fully restrained against thermal expansion or contraction develop, at most, a biaxial stress state ($\hat{\alpha}_3 = 0$). When $\hat{\alpha}_1$ and $\hat{\alpha}_2$ are both positive valued, a laminate is loaded by uniform biaxial compression when heated uniformly. In contrast, when $\hat{\alpha}_1 > 0$ and $\hat{\alpha}_2 < 0$, a laminate is loaded by uniform axial compression and transverse tension ($N_{y1} < 0$) when heated uniformly. A

similar stress state exists when $\hat{\alpha}_1 < 0$ and $\hat{\alpha}_2 > 0$ and the laminate is uniformly cooled. However, for all three of these loading conditions, $L_1 = 1$, $L_3 = 0$, and L_2 is given by equation (47). The critical temperature change $\frac{12b^2}{\pi^2 t^2}\Theta_0^{cr}$ is obtained by dividing both sides of equation (49) by $\hat{\alpha}_1$ once $\tilde{p}_{cr}(\beta, \gamma, \delta, L_1, L_2)$ is known. The appropriate value for $\tilde{p}_{cr}$ is obtained from generic buckling design charts by noting that equations (44) and (45) give $K_x = \tilde{p}_{cr}$ and $K_y = L_2\ \tilde{p}_{cr}$, respectively, and that $L_2 = K_y/K_x$. Thus, the critical value of the loading parameter for balanced laminates can be obtained from traditional K_x-K_y buckling interaction curves that are given as a function of the nondimensional parameters β, γ, δ, and the flexural boundary conditions.

When $\hat{\alpha}_1$ and $\hat{\alpha}_2$ are both positive valued and the laminate is subjected to uniform cooling, or when $\hat{\alpha}_1$ and $\hat{\alpha}_2$ are both negative valued and the laminate is subjected to uniform heating, a state of biaxial tension exists in the laminate. For this loading condition, elastic buckling is not possible. When $\hat{\alpha}_1 > 0$ and $\hat{\alpha}_2 < 0$, a laminate is loaded by uniform axial tension and by transverse compression when cooled uniformly. A similar stress state exists when $\hat{\alpha}_1 < 0$ and $\hat{\alpha}_2 > 0$ and the laminate is uniformly heated. For both of these cases, $L_1 = -1$, $L_3 = 0$, and L_2 is given by equation (50). More importantly, because the only destabilizing load is a transverse compression load, a wide-column buckling mode is the only possibility. Thus, the critical temperature change $\frac{12b^2}{\pi^2 t^2}\Theta_0^{cr}$ is obtained by dividing both sides of equation (52b) by $\hat{\alpha}_1$. For this special case, $K_y = 1$ and $K_y = 4$ for simply supported and clamped plates, respectively, and $K_x = -K_y/L_2$.

When $\hat{\alpha}_1 = 0$ and $\hat{\alpha}_2 < 0$, a laminate is loaded by uniform transverse tension when heated uniformly. A similar stress state exists when $\hat{\alpha}_1 = 0$ and $\hat{\alpha}_2 > 0$ and the laminate is uniformly cooled. For this loading condition, elastic buckling is also not possible. For the cases where $\hat{\alpha}_1 = 0$ and $\hat{\alpha}_2 < 0$ and the laminate is cooled uniformly, and where $\hat{\alpha}_1 = 0$ and $\hat{\alpha}_2 > 0$ and the laminate is heated uniformly, a state of transverse compression exists. A wide-column buckling mode is the only possibility. The critical temperature change $\frac{12b^2}{\pi^2 t^2}\Theta_0^{cr}$ is obtained by dividing both sides of equation (54b) by $\hat{\alpha}_2$. For this special case, $K_y = 1$ and $K_y = 4$ for simply supported and clamped plates, respectively.

Examples of traditional K_x-K_y buckling interaction curves that can be used to obtain $\tilde{p}_{cr}(\beta, \gamma, \delta, L_1, L_2)$ described in the previous paragraphs are presented in figure 25 for specially orthotropic plates that have negligible flexural anisotropy ($\gamma = \delta = 0$). In particular, two sets of generic buckling curves are shown in figure 25 for plates that are subjected to combined axial compression and transverse tension ($K_y < 0$) or compression ($K_y > 0$) loads. Results are shown in the figure for six values of the orthotropy parameter β that cover a very wide range of laminate constructions. The solid and dashed curves correspond to results for clamped and simply supported plates, respectively, and the curves for $\beta = 1$ correspond to results for isotropic plates. Similar curves that show the effects of flexural anisotropy are presented in reference 1, along with a discussion of the behavioral characteristics. For the K_x-K_y buckling interaction curves shown in figure 25, the load factor L_2 appears implicitly as the slope of a line emanating from the origin of the graph. The buckling coefficient that corresponds to a

given value of L_2 is determined by the point of intersection of the line and the appropriate buckling interaction curve. Several representative points of intersection are depicted in figure 25 for the simply supported and clamped plates by the open and filled circular symbols, respectively. Points of intersection that are on the horizontal portion of the curves, given by $K_y = 1$ and $K_y = 4$ for the simply supported and clamped plates, respectively, correspond to wide-column buckling modes. Similarly, results for negative values of K_x, although not shown in figure 25, correspond to horizontal extrapolations of the lines $K_y = 1$ and $K_y = 4$ and also correspond to wide-column buckling modes. With the value of L_2 determined from equation (47), unique values of K_x and K_y are determined from a figure like figure 25, where $\tilde{p}_{\text{cr}} = K_x$.

Results that are directly analogous to those presented in figure 25 are presented in figures 26 and 27 and in tables 35 and 36, in which the buckling coefficient K_x, or equivalently $\tilde{p}_{\text{cr}}$, is given explicitly in terms of the load factor L_2. An interesting characteristic of figure 26 is that the family of curves for the simply supported plates (dashed) and the clamped plates (solid) terminate at points on the gray, solid curves given by $K_x = \frac{1}{L_2}$ and $K_x = \frac{4}{L_2}$, respectively. The curves $K_x = \frac{1}{L_2}$ and $K_x = \frac{4}{L_2}$ correspond to the horizontal portion of the curves in figure 25 that are given by $K_y = 1$ and $K_y = 4$ for the simply supported plates (dashed) and the clamped plates (solid), respectively, and represent the wide-column buckling modes. Like figure 25, negative values of K_x (not shown) correspond to wide-column buckling modes. The results in figure 27 show an increase in the buckling coefficient K_x as the load factor L_2 decreases. For negative values of L_2, this increase in buckling resistance corresponds to an increase in the magnitude of the transverse tension load, which has a well-known stabilizing effect.

Typically, when studying the behavior of a plate that possesses flexural anisotropy, one likes to know the importance of the anisotropy. Generic curves for simply supported plates that can be used in conjunction with figures 26 and 27 to obtain this information are presented in figures 28 and 29. Some corresponding numerical values are given in tables 37–39. The curves in figures 28 and 29 indicate the effects of plate flexural anisotropy on the ratio of the buckling coefficients that include and neglect this anisotropy, respectively, as a function of β and L_2. Buckling coefficients that correspond to the neglect of flexural anisotropy are denoted by $K_x\big|_{\gamma=\delta=0}$. Six groups of curves are shown in each figure that correspond to equal values of the flexural anisotropy parameters. Moreover, three curves are contained in each group that correspond to different values of L_2.

Charts for unbalanced laminates. Unbalanced laminates that are subjected to uniform heating or cooling and that are fully restrained against thermal expansion or contraction can generally develop a prebuckling stress state that consists of combinations of axial tension or compression, transverse tension or compression, and positive or negative shear. The specific form of the prebuckling stress state is determined by the values of the parameters $\hat{\alpha}_1$, $\hat{\alpha}_2$, and $\hat{\alpha}_3$, which determine the values of the load factors L_1, L_2, and L_3. The specific values of L_1, L_2, and L_3 are obtained by following the same logic presented previously for the balanced laminates and discussed during the presentation of equations (47)–(58). Once L_1, L_2, and L_3 are determined, $\tilde{p}_{\text{cr}}(\beta, \gamma, \delta, L_1, L_2, L_3)$ can be determined from generic results that give either $\tilde{p}_{\text{cr}}$ or K_x-K_y-K_s buckling interaction surfaces (or level curves) as a function of L_1, L_2, L_3, β, γ, δ, and the flexural boundary conditions. Then, the critical temperature

change $\frac{12b^2}{\pi^2 t^2}\Theta_0^{cr}$ is determined by using the appropriate one of equations (49), (52a), (54a), (56), (57), and (58).

Examples of generic buckling curves are shown in figure 30 for plates with negligible flexural anisotropy ($\gamma = \delta = 0$) and that are subjected to combined axial compression, transverse tension or compression, and shear. These results are applicable to unbalanced, symmetric laminates with negligible flexural anisotropy that develop biaxial and shear loads when restrained from thermal expansion or contraction and can be used to obtain $\tilde{p}_{cr}$ described in the previous paragraph. The results shown in figure 30 represent the traditional buckling interaction curves and are for a value of $\beta = 1$, which corresponds to results for isotropic plates. The load factors L_2 and L_3 are included in the results in an implicit manner. The solid and dashed curves correspond to results for clamped and simply supported plates, respectively, and are level curves of the corresponding K_x-K_y-K_s buckling interaction surface. Each curve in the figure corresponds to a different magnitude of the shear loading. Moreover, positive and negative values of the shear-buckling coefficient K_s correspond to positive and negative directions of the shear loading (see fig. 2(b)). The buckling coefficients that correspond to given values of the load factors L_2 and L_3 are determined by the point of intersection of the line emanating from the origin of the graph and the appropriate buckling interaction curve. These points of intersection are depicted in figure 30 for the simply supported and clamped plates by the open and filled circular symbols, respectively. Points of intersection that occur on the horizontal portion of the curves given by $K_y = 1$ and $K_y = 4$ for the simply supported and clamped plates, respectively, correspond to wide-column buckling modes. With the values of L_1, L_2, and L_3 determined from the values of the parameters $\hat{\alpha}_1$, $\hat{\alpha}_2$, and $\hat{\alpha}_3$, unique values of K_x, K_y, and K_s are determined from a figure like figure 30, and $\tilde{p}_{cr}$ is determined from equations (44)–(46). It is worth mentioning that very few results of this type are available in the technical literature.

Results that are directly analogous to those presented in figure 30 are presented in figures 31–44 and in tables 40–53 for simply supported plates in which the buckling coefficient K_x, or equivalently $\tilde{p}_{cr}$, is given explicitly in terms of the load factors L_2 and L_3, with $L_1 = 1$. Thus, the results in these figures and tables are applicable to plates for which the axial load is a compression load. More precisely, K_x is given as a function of L_2 for selected values of L_3, and three different curves, for most figures, and two different curves, in some figures, are shown in each figure that correspond to different values of β.

The curves in figures 31 and 32 (see tables 40 and 41) are for specially orthotropic plates ($\gamma = \delta = 0$) with values of $\beta = 0.5$, 1, and 1.5 and with values of $\beta = 2$, 2.5, and 3, respectively. Curves are given in these figures that apply to both positive and negative shear loads. Similarly, the curves in figures 33 and 34 and in figures 35 and 36 (see tables 42–45) are for plates with $\gamma = \delta = 0.2$ (slight anisotropy) and for values of $\beta = 0.5$, 1, and 1.5 and for values of $\beta = 2$, 2.5, and 3, respectively. Likewise, the curves in figures 37 and 38, and in figures 39 and 40 (see tables 46– 49) are for plates with $\gamma = \delta = 0.4$ and for values of $\beta = 0.6$, 1, and 1.5 and for values of $\beta = 2$, 2.5, and 3, respectively. The curves in figures 41 and 42 and in figures 43 and 44 (see tables 50–53) are for plates with $\gamma = \delta = 0.6$ and for values of $\beta = 1.5$ and 2 and for values of $\beta = 2.5$ and 3, respectively. Moreover, the results in figures 33, 35, 37, 39, 41, and 43 are primarily for positive shear loads ($L_3 > 0$), and those in figures 34, 36, 38, 40, 42, and 44 are for negative shear loads ($L_3 < 0$). The distinction between positive and negative shear loads and the differences in the corresponding results is caused by the presence of flexural anisotropy. Although it is not shown for all curves, the curves in figures 31–44 terminate at points on the gray, solid curves given by $K_x = \frac{1}{L_2}$, which represent the wide-column buckling modes.

Examples

To illustrate the use of the generic figures that have been presented herein, first consider a simply supported $[(\pm 45/0/90)_8]_s$ laminate made of IM7/5260 graphite-bismaleimide material. From figures 17 and 18, and tables 17–22, one gets $\beta = 1.1$, $\gamma = \delta \approx 0$, $\hat{\alpha}_1 = 1.51 \times 10^{-6}$/°F, and $\hat{\alpha}_2 = 1.55 \times 10^{-6}$/°F. The parameter $\hat{\alpha}_3 = 0$ because the laminate is balanced. For this laminate, the only destabilizing loads are biaxial compression loads that are obtained for uniform heating. For this case, $L_1 = 1$, $L_3 = 0$, and $L_2 = 1.03 \approx 1$ is obtained from equation (47). For $L_1 = 1$, $K_x = \tilde{p}_{cr}$. The value of K_x is obtained from figure 26 (or table 35) by interpolating the results in the figure for $\beta = 1$ and $\beta = 1.5$. For $\beta = 1$ and $L_2 = 1$, table 35 gives $K_x = 1.0$, which corresponds to a wide-column buckling mode. Similarly, for $\beta = 1.5$ and $L_2 = 1$, table 35 also gives $K_x = 1.0$. Therefore, $K_x = 1.0$ for $\beta = 1.1$. Substituting $K_x = 1.0$ for $\tilde{p}_{cr}$ and $\hat{\alpha}_1 = 1.51 \times 10^{-6}$/°F into equation (49) gives $\frac{12b^2}{\pi^2 t^2}\Theta_0^{cr} = 0.66 \times 10^6$ °F. Next, let the plate width be given such that the plate width-to-thickness ratio is $b/t = 100$. For this plate, $\Theta_0^{cr} \approx 54$ °F.

Next, consider a simply supported $[\pm 45/0/90]_s$ laminate made of IM7/5260 graphite-bismaleimide material. From figures 17 and 18, and tables 17–22, one gets $\beta \approx 2.0$, $\gamma = \delta \approx 0.2$, $\hat{\alpha}_1 = 1.85 \times 10^{-6}$/°F, and $\hat{\alpha}_2 = 2.10 \times 10^{-6}$/°F. The parameter $\hat{\alpha}_3 = 0$ because the laminate is also balanced. For this laminate, the only destabilizing loads are also biaxial compression loads that are obtained for uniform heating. Thus, for this case, $L_1 = 1$, $L_3 = 0$, and $L_2 = 1.14$ is obtained from equation (47). Again, for $L_1 = 1$, $K_x = \tilde{p}_{cr}$. The value of K_x is obtained directly from figure 35 by noting that all values of K_x for $L_2 > 1$ also fall on the solid gray curve given by $K_x = 1/L_2$. For $L_2 = 1.14$, $K_x = 0.88$, which also corresponds to a wide-column buckling mode. Substituting $K_x = 0.88$ for $\tilde{p}_{cr}$ and $\hat{\alpha}_1 = 1.85 \times 10^{-6}$/°F into equation (49) gives $\frac{12b^2}{\pi^2 t^2}\Theta_0^{cr} = 0.48 \times 10^6$ °F. Next, let the plate width be given such that the plate width-to-thickness ratio is $b/t = 100$. For this plate, $\Theta_0^{cr} \approx 39$ °F.

Finally, consider a simply supported $[(+45_2/0/90)_8]_s$ unbalanced laminate made of IM7/5260 graphite-bismaleimide material. Although results for these laminates are not presented in figures 17–24, by using a laminate analysis code or a set of charts like those shown in figures 17–24, one could get $\beta \approx 1$, $\gamma = \delta \approx 0.3$, $\hat{\alpha}_1 = 1.51 \times 10^{-6}$/°F, $\hat{\alpha}_2 = 1.55 \times 10^{-6}$/°F, and $\hat{\alpha}_3 = 0.44 \times 10^{-6}$/°F. For this laminate, a state of biaxial compression and positive shear loads arise for uniform heating. Thus, for this case, $L_1 = 1$, $L_2 = 1.03 \approx 1$ is obtained from equation (47), and $L_3 = 0.3$ is obtained from equation (48). Again, for $L_1 = 1$, $K_x = \tilde{p}_{cr}$. The results presented in figure 33 for $\beta = 1$, $\gamma = \delta = 0.2$, $L_3 = 0$, and $L_3 = 0.5$, and in figure 37 for $\beta = 1$, $\gamma = \delta = 0.4$, $L_3 = 0$, and $L_3 = 0.5$ indicate that K_x for $L_2 = 1$ and $L_3 = 0.3$ are given by $K_x = 1/L_2$ (solid gray curve). For $L_2 = 1$, $K_x = 1.0$, which also corresponds to a wide-column buckling mode. Substituting $K_x = 1.0$ for $\tilde{p}_{cr}$ and $\hat{\alpha}_1 = 1.51 \times 10^{-6}$/°F into equation (49) gives $\frac{12b^2}{\pi^2 t^2}\Theta_0^{cr} = 0.66 \times 10^6$ °F. Next, let the plate width be given such that the plate width-to-thickness ratio is $b/t = 100$. For this plate, $\Theta_0^{cr} \approx 54$ °F. Comparing this result with the result for the corresponding $[(\pm 45/0/90)_8]_s$ laminate discussed previously shows that the unbalanced laminate is

equally buckling resistant, even with its higher degree of flexural anisotropy and the presence of a shear load. This similarity in buckling resistance is a manifestation of the fact that both the $[(\pm 45/0/90)_8]_s$ and the $[(+45_2/0/90)_8]_s$ laminates buckle into a wide-column mode. For the case of uniform cooling, biaxial tension and negative shear loads are induced by the restrained deformation. The load factors for this case are obtained from equations (50) and (51), where $L_1 = -1$. These equations yield $L_2 \approx -1$ and $L_3 = -0.3$. Examination of the load factors indicates that the axial and transverse tension loads are approximately 3.3 times the magnitude of the destabilizing shear load. For this loading condition, the tension loads are dominant and elastic buckling is not likely.

Concluding Remarks

An analytical approach for synthesizing buckling results and behavior for long, balanced and unbalanced symmetric laminates that are subjected to uniform heating or cooling and fully restrained thermal expansion or contraction has been presented. A nondimensional buckling analysis for long flexurally anisotropic plates that are subjected to combined loads has been described and useful nondimensional parameters have been presented. In particular, stiffness-weighted thermal-expansion parameters have been presented that can be used to determine critical temperature changes for a wide range of laminate constructions in terms of physically intuitive, well-known mechanical buckling coefficients. Moreover, the effects of membrane orthotropy and membrane anisotropy on the mechanically and thermally induced prebuckling stress state have been determined.

A large number of results have been presented herein for some common laminates that are intended, to some extent, to facilitate a structural designer's transition to the use of the generic buckling design curves that are included in the paper. Many of the results were previously unknown. In addition, several results have been presented that show the effect of laminate construction on the buckling behavior, and several cases are presented that indicate when a laminate will buckle because of uniform cooling. Results of this type could be important in the design of vehicles that use liquid fuels. Generic buckling design curves have also been presented that provide physical insight into the buckling problem of the present paper in addition to providing useful design data. Also, examples have been presented that demonstrate the use of the generic design curves. Overall, the analysis approach and generic results that have been presented identify the effects or characteristics of laminate thermal expansion, membrane orthotropy and anisotropy, and flexural orthotropy and anisotropy on laminated-plate buckling in a very general and unifying manner. Although the results are based on classical laminated-plate theory and have been demonstrated for infinitely long plates, the approach is applicable to more sophisticated plate theories that incorporate effects such as transverse-shear flexibility and can be used for finite-length plates.

References

1. Nemeth, M. P.: *Buckling Behavior of Long Symmetrically Laminated Plates Subjected to Combined Loadings*. NASA TP-3195, 1992.

2. Nemeth, M. P.: Buckling Behavior of Long Symmetrically Laminated Plates Subjected to Compression, Shear, and Inplane Bending Loads. *AIAA J.*, vol. 30, no. 12, 1992, pp. 2959–2965.

3. Nemeth, M. P.: *Buckling Behavior of Long Anistropic Plates Subjected to Combined Loads*. NASA TP-3568, 1995.

4. Nemeth, M. P.: *Buckling Behavior of Long Symmetrically Laminated Plates Subjected to Shear and Linearly Varying Axial Edge Loads*. NASA TP-3659, 1997.

5. Nemeth, M. P.: Buckling Behavior of Long Anisotropic Plates Subjected to Restrained Thermal Expansion and Mechanical Loads. *Journal of Thermal Stresses*, vol. 23, 2000, pp. 873–916.

6. Nemeth, M. P.: Importance of Anisotropy on Buckling of Compression-Loaded Symmetric Composite Plates. *AIAA J.*, vol. 24, no. 11, 1986, pp. 1831–1835.

7. Whitney, J. M.: *Structural Analysis of Laminated Anisotropic Plates*. Technomic Publishing Co., Inc., Lancaster, Pennsylvania, 1987.

8. Hyer, M. W.: *Stress Analysis of Fiber-Reinforced Composite Materials.* WCB/McGraw Hill Publishing Co., Inc., Boston, 1998.

9. Romeo, G.; and Ferrero, G.: Analytical/Experimental Behavior of Anisotropic Rectangular Panels Under Linearly Varying Combined Loads. *AIAA J.*, vol. 39, no. 5, 2001, pp. 932–941.

10. Batdorf, S. B.; Stein, M.; and Libove, C.: *Critical Combinations of Longitudinal and Transverse Direct Stress for an Infinitely Long Flat Plate With Edges Elastically Restrained Against Rotation*. NACA WR L-49, 1946.

Table 1. Typical Properties of Selected Engineering Metals

Property	Material				
	Aluminum	Steel	Titanium	Brass	Copper
Elastic modulus, E, Msi	10.0	30.0	16.0	14.8	17.0
Poisson's ratio, ν	0.33	0.25	0.33	0.34	0.31
Coefficient of thermal expansion, $\alpha \times 10^6$/°F	13.0	6.5	4.8	10.5	9.5

Table 2. Lamina Properties

Lamina property*	Material systems								
	Boron-Al	S-glass-epoxy	Kevlar 49-epoxy	IM7/5260	AS4/3502	AS4/3501-6	Boron-epoxy	IM7/PETI-5	P-100/3502
E_L, Msi	33	7.5	11.02	22.1	18.5	20.01	29.58	20.35	53.5
E_T, Msi	21	1.7	0.8	1.457	1.64	1.30	2.68	1.16	0.73
ν_{LT}	0.23	0.25	0.34	0.258	0.30	0.30	0.23	0.29	0.31
G_{LT}, Msi	7.0	0.80	0.33	0.860	0.87	1.03	0.81	0.61	0.76
$\alpha_L \times 10^6$/°F	3.2	3.5	–2.22	0.0125	0.25	–0.167	3.38	–0.14	–0.64
$\alpha_T \times 10^6$/°F	11.0	11.0	43.89	14.91	16.2	15.6	16.83	16.85	17.2

*The symbols L and T denote the longitudinal fiber and transverse matrix directions of a specially orthotropic lamina, respectively.

Table 3. Parameters, Buckling Coefficients, and Critical Temperature Change for Simply Supported and Clamped $[(\pm 45/0/90)_m]_s$ Plates Made of IM7/5260 Material and Totally Restrained Against Thermal Expansion (see figs. 6, 7, 12, and 13)

m*	$\hat{\alpha}_1 \times 10^6$/°F	$L_2 = \frac{\hat{\alpha}_2}{\hat{\alpha}_1}$	Simply supported				Clamped			
			K_x	K_y	$\frac{\lambda_{cr}}{b}$	$\frac{12b^2}{\pi^2 t^2}\Theta_0^{cr} \times 10^{-6}$ °F	K_x	K_y	$\frac{\lambda_{cr}}{b}$	$\frac{12b^2}{\pi^2 t^2}\Theta_0^{cr} \times 10^{-6}$ °F
1	1.85	1.14	.879	1.00	∞†	.476	3.52	4.00	∞	1.90
2	1.64	1.09	.917	1.00	∞	.559	3.67	4.00	∞	2.24
3	1.58	1.06	.940	1.00	∞	.595	3.74	3.97	2.32	2.36
4	1.55	1.05	.954	1.00	∞	.614	3.75	3.94	1.86	2.42
5	1.54	1.04	.962	1.00	∞	.626	3.76	3.91	1.69	2.45
6	1.53	1.03	.968	1.00	∞	.634	3.76	3.89	1.60	2.47
7	1.52	1.03	.972	1.00	∞	.640	3.76	3.87	1.55	2.48
8	1.51	1.03	.975	1.00	∞	.645	3.76	3.86	1.51	2.49

*$L_1 = 1$, $L_3 = 0$, and $N_{y1} = N_{x1}^c$ (see discussion of eqs. (47)–(49)).
†The symbol ∞ denotes a wide-column buckling mode.

Table 4. Parameters, Buckling Coefficients, and Critical Temperature Change for Simply Supported and Clamped $[(+45_2/0/90)_m]_s$ Plates Made of IM7/5260 Material and Totally Restrained Against Thermal Expansion (see figs. 6, 7, 8, 12, and 13)

m*	$\hat{\alpha}_1 \times 10^6$/°F	$L_2 = \frac{\hat{\alpha}_2}{\hat{\alpha}_1}$	$L_3 = \frac{\hat{\alpha}_3}{\hat{\alpha}_1}$	Simply supported					Clamped				
				K_x	K_y	K_s	$\frac{\lambda_{cr}}{b}$	$\frac{12b^2}{\pi^2 t^2}\Theta_0^{cr} \times 10^{-6}$ °F	K_x	K_y	K_s	$\frac{\lambda_{cr}}{b}$	$\frac{12b^2}{\pi^2 t^2}\Theta_0^{cr} \times 10^{-6}$ °F
1	1.85	1.14	.306	.863	.982	.264	2.80	.467	2.10	2.38	.641	.85	1.13
2	1.64	1.09	.300	.917	1.00	.275	∞†	.559	2.59	2.83	.777	.91	1.58
3	1.58	1.06	.296	.940	1.00	.278	∞	.595	2.73	2.90	.807	.91	1.73
4	1.55	1.05	.294	.954	1.00	.280	∞	.614	2.79	2.93	.820	.91	1.80
5	1.54	1.04	.293	.962	1.00	.281	∞	.626	2.82	2.94	.826	.90	1.84
6	1.53	1.03	.292	.968	1.00	.282	∞	.634	2.85	2.94	.831	.90	1.87
7	1.52	1.03	.291	.972	1.00	.283	∞	.640	2.86	2.95	.833	.90	1.89
8	1.51	1.03	.291	.975	1.00	.283	∞	.645	2.88	2.95	.836	.90	1.90

*$L_1 = 1$, $N_{y1} = N_{x1}^c$, and $N_{xy1} = 0.29 N_{x1}^c$ (see discussion of eqs. (47)–(49)).
†The symbol ∞ denotes a wide-column buckling mode.

Table 5. Parameters, Buckling Coefficients, and Critical Temperature Change for Simply Supported and Clamped $[(\pm 45/0_2)_m]_s$ Plates Made of IM7/5260 Material and Totally Restrained Against Thermal Expansion (see figs. 6, 7, 12, and 13)

m*	$\hat{\alpha}_1 \times 10^6$/°F	$L_2 = \frac{\hat{\alpha}_2}{\hat{\alpha}_1}$	Simply supported				Clamped			
			K_x	K_y	$\frac{\lambda_{cr}}{b}$	$\frac{12b^2}{\pi^2 t^2}\Theta_0^{cr} \times 10^{-6}$ °F	K_x	K_y	$\frac{\lambda_{cr}}{b}$	$\frac{12b^2}{\pi^2 t^2}\Theta_0^{cr} \times 10^{-6}$ °F
1	1.33	2.15	.466	1.00	∞†	.352	1.86	4.00	∞	1.41
2	1.26	2.70	.371	1.00	∞	.294	1.48	4.00	∞	1.18
3	1.25	2.90	.344	1.00	∞	.275	1.38	4.00	∞	1.10
4	1.25	3.01	.332	1.00	∞	.265	1.33	4.00	∞	1.06
5	1.25	3.08	.325	1.00	∞	.259	1.30	4.00	∞	1.04
6	1.25	3.12	.320	1.00	∞	.255	1.28	4.00	∞	1.02
7	1.25	3.15	.317	1.00	∞	.253	1.27	4.00	∞	1.01
8	1.26	3.18	.315	1.00	∞	.251	1.26	4.00	∞	1.00

*$L_1 = 1$, $L_3 = 0$, and $N_{y1} = 1.81 N_{x1}^c$ (see discussion of eqs. (47)–(49)).
†The symbol ∞ denotes a wide-column buckling mode.

Table 6. Parameters, Buckling Coefficients, and Critical Temperature Change for Simply Supported and Clamped $[(+45_2/0_2)_m]_s$ Plates Made of IM7/5260 Material and Totally Restrained Against Thermal Expansion (see figs. 6, 7, 8, 12, and 13)

				Simply supported					Clamped				
m*	$\hat{\alpha}_1 \times 10^6$/°F	$L_2 = \frac{\hat{\alpha}_2}{\hat{\alpha}_1}$	$L_3 = \frac{\hat{\alpha}_3}{\hat{\alpha}_1}$	K_x	K_y	K_s	$\frac{\lambda_{cr}}{b}$	$\frac{12b^2}{\pi^2 t^2}\Theta_0^{cr}$ $\times 10^{-6}$ °F	K_x	K_y	K_s	$\frac{\lambda_{cr}}{b}$	$\frac{12b^2}{\pi^2 t^2}\Theta_0^{cr}$ $\times 10^{-6}$ °F
1	1.33	2.15	.439	.466	1.00	.205	∞†	.352	1.30	2.79	0.571	.97	.982
2	1.26	2.70	.492	.371	1.00	.182	∞	.294	1.18	3.18	.580	1.25	.935
3	1.25	2.90	.510	.344	1.00	.176	∞	.275	1.14	3.30	.580	1.36	.907
4	1.25	3.01	.520	.332	1.00	.173	∞	.265	1.12	3.36	.580	1.42	.890
5	1.25	3.08	.525	.325	1.00	.171	∞	.259	1.10	3.39	.580	1.45	.880
6	1.25	3.12	.529	.320	1.00	.170	∞	.255	1.10	3.42	.580	1.48	.873
7	1.25	3.15	.532	.317	1.00	.169	∞	.253	1.09	3.43	.579	1.50	.868
8	1.26	3.18	.534	.315	1.00	.168	∞	.251	1.08	3.45	.579	1.51	.864

*$L_1 = 1$, $N_{y1} = 1.81 N_{x1}^c$, and $N_{xy1} = 0.40\, N_{x1}^c$ (see discussion of eqs. (47)–(49)).
†The symbol ∞ denotes a wide-column buckling mode.

Table 7. Parameters, Buckling Coefficients, and Critical Temperature Change for Simply Supported and Clamped $[(\pm 45/90_2)_m]_s$ Plates Made of IM7/5260 Material and Totally Restrained Against Thermal Expansion (see figs. 6, 7, 12, and 13)

			Simply supported				Clamped			
m*	$\hat{\alpha}_1 \times 10^6$/°F	$L_2 = \frac{\hat{\alpha}_2}{\hat{\alpha}_1}$	K_x	K_y	$\frac{\lambda_{cr}}{b}$	$\frac{12b^2}{\pi^2 t^2}\Theta_0^{cr}$ $\times 10^{-6}$ °F	K_x	K_y	$\frac{\lambda_{cr}}{b}$	$\frac{12b^2}{\pi^2 t^2}\Theta_0^{cr}$ $\times 10^{-6}$ °F
1	2.39	.466	2.15	1.00	∞†	.897	6.78	3.158	.86	2.83
2	2.28	.371	2.70	1.00	∞	1.19	6.66	2.466	.67	2.93
3	2.26	.344	2.90	.999	4.44	1.28	6.56	2.259	.63	2.90
4	2.26	.332	2.97	.985	2.23	1.31	6.50	2.160	.61	2.87
5	2.26	.325	2.99	.972	1.88	1.32	6.47	2.102	.60	2.86
6	2.26	.320	3.00	.962	1.72	1.33	6.44	2.064	.60	2.85
7	2.27	.317	3.01	.954	1.64	1.33	6.43	2.037	.59	2.84
8	2.27	.315	3.01	.948	1.58	1.33	6.41	2.017	.59	2.83

*$L_1 = 1$, $L_3 = 0$, and $N_{y1} = 0.55 N_{x1}^c$ (see discussion of eqs. (47)–(49)).
†The symbol ∞ denotes a wide-column buckling mode.

Table 8. Parameters, Buckling Coefficients, and Critical Temperature Change for Simply Supported and Clamped $[(+45_2/90_2)_m]_s$ Plates Made of IM7/5260 Material and Totally Restrained Against Thermal Expansion (see figs. 6, 7, 8, 12, and 13)

				Simply supported					Clamped				
m*	$\hat{\alpha}_1 \times 10^6$/°F	$L_2 = \frac{\hat{\alpha}_2}{\hat{\alpha}_1}$	$L_3 = \frac{\hat{\alpha}_3}{\hat{\alpha}_1}$	K_x	K_y	K_s	$\frac{\lambda_{cr}}{b}$	$\frac{12b^2}{\pi^2 t^2}\Theta_0^{cr} \times 10^{-6}$ °F	K_x	K_y	K_s	$\frac{\lambda_{cr}}{b}$	$\frac{12b^2}{\pi^2 t^2}\Theta_0^{cr} \times 10^{-6}$ °F
1	2.39	.466	.205	1.87	.871	.382	1.34	.781	3.57	1.66	.730	.59	1.49
2	2.28	.371	.182	2.30	.854	.420	1.14	1.01	4.31	1.60	.787	.52	1.89
3	2.26	.344	.176	2.40	.825	.421	1.06	1.06	4.48	1.54	788	.50	1.98
4	2.26	.332	.173	2.43	.809	.420	1.02	1.08	4.56	1.51	.787	.50	2.01
5	2.26	.325	.171	2.45	.798	.419	1.00	1.09	4.60	1.50	.785	.49	2.03
6	2.26	.320	.170	2.47	.791	.419	.99	1.09	4.62	1.48	.784	.49	2.04
7	2.27	.317	.169	2.48	.785	.418	.98	1.09	4.64	1.47	.783	.49	2.05
8	2.27	.315	.168	2.48	.781	.417	.97	1.10	4.66	1.47	.783	.49	2.06

*$L_1 = 1$, $N_{y1} = 0.55N_{x1}^c$, and $N_{xy1} = 0.22N_{x1}^c$ (see discussion of eqs. (47)–(49)).

Table 9. Parameters, Buckling Coefficients, and Critical Temperature Change for Simply Supported and Clamped $[(\pm 45/10_2)_m]_s$ Plates Made of IM7/5260 Material and Totally Restrained Against Thermal Expansion (see figs. 6, 7, 8, 12, and 13)

				Simply supported					Clamped				
m*	$\hat{\alpha}_1 \times 10^6$/°F	$L_2 = \frac{\hat{\alpha}_2}{\hat{\alpha}_1}$	$L_3 = \frac{\hat{\alpha}_3}{\hat{\alpha}_1}$	K_x	K_y	K_s	$\frac{\lambda_{cr}}{b}$	$\frac{12b^2}{\pi^2 t^2}\Theta_0^{cr} \times 10^{-6}$ °F	K_x	K_y	K_s	$\frac{\lambda_{cr}}{b}$	$\frac{12b^2}{\pi^2 t^2}\Theta_0^{cr} \times 10^{-6}$ °F
1	1.37	2.05	.146	.488	1.00	.071	∞†	.357	1.95	4.00	.285	∞	1.43
2	1.31	2.55	.163	.392	1.00	.064	∞	.299	1.57	4.00	.255	∞	1.20
3	1.30	2.74	.169	.365	1.00	.062	∞	.280	1.46	4.00	.246	∞	1.12
4	1.30	2.84	.172	.352	1.00	.061	∞	.270	1.41	4.00	.242	∞	1.08
5	1.31	2.90	.174	.345	1.00	.060	∞	.264	1.38	4.00	.239	∞	1.06
6	1.31	2.94	.175	.340	1.00	.059	∞	.260	1.36	4.00	.238	∞	1.04
7	1.31	2.97	.176	.337	1.00	.059	∞	.258	1.35	4.00	.237	∞	1.03
8	1.31	2.99	.176	.334	1.00	.059	∞	.255	1.34	4.00	.236	∞	1.02

*$L_1 = 1$, $N_{y1} = 1.74N_{x1}^c$, and $N_{xy1} = 0.13N_{x1}^c$ (see discussion of eqs. (47)–(49)).
†The symbol ∞ denotes a wide-column buckling mode.

Table 10. Parameters, Buckling Coefficients, and Critical Temperature Change for Simply Supported and Clamped $[(\pm 45/30_2)_m]_s$ Plates Made of IM7/5260 Material and Totally Restrained Against Thermal Expansion (see figs. 6, 7, 8, 12, and 13)

m*	$\hat{\alpha}_1 \times 10^6$/°F	$L_2 = \frac{\hat{\alpha}_2}{\hat{\alpha}_1}$	$L_3 = \frac{\hat{\alpha}_3}{\hat{\alpha}_1}$	Simply supported					Clamped				
				K_x	K_y	K_s	$\frac{\lambda_{cr}}{b}$	$\frac{12b^2}{\pi^2 t^2}\Theta_0^{cr} \times 10^{-6}$ °F	K_x	K_y	K_s	$\frac{\lambda_{cr}}{b}$	$\frac{12b^2}{\pi^2 t^2}\Theta_0^{cr} \times 10^{-6}$ °F
1	1.68	1.46	.304	.684	1.00	.208	∞†	0.408	2.73	4.00	.831	∞	1.63
2	1.66	1.67	.325	.599	1.00	.194	∞	0.361	2.39	4.00	.777	∞	1.44
3	1.66	1.75	.332	.573	1.00	.190	∞	0.345	2.29	4.00	.760	∞	1.38
4	1.66	1.78	.336	.560	1.00	.188	∞	0.338	2.24	4.00	.752	∞	1.35
5	1.66	1.81	.338	.553	1.00	.187	∞	0.333	2.21	4.00	.747	∞	1.33
6	1.66	1.82	.339	.548	1.00	.186	∞	0.330	2.19	4.00	.744	∞	1.32
7	1.66	1.84	.340	.545	1.00	.185	∞	0.328	2.18	4.00	.741	∞	1.31
8	1.66	1.85	.341	.542	1.00	.185	∞	0.326	2.17	4.00	.740	∞	1.30

*$L_1 = 1$, $\mathcal{N}_{y1} = 1.34\mathcal{N}_{x1}^c$, and $\mathcal{N}_{xy1} = 0.29\mathcal{N}_{x1}^c$ (see discussion of eqs. (47)–(49)).
†The symbol ∞ denotes a wide-column buckling mode.

Table 11. Parameters, Buckling Coefficients, and Critical Temperature Change for Simply Supported and Clamped $[\pm\theta]_s$ Plates Made of IM7/5260 Material and Totally Restrained Against Thermal Expansion (see figs. 9, 10, and 14)

θ, deg*	$\hat{\alpha}_1 \times 10^6$/°F	$L_2 = \frac{\hat{\alpha}_2}{\hat{\alpha}_1}$	$\frac{\mathcal{N}_{y1}}{\mathcal{N}_{x1}^c}$	Simply supported				Clamped			
				K_x	K_y	$\frac{\lambda_{cr}}{b}$	$\frac{12b^2}{\pi^2 t^2}\Theta_0^{cr} \times 10^{-6}$ °F	K_x	K_y	$\frac{\lambda_{cr}}{b}$	$\frac{12b^2}{\pi^2 t^2}\Theta_0^{cr} \times 10^{-6}$ °F
0	1.04	14.4	3.69	.069	1.00	∞†	.067	.278	4.00	∞	.268
5	1.06	13.9	3.60	.072	1.00	∞	.068	.288	4.00	∞	.272
10	1.13	12.4	3.34	.080	1.00	∞	.071	.322	4.00	∞	.285
15	1.23	10.3	2.98	.097	1.00	∞	.079	.388	4.00	∞	.315
20	1.35	7.90	2.57	.127	1.00	∞	.094	.506	4.00	∞	.376
25	1.46	5.64	2.17	.177	1.00	∞	.122	.709	4.00	∞	.487
30	1.56	3.81	1.81	.262	1.00	∞	.168	1.05	4.00	∞	.672
35	1.68	2.48	1.49	.403	1.00	∞	.240	1.61	4.00	∞	.962
40	1.82	1.58	1.22	.632	1.00	∞	.348	2.50	3.96	2.82	1.38
45	1.99	1.00	1.00	1.00	1.00	∞	.502	3.64	3.64	1.33	1.83
50	2.22	.632	.819	1.58	1.00	∞	.714	4.78	3.02	.85	2.16
55	2.50	.403	.672	2.47	.994	2.92	.988	5.63	2.27	.63	2.26
60	2.82	.262	.554	3.10	.813	1.07	1.10	6.11	1.60	.51	2.17
65	3.16	.177	.461	3.32	.588	.78	1.05	6.26	1.11	.44	1.98
70	3.46	.127	.389	3.26	.413	.66	.943	6.15	.778	.40	1.78
75	3.67	.097	.336	3.05	.296	.59	.831	5.87	.570	.37	1.60
80	3.78	.080	.299	2.80	.225	.55	.741	5.56	.447	.35	1.47
85	3.82	.072	.278	2.62	.189	.54	.685	5.33	.384	.35	1.39
90	3.83	.069	.271	2.55	.177	.53	.666	5.24	.364	.34	1.37

*$L_1 = 1$ and $L_3 = 0$ (see discussion of eqs. (47)–(49)).
†The symbol ∞ denotes a wide-column buckling mode.

Table 12. Parameters, Buckling Coefficients, and Critical Temperature Change for Simply Supported and Clamped $[(\pm\theta)_m]_s$ Plates Made of IM7/5260 Material and Totally Restrained Against Thermal Expansion ($m > 5$, see figs. 9, 10, and 14)

θ, deg*	$\hat{\alpha}_1 \times 10^6/°F$	$L_2 = \frac{\hat{\alpha}_2}{\hat{\alpha}_1}$	$\frac{N_{y1}}{N_{x1}^c}$	Simply supported				Clamped			
				K_x	K_y	$\frac{\lambda_{cr}}{b}$	$\frac{12b^2}{\pi^2 t^2}\Theta_0^{cr} \times 10^{-6}$ °F	K_x	K_y	$\frac{\lambda_{cr}}{b}$	$\frac{12b^2}{\pi^2 t^2}\Theta_0^{cr} \times 10^{-6}$ °F
0	1.04	14.4	3.69	.069	1.00	∞†	.067	.278	4.00	∞	.268
5	1.06	13.9	3.60	.072	1.00	∞	.068	.288	4.00	∞	.272
10	1.13	12.4	3.34	.080	1.00	∞	.071	.322	4.00	∞	.285
15	1.23	10.3	2.98	.097	1.00	∞	.079	.388	4.00	∞	.315
20	1.35	7.90	2.57	.127	1.00	∞	.094	.506	4.00	∞	.376
25	1.46	5.64	2.17	.177	1.00	∞	.122	.709	4.00	∞	.487
30	1.56	3.81	1.81	.262	1.00	∞	.168	1.05	4.00	∞	.672
35	1.68	2.48	1.49	.403	1.00	∞	.240	1.61	4.00	∞	.962
40	1.82	1.58	1.22	.632	1.00	∞	.348	2.53	4.00	∞	1.39
45	1.99	1.00	1.00	1.00	1.00	∞	.502	4.00	4.00	∞	2.01
50	2.22	.632	.819	1.58	1.00	∞	.714	6.32	3.99	2.70	2.85
55	2.50	.403	.672	2.48	1.00	∞	.994	7.75	3.12	.72	3.11
60	2.82	.262	.554	3.81	1.00	∞	1.352	8.15	2.14	.54	2.89
65	3.16	.177	.461	4.43	.785	.910	1.404	7.96	1.41	.45	2.52
70	3.46	.127	.389	4.16	.527	.690	1.204	7.39	.936	.40	2.14
75	3.67	.097	.336	3.62	.352	.600	.988	6.64	.644	.37	1.81
80	3.78	.080	.299	3.07	.247	.560	.814	5.92	.476	.35	1.57
85	3.82	.072	.278	2.69	.194	.540	.703	5.42	.390	.35	1.42
90	3.83	.069	.271	2.55	.177	.530	.666	5.24	.364	.34	1.37

*$L_1 = 1$ and $L_3 = 0$ (see discussion of eqs. (47)–(49)).
†The symbol ∞ denotes a wide-column buckling mode.

Table 13. Parameters, Buckling Coefficients, and Critical Temperature Change for Simply Supported and Clamped $[(+\theta)_{2m}]_s$ (m = 1, 2, ...) Plates Made of IM7/5260 Material and Totally Restrained Against Thermal Expansion (see figs. 9, 10, 11, and 14)

θ, deg*	$\hat{\alpha}_1 \times 10^6$/°F	$L_2 = \frac{\hat{\alpha}_2}{\hat{\alpha}_1}$	$L_3 = \frac{\hat{\alpha}_3}{\hat{\alpha}_1}$	$\frac{N_{y1}}{N^c_{x1}}$	$\frac{N_{xy1}}{N^c_{x1}}$	Simply supported					Clamped				
						K_x	K_y	K_s	$\frac{\lambda_{cr}}{b}$	$\frac{12b^2}{\pi^2 t^2}\Theta_0^{cr} \times 10^{-6}$ °F	K_x	K_y	K_s	$\frac{\lambda_{cr}}{b}$	$\frac{12b^2}{\pi^2 t^2}\Theta_0^{cr} \times 10^{-6}$ °F
0	1.04	14.4	0	3.70	0	.069	1.00	0	∞†	.067	.278	4.00	0	∞	.268
5	1.06	13.9	.450	3.60	.229	.072	1.00	.032	∞	.068	.288	4.00	.130	∞	.272
10	1.13	12.4	.822	3.34	.426	.080	1.00	.066	∞	.071	.322	4.00	.265	∞	.285
15	1.23	10.3	1.06	2.98	.571	.097	1.00	.103	∞	.079	.388	4.00	.412	∞	.315
20	1.35	7.90	1.16	2.57	.658	.127	1.00	.146	∞	.094	.506	4.00	.585	∞	.376
25	1.46	5.64	1.12	2.17	.697	.177	1.00	.199	∞	.122	.706	3.98	.793	3.99	.485
30	1.56	3.81	1.01	1.81	.697	.262	1.00	.266	∞	.168	.916	3.49	.928	1.54	.586
35	1.68	2.48	.866	1.49	.671	.403	1.00	.349	∞	.240	1.14	2.83	.986	1.08	.679
40	1.82	1.58	.715	1.22	.628	.622	.984	.444	3.01	.343	1.40	2.21	1.00	.84	.771
45	1.99	1.00	.574	1.00	.574	.836	.836	.480	1.45	.420	1.72	1.72	.986	.69	.863
50	2.22	.632	.452	.819	.514	1.06	.672	.480	1.07	.480	2.11	1.34	.954	.59	.953
55	2.50	.403	.349	.672	.451	1.32	.532	.461	.87	.529	2.59	1.05	.906	.51	1.04
60	2.82	.262	.266	.554	.386	1.61	.421	.427	.75	.570	3.16	.828	.839	.46	1.12
65	3.16	.177	.199	.461	.321	1.90	.337	.379	.67	.602	3.76	.666	.749	.42	1.19
70	3.46	.127	.146	.389	.256	2.17	.274	.317	.61	.627	4.33	.548	.633	.39	1.25
75	3.67	.097	.103	.336	.192	2.37	.230	.244	.58	.645	4.78	.464	.492	.37	1.30
80	3.78	.080	.066	.299	.128	2.48	.200	.164	.55	.657	5.06	.407	.335	.35	1.34
85	3.82	.072	.032	.278	.064	2.54	.183	.082	.54	.664	5.20	.375	.169	.35	1.36
90	3.83	.069	0	.271	0	2.55	.177	0	.53	.666	5.24	.364	0	.34	1.37

*L_1 = 1 (see discussion of eqs. (47)–(49)).

†The symbol ∞ denotes a wide-column buckling mode.

Table 14. Parameters, Buckling Coefficients, and Critical Temperature Change for Simply Supported and Clamped $[(\pm 45/0/90) + \theta]_s$ Plates Made of IM7/5260 Material and Totally Restrained Against Thermal Expansion (see figs. 9, 10, and 15)

θ, deg*	$\hat{\alpha}_1 \times 10^6$/°F	$L_2 = \frac{\hat{\alpha}_2}{\hat{\alpha}_1}$	Simply supported				Clamped			
			K_x	K_y	$\frac{\lambda_{cr}}{b}$	$\frac{12b^2}{\pi^2 t^2}\Theta_0^{cr} \times 10^{-6}$ °F	K_x	K_y	$\frac{\lambda_{cr}}{b}$	$\frac{12b^2}{\pi^2 t^2}\Theta_0^{cr} \times 10^{-6}$ °F
0	1.85	1.14	.879	1.00	∞†	.476	3.52	4.00	∞	1.91
5	1.81	1.06	.943	1.00	∞	.522	3.77	4.00	∞	2.09
10	1.73	.990	1.01	1.00	∞	.583	3.91	3.86	1.73	2.25
15	1.64	.930	1.08	1.00	∞	.656	3.88	3.61	1.27	2.37
20	1.54	.882	1.13	1.00	∞	.736	3.79	3.34	1.06	2.46
25	1.45	.846	1.18	.999	6.54	.816	3.67	3.10	.94	2.54
30	1.37	.818	1.20	.980	2.49	.873	3.57	2.92	.86	2.60
35	1.32	.797	1.20	.955	1.96	.909	3.50	2.79	.81	2.66
40	1.29	.780	1.20	.938	1.77	.935	3.48	2.72	.78	2.71
45	1.28	.767	1.22	.935	1.73	.954	3.52	2.70	.76	2.75
50	1.30	.755	1.25	.947	1.81	.966	3.61	2.73	.76	2.78
55	1.34	.746	1.30	.969	2.09	.969	3.76	2.81	.78	2.81
60	1.41	.740	1.34	.993	3.07	.954	3.97	2.94	.81	2.82
65	1.49	.738	1.35	1.00	∞	.907	4.22	3.11	.86	2.82
70	1.60	.743	1.35	1.00	∞	.844	4.48	3.33	.95	2.81
75	1.70	.757	1.32	1.00	∞	.778	4.70	3.56	1.08	2.77
80	1.79	.784	1.28	1.00	∞	.715	4.83	3.79	1.31	2.71
85	1.84	.825	1.21	1.00	∞	.660	4.80	3.96	1.95	2.61
90	1.85	.879	1.14	1.00	∞	.616	4.55	4.00	∞	2.47

*$L_1 = 1$, $\mathcal{N}_{y1} = \mathcal{N}_{x1}^c$, and $L_3 = 0$ (see discussion of eqs. (47)–(49)).
†The symbol ∞ denotes a wide-column buckling mode.

Table 15. Parameters, Buckling Coefficients, and Critical Temperature Change for Simply Supported and Clamped $[\pm\theta/0/90]_s$ Plates Made of IM7/5260 Material and Totally Restrained Against Thermal Expansion (see figs. 9, 10, and 15)

θ, deg*	$\hat{\alpha}_1 \times 10^6/^\circ\mathrm{F}$	$L_2 = \frac{\hat{\alpha}_2}{\hat{\alpha}_1}$	$\frac{N_{y1}}{N_{x1}^c}$	Simply supported				Clamped			
				K_x	K_y	$\frac{\lambda_{cr}}{b}$	$\frac{12b^2}{\pi^2 t^2}\Theta_0^{cr} \times 10^{-6}\ ^\circ\mathrm{F}$	K_x	K_y	$\frac{\lambda_{cr}}{b}$	$\frac{12b^2}{\pi^2 t^2}\Theta_0^{cr} \times 10^{-6}\ ^\circ\mathrm{F}$
0	1.58	6.31	1.81	.158	1.00	∞†	.100	.633	4.00	∞	.401
5	1.60	6.20	1.79	.161	1.00	∞	.101	.645	4.00	∞	.404
10	1.64	5.86	1.74	.171	1.00	∞	.104	.683	4.00	∞	.417
15	1.69	5.28	1.66	.189	1.00	∞	.112	.757	4.00	∞	.448
20	1.74	4.52	1.56	.221	1.00	∞	.127	.884	4.00	∞	.509
25	1.77	3.67	1.45	.273	1.00	∞	.154	1.09	4.00	∞	.616
30	1.79	2.84	1.34	.352	1.00	∞	.197	1.41	4.00	∞	.789
35	1.80	2.12	1.22	.471	1.00	∞	.262	1.88	4.00	∞	1.05
40	1.81	1.56	1.11	.642	1.00	∞	.354	2.57	4.00	∞	1.42
45	1.85	1.14	1.00	.879	1.00	∞	.476	3.52	4.00	∞	1.90
50	1.90	.837	.905	1.20	1.00	∞	.630	4.75	3.97	2.21	2.50
55	1.96	.627	.821	1.60	1.00	∞	.816	5.59	3.50	.96	2.86
60	2.02	.483	.749	2.07	1.00	∞	1.03	5.88	2.84	.72	2.92
65	2.06	.387	.689	2.53	.976	1.92	1.23	5.81	2.24	.61	2.82
70	2.09	.323	.640	2.54	.820	1.09	1.22	5.51	1.78	.54	2.64
75	2.09	.282	.602	2.36	.666	.90	1.13	5.14	1.45	.51	2.46
80	2.08	.257	.575	2.15	.554	.82	1.03	4.81	1.24	.49	2.31
85	2.07	.244	.559	2.00	.488	.78	.965	4.58	1.12	.47	2.21
90	2.07	.240	.554	1.95	.467	.77	.941	4.50	1.08	.47	2.18

*$L_1 = 1$ and $L_3 = 0$ (see discussion of eqs. (47)–(49)).

†The symbol ∞ denotes a wide-column buckling mode.

Table 16. Parameters, Buckling Coefficients, and Critical Temperature Change for Simply Supported and Clamped $[+\theta_2/0/90]_s$ Plates Made of IM7/5260 Material and Totally Restrained Against Thermal Expansion (see figs. 9, 10, 11, and 15)

θ, deg*	$\hat{\alpha}_1 \times 10^6$/°F	$L_2 = \frac{\hat{\alpha}_2}{\hat{\alpha}_1}$	$L_3 = \frac{\hat{\alpha}_3}{\hat{\alpha}_1}$	$\frac{N_{y1}}{N^c_{x1}}$	$\frac{N_{xy1}}{N^c_{x1}}$	Simply supported					Clamped				
						K_x	K_y	K_s	$\frac{\lambda_{cr}}{b}$	$\frac{12b^2}{\pi^2 t^2}\Theta_0^{cr} \times 10^{-6}$ °F	K_x	K_y	K_s	$\frac{\lambda_{cr}}{b}$	$\frac{12b^2}{\pi^2 t^2}\Theta_0^{cr} \times 10^{-6}$ °F
0	1.58	6.31	0	1.81	0	.158	1.00	0	∞†	.100	.633	4.00	0	∞	.401
5	1.60	6.20	.129	1.79	.069	.161	1.00	.021	∞	.101	.645	4.00	.083	∞	.404
10	1.64	5.86	.247	1.74	.134	.171	1.00	.042	∞	.104	.683	4.00	.169	∞	.417
15	1.69	5.28	.341	1.66	.191	.189	1.00	.064	∞	.112	.757	4.00	.258	∞	.448
20	1.74	4.52	.402	1.56	.236	.221	1.00	.089	∞	.127	.884	4.00	.356	∞	.509
25	1.77	3.67	.428	1.45	.270	.273	1.00	.117	∞	.154	1.09	4.00	.467	∞	.616
30	1.79	2.84	.423	1.34	.290	.352	1.00	.149	∞	.197	1.35	3.82	.570	2.02	.755
35	1.80	2.12	.395	1.22	.299	.471	1.00	.186	∞	.262	1.57	3.34	.621	1.32	.877
40	1.81	1.56	.353	1.11	.297	.642	1.00	.227	∞	.354	1.82	2.83	.641	1.03	1.00
45	1.85	1.14	.306	1.00	.287	.863	.982	.264	2.80	.467	2.10	2.38	.641	.85	1.13
50	1.90	.837	.259	.905	.269	1.06	.886	.274	1.60	.558	2.42	2.03	.627	.74	1.28
55	1.96	.627	.215	.821	.246	1.25	.780	.267	1.25	.637	2.79	1.75	.599	.65	1.43
60	2.02	.483	.175	.749	.217	1.43	.689	.249	1.06	.708	3.19	1.54	.556	.60	1.58
65	2.06	.387	.139	.689	.186	1.59	.615	.221	.950	.772	3.57	1.38	.497	.55	1.73
70	2.09	.323	.107	.640	.151	1.73	.559	.186	.880	.829	3.91	1.26	.420	.52	1.88
75	2.09	.282	.079	.602	.115	1.83	.517	.144	.830	.876	4.18	1.18	.329	.50	2.00
80	2.08	.257	.052	.575	.077	1.90	.489	.098	.790	.911	4.36	1.12	.226	.48	2.09
85	2.07	.244	.026	.559	.039	1.94	.472	.050	.780	.933	4.47	1.09	.115	.47	2.16
90	2.07	.240	0	.554	0	1.95	.467	0	.770	.941	4.50	1.08	0	.47	2.18

*$L_1 = 1$ (see discussion of eqs. (47)–(49)).
†The symbol ∞ denotes a wide-column buckling mode.

Table 17. Values of Stiffness-Weighted Laminate Thermal-Expansion Parameter $\hat{\alpha}_1 \times 10^6$/°F for $[(\pm 45/0/90)_m]_s$ Laminates (see fig. 17)

m	Material systems								
	Boron-Al	S-glass-epoxy	Kevlar 49-epoxy	IM7/5260	AS4/3502	AS4/3501-6	Boron-epoxy	IM7/PETI-5	P-100/3502
1	8.73	7.40	2.97	1.85	2.98	1.64	7.90	1.67	−.567
2	8.43	6.90	2.63	1.64	2.67	1.47	6.96	1.48	−.490
3	8.34	6.75	2.53	1.58	2.58	1.42	6.70	1.42	−.469
4	8.29	6.68	2.48	1.55	2.54	1.40	6.57	1.39	−.459
5	8.26	6.64	2.46	1.54	2.52	1.38	6.50	1.38	−.453
6	8.25	6.61	2.44	1.53	2.50	1.38	6.45	1.37	−.449
7	8.23	6.59	2.43	1.52	2.49	1.37	6.42	1.36	−.447
8	8.22	6.57	2.42	1.51	2.48	1.37	6.39	1.36	−.445

Table 18. Values of Stiffness-Weighted Laminate Thermal-Expansion Parameter $\hat{\alpha}_2 \times 10^6/°F$ for $[(\pm 45/0/90)_m]_s$ Laminates (see figs. 17 and 18)

m	Material systems								
	Boron-Al	S-glass-epoxy	Kevlar 49-epoxy	IM7/5260	AS4/3502	AS4/3501-6	Boron-epoxy	IM7/PETI-5	P-100/3502
1	8.95	8.01	3.38	2.10	3.36	1.86	8.96	1.92	–0.662
2	8.58	7.30	2.86	1.79	2.90	1.60	7.57	1.61	–0.542
3	8.45	7.03	2.69	1.68	2.74	1.51	7.10	1.51	–0.504
4	8.37	6.89	2.60	1.63	2.66	1.47	6.88	1.46	–0.485
5	8.33	6.81	2.55	1.60	2.61	1.44	6.74	1.43	–0.474
6	8.30	6.75	2.52	1.58	2.58	1.42	6.66	1.41	–0.467
7	8.28	6.71	2.49	1.56	2.56	1.41	6.60	1.40	–0.462
8	8.26	6.68	2.48	1.55	2.54	1.40	6.54	1.39	–0.458

Table 19. Values of Load Factor $L_2 = \dfrac{\hat{\alpha}_2}{\hat{\alpha}_1}$ for $[(\pm 45/0/90)_m]_s$ Laminates (see fig. 18)

m*	Material systems								
	Boron-Al	S-glass-epoxy	Kevlar 49-epoxy	IM7/5260	AS4/3502	AS4/3501-6	Boron-epoxy	IM7/PETI-5	P-100/3502
1	1.02	1.08	1.14	1.14	1.13	1.13	1.13	1.14	1.17
2	1.02	1.06	1.09	1.09	1.08	1.09	1.09	1.09	1.11
3	1.01	1.04	1.06	1.06	1.06	1.06	1.06	1.07	1.07
4	1.01	1.03	1.05	1.05	1.05	1.05	1.05	1.05	1.06
5	1.01	1.03	1.04	1.04	1.04	1.04	1.04	1.04	1.05
6	1.01	1.02	1.03	1.03	1.03	1.03	1.03	1.03	1.04
7	1.01	1.02	1.03	1.03	1.03	1.03	1.03	1.03	1.03
8	1.00	1.02	1.02	1.03	1.02	1.02	1.02	1.03	1.03

*$L_1 = 1$, $L_3 = 0$, and $N_{y1} = N_{x1}^c$ (see discussion of eqs. (47)–(52)).

Table 20. Values of $\beta = \dfrac{D_{12} + 2D_{66}}{\sqrt{D_{11}D_{22}}}$ for $[(\pm 45/0/90)_m]_s$ Laminates (see ref. 5, fig. 20)

m	Material systems								
	Boron-Al	S-glass-epoxy	Kevlar 49-epoxy	IM7/5260	AS4/3502	AS4/3501-6	Boron-epoxy	IM7/PETI-5	P-100/3502
1	1.28	1.57	2.02	1.98	1.90	1.89	2.05	2.04	2.21
2	1.14	1.26	1.45	1.44	1.40	1.40	1.46	1.46	1.53
3	1.09	1.17	1.29	1.28	1.26	1.26	1.30	1.29	1.33
4	1.07	1.13	1.21	1.21	1.19	1.19	1.22	1.22	1.24
5	1.05	1.10	1.17	1.16	1.15	1.15	1.17	1.17	1.19
6	1.04	1.08	1.14	1.13	1.13	1.12	1.14	1.14	1.16
7	1.04	1.07	1.12	1.11	1.11	1.11	1.12	1.12	1.14
8	1.03	1.06	1.10	1.10	1.09	1.09	1.11	1.11	1.12

Table 21. Values of $\gamma = \frac{D_{16}}{\left(D_{11}^3 D_{22}\right)^{1/4}}$ for $[(\pm 45/0/90)_m]_s$ Laminates (see ref. 5, fig. 21)

m	Material systems								
	Boron-Al	S-glass-epoxy	Kevlar 49-epoxy	IM7/5260	AS4/3502	AS4/3501-6	Boron-epoxy	IM7/PETI-5	P-100/3502
1	.036	.114	.182	.182	.170	.176	.178	.189	.217
2	.015	.045	.069	.069	.065	.067	.067	.071	.080
3	.009	.027	.042	.042	.039	.041	.040	.043	.048
4	.006	.020	.030	.030	.028	.029	.029	.031	.035
5	.005	.015	.023	.023	.022	.023	.022	.024	.027
6	.004	.013	.019	.019	.018	.019	.018	.020	.022
7	.003	.011	.016	.016	.015	.016	.016	.017	.019
8	.003	.009	.014	.014	.013	.014	.013	.014	.016

Table 22. Values of $\delta = \frac{D_{26}}{\left(D_{11} D_{22}^3\right)^{1/4}}$ for $[(\pm 45/0/90)_m]_s$ Laminates (see ref. 5, fig. 22)

m	Material systems								
	Boron-Al	S-glass-epoxy	Kevlar 49-epoxy	IM7/5260	AS4/3502	AS4/3501-6	Boron-epoxy	IM7/PETI-5	P-100/3502
1	.037	.123	.207	.207	.191	.200	.202	.216	.253
2	.015	.047	.075	.075	.070	.073	.073	.078	.089
3	.009	.028	.044	.044	.042	.044	.043	.046	.052
4	.007	.020	.031	.031	.029	.031	.030	.032	.037
5	.005	.016	.024	.024	.023	.024	.023	.025	.028
6	.004	.013	.020	.020	.018	.019	.019	.020	.023
7	.004	.011	.016	.017	.016	.016	.016	.017	.019
8	.003	.009	.014	.014	.013	.014	.014	.015	.017

Table 23. Values of $\left(\frac{D_{11}}{D_{22}}\right)^{1/4}$ for $[(\pm 45/0/90)_m]_s$ Laminates

m	Material systems								
	Boron-Al	S-glass-epoxy	Kevlar 49-epoxy	IM7/5260	AS4/3502	AS4/3501-6	Boron-epoxy	IM7/PETI-5	P-100/3502
1	1.01	1.04	1.07	1.07	1.06	1.06	1.07	1.07	1.08
2	1.01	1.03	1.04	1.04	1.04	1.04	1.04	1.05	1.05
3	1.01	1.02	1.03	1.03	1.03	1.03	1.03	1.03	1.04
4	1.01	1.02	1.02	1.02	1.02	1.02	1.02	1.02	1.03
5	1.00	1.01	1.02	1.02	1.02	1.02	1.02	1.02	1.02
6	1.00	1.01	1.02	1.02	1.02	1.02	1.02	1.02	1.02
7	1.00	1.01	1.01	1.01	1.01	1.01	1.01	1.01	1.02
8	1.00	1.01	1.01	1.01	1.01	1.01	1.01	1.01	1.01

Table 24. Values of Stiffness-Weighted Laminate Thermal-Expansion Parameter $\hat{\alpha}_1 \times 10^6$/°F for $[(\pm\theta)_m]_s$ and $[(+\theta)_{2m}]_s$ Laminates With m = 1, 2, ... (see fig. 19)

θ, deg	Material systems								
	Boron-Al	S-glass-epoxy	Kevlar 49-epoxy	IM7/5260	AS4/3502	AS4/3501-6	Boron-epoxy	IM7/PETI-5	P-100/3502
0	6.03	8.66	–4.22	1.04	2.29	.538	12.4	.580	–4.86
5	6.08	8.67	–4.12	1.06	2.31	.563	12.4	.609	–4.78
10	6.23	8.70	–3.81	1.13	2.39	.638	12.5	.692	–4.47
15	6.48	8.73	–3.24	1.23	2.50	.752	12.6	.817	–3.84
20	6.82	8.72	–2.41	1.35	2.62	.891	12.3	.967	–3.03
25	7.22	8.65	–1.38	1.46	2.72	1.04	11.8	1.12	–2.28
30	7.67	8.50	–.245	1.56	2.81	1.19	11.0	1.27	–1.69
35	8.12	8.28	.901	1.68	2.90	1.36	10.1	1.42	–1.24
40	8.56	8.02	2.04	1.82	3.03	1.54	9.27	1.60	–.900
45	8.93	7.74	3.22	1.99	3.20	1.75	8.58	1.81	–.622
50	9.23	7.46	4.46	2.22	3.43	2.01	8.06	2.08	–.373
55	9.42	7.17	5.82	2.50	3.71	2.31	7.66	2.40	–.126
60	9.53	6.88	7.27	2.82	4.03	2.66	7.32	2.78	.148
65	9.55	6.59	8.71	3.16	4.35	3.03	6.96	3.19	.479
70	9.53	6.30	9.95	3.46	4.60	3.38	6.54	3.56	.886
75	9.47	6.04	10.8	3.67	4.76	3.66	6.08	3.82	1.33
80	9.42	5.83	11.3	3.78	4.83	3.84	5.67	3.95	1.71
85	9.38	5.70	11.6	3.82	4.84	3.94	5.40	4.00	1.92
90	9.36	5.65	11.6	3.83	4.85	3.96	5.30	4.01	1.99

Table 25. Values of Stiffness-Weighted Laminate Thermal-Expansion Parameter $\hat{\alpha}_2 \times 10^6$/°F for $[(\pm\theta)_m]_s$ and $[(+\theta)_{2m}]_s$ Laminates With m = 1, 2, ... (see fig. 20)

θ, deg	Material systems								
	Boron-Al	S-glass-epoxy	Kevlar 49-epoxy	IM7/5260	AS4/3502	AS4/3501-6	Boron-epoxy	IM7/PETI-5	P-100/3502
0	11.7	11.9	43.1	14.9	16.3	15.5	17.6	16.8	17.0
5	11.7	11.9	42.6	14.7	16.1	15.2	17.8	16.6	16.2
10	11.7	11.9	40.5	14.0	15.5	14.2	18.3	15.8	13.3
15	11.6	11.9	36.4	12.7	14.4	12.5	18.7	14.2	8.73
20	11.5	11.6	30.0	10.6	12.6	10.1	18.5	11.7	4.46
25	11.2	11.2	22.4	8.21	10.3	7.66	17.2	8.76	1.76
30	10.8	10.5	15.3	5.95	7.96	5.47	15.0	6.12	.391
35	10.3	9.64	9.70	4.16	5.93	3.78	12.6	4.11	–.240
40	9.66	8.68	5.78	2.87	4.35	2.58	10.4	2.73	–.514
45	8.93	7.74	3.22	1.99	3.20	1.75	8.58	1.81	–.622
50	8.17	6.89	1.58	1.40	2.38	1.20	7.19	1.22	–.654
55	7.43	6.16	.540	1.01	1.82	.830	6.14	.833	–.653
60	6.75	5.56	–.116	.740	1.42	.580	5.36	.578	–.638
65	6.16	5.09	–.534	.559	1.15	.411	4.79	.408	–.620
70	5.67	4.72	–.799	.437	.956	.297	4.37	.294	–.602
75	5.29	4.45	–.965	.356	.826	.221	4.08	.220	–.587
80	5.02	4.27	–1.07	.304	.743	.172	3.88	.173	–.576
85	4.86	4.16	–1.12	.275	.696	.146	3.77	.147	–.570
90	4.81	4.12	–1.14	.266	.681	.137	3.73	.139	–.567

Table 26. Values of Stiffness-Weighted Laminate Thermal-Expansion Parameter $\hat{\alpha}_3 \times 10^6/°F$ for $[(+\theta)_{2m}]_s$ Laminates With $m = 1, 2, ...$ (see fig. 21)

θ, deg	Material systems								
	Boron-Al	S-glass-epoxy	Kevlar 49-epoxy	IM7/5260	AS4/3502	AS4/3501-6	Boron-epoxy	IM7/PETI-5	P-100/3502
0	0	0	0	0	0	0	0	0	0
5	.325	–.379	2.65	.478	.407	.585	–1.13	.609	1.71
10	.646	–.746	5.21	.929	.795	1.12	–2.24	1.19	3.13
15	.956	–1.09	7.45	1.31	1.13	1.55	–3.28	1.67	3.82
20	1.25	–1.38	9.01	1.55	1.38	1.81	–4.09	1.97	3.69
25	1.51	–1.60	9.65	1.64	1.49	1.89	–4.52	2.04	3.15
30	1.72	–1.73	9.44	1.58	1.49	1.82	–4.56	1.94	2.58
35	1.87	–1.77	8.72	1.45	1.41	1.68	–4.29	1.76	2.11
40	1.94	–1.73	7.80	1.30	1.28	1.51	–3.88	1.55	1.75
45	1.93	–1.63	6.88	1.14	1.15	1.33	–3.44	1.36	1.48
50	1.85	–1.48	6.02	1.00	1.01	1.17	–3.01	1.18	1.27
55	1.71	–1.32	5.23	.872	.882	1.03	–2.61	1.03	1.11
60	1.51	–1.13	4.48	.749	.756	.886	–2.22	.885	.978
65	1.28	–.940	3.74	.629	.630	.746	–1.84	.744	.857
70	1.04	–.746	2.99	.505	.503	.603	–1.45	.599	.733
75	.780	–.554	2.22	.378	.374	.455	–1.06	.449	.584
80	.520	–.366	1.46	.250	.247	.303	–.695	.297	.404
85	.260	–.182	.721	.124	.122	.151	–.342	.147	.204
90	0	0	0	0	0	0	0	0	0

Table 27. Values of $\frac{N_{y1}}{N_{x1}^c}$ for $[(\pm\theta)_m]_s$ and $[(+\theta)_{2m}]_s$ Laminates ($m = 1, 2, ...$)

θ, deg	Material systems								
	Boron-Al	S-glass-epoxy	Kevlar 49-epoxy	IM7/5260	AS4/3502	AS4/3501-6	Boron-epoxy	IM7/PETI-5	P-100/3502
0	1.55	.653	–2.75	3.69	2.12	7.37	.428	6.92	–.409
5	1.54	.657	–2.81	3.60	2.09	6.99	.434	6.58	–.403
10	1.51	.670	–2.98	3.34	2.02	6.02	.453	5.72	–.383
15	1.46	.692	–3.34	2.98	1.90	4.87	.485	4.67	–.347
20	1.40	.723	–4.13	2.57	1.76	3.80	.530	3.68	–.292
25	1.32	.762	–6.33	2.17	1.60	2.92	.590	2.85	–.210
30	1.24	.810	–29.6	1.81	1.44	2.23	.666	2.19	–.088
35	1.16	.866	6.46	1.49	1.28	1.70	.759	1.69	.102
40	1.08	.930	2.18	1.22	1.13	1.30	.870	1.30	.415
45	1.00	1.00	1.00	1.00	1.00	1.00	1.00	1.00	1.00
50	.928	1.08	.458	.819	.883	.767	1.15	.770	2.41
55	.862	1.15	.155	.672	.781	.587	1.32	.593	9.83
60	.805	1.23	–.033	.554	.696	.449	1.50	.456	–11.4
65	.756	1.31	–.158	.461	.625	.343	1.69	.351	–4.76
70	.715	1.38	–.242	.389	.569	.263	1.89	.272	–3.42
75	.684	1.44	–.299	.336	.526	.206	2.06	.214	–2.88
80	.662	1.49	–.336	.299	.496	.166	2.21	.175	–2.61
85	.649	1.52	–.356	.278	.478	.143	2.31	.152	–2.48
90	.644	1.53	–.363	.271	.472	.136	2.34	.145	–2.45

Table 28. Values of $\frac{N_{xy1}}{N^c_{x1}}$ for $[(+\theta)_{2m}]_s$ Laminates (m = 1, 2, ...)

θ, deg	Material systems								
	Boron-Al	S-glass-epoxy	Kevlar 49-epoxy	IM7/5260	AS4/3502	AS4/3501-6	Boron-epoxy	IM7/PETI-5	P-100/3502
0	0	0	0	0	0	0	0	0	0
5	.048	–.030	–.336	.229	.096	.523	–.050	.492	–.124
10	.093	–.060	–.724	.426	.185	.914	–.100	.859	–.252
15	.133	–.089	–1.25	.571	.260	1.12	–.149	1.06	–.389
20	.167	–.116	–2.15	.659	.318	1.17	–.197	1.12	–.542
25	.193	–.142	–4.37	.697	.357	1.14	–.244	1.10	–.721
30	.210	–.165	–26.5	.697	.379	1.06	–.289	1.03	–.942
35	.220	–.184	7.50	.671	.384	.967	–.331	.943	–1.23
40	.222	–.200	3.35	.628	.377	.864	–.369	.846	–1.66
45	.217	–.210	2.14	.574	.359	.761	–.401	.747	–2.38
50	.205	–.215	1.54	.514	.333	.662	–.424	.652	–4.01
55	.189	–.213	1.16	.451	.300	.568	–.437	.559	–12.1
60	.169	–.203	.895	.386	.264	.477	–.434	.471	10.8
65	.146	–.186	.690	.321	.223	.392	–.414	.387	3.43
70	.119	–.161	.521	.256	.181	.309	–.372	.306	1.85
75	.091	–.128	.375	.192	.137	.229	–.307	.227	1.12
80	.062	–.090	.243	.128	.092	.152	–.220	.150	.658
85	.031	–.046	.120	.064	.046	.076	–.115	.075	.307
90	0	0	0	0	0	0	0	0	0

Table 29. Values of $\beta = \frac{D_{12} + 2D_{66}}{\sqrt{D_{11}D_{22}}}$ for $[(\pm\theta)_m]_s$ and $[(+\theta)_{2m}]_s$ Laminates With m = 1, 2, ... (see ref. 5, fig. 25)

θ, deg	Material systems								
	Boron-Al	S-glass-epoxy	Kevlar 49-epoxy	IM7/5260	AS4/3502	AS4/3501-6	Boron-epoxy	IM7/PETI-5	P-100/3502
0	.697	.561	.312	.368	.403	.478	.250	.319	.279
5	.715	.596	.390	.447	.469	.551	.324	.406	.460
10	.768	.699	.617	.674	.661	.757	.539	.659	.954
15	.851	.860	.966	1.02	.954	1.06	.880	1.04	1.57
20	.957	1.06	1.38	1.41	1.30	1.40	1.30	1.47	2.09
25	1.08	1.28	1.77	1.77	1.64	1.72	1.72	1.86	2.42
30	1.19	1.48	2.09	2.06	1.92	1.96	2.08	2.16	2.60
35	1.29	1.65	2.30	2.26	2.12	2.13	2.33	2.36	2.70
40	1.36	1.75	2.42	2.36	2.24	2.23	2.47	2.46	2.74
45	1.38	1.79	2.46	2.40	2.28	2.26	2.51	2.50	2.76
50	1.36	1.75	2.42	2.36	2.24	2.23	2.47	2.46	2.74
55	1.29	1.65	2.30	2.26	2.12	2.13	2.33	2.36	2.70
60	1.19	1.48	2.09	2.06	1.92	1.96	2.78	2.16	2.60
65	1.08	1.28	1.77	1.77	1.64	1.72	1.72	1.86	2.42
70	.957	1.06	1.38	1.41	1.30	1.40	1.30	1.47	2.09
75	.851	.860	.966	1.02	.954	1.06	.880	1.04	1.57
80	.768	.699	.617	.674	.661	.757	.539	.659	.954
85	.715	.596	.390	.447	.469	.551	.324	.406	.460
90	.697	.561	.312	.368	.403	.478	.250	.319	.279

Table 30. Values of $\gamma = \frac{D_{16}}{\left(D_{11}^3 D_{22}\right)^{1/4}}$ for $[\pm\theta]_s$ Laminates (see ref. 5, fig. 26)

θ, deg	Material systems								
	Boron-Al	S-glass-epoxy	Kevlar 49-epoxy	IM7/5260	AS4/3502	AS4/3501-6	Boron-epoxy	IM7/PETI-5	P-100/3502
0	0	0	0	0	0	0	0	0	0
5	.032	.069	.115	.116	.105	.113	.110	.123	.184
10	.063	.136	.228	.230	.208	.222	.219	.243	.356
15	.090	.199	.333	.335	.303	.322	.322	.355	.496
20	.112	.255	.425	.424	.386	.405	.414	.449	.589
25	.127	.300	.496	.493	.452	.469	.488	.519	.642
30	.133	.332	.543	.538	.497	.512	.538	.565	.670
35	.131	.348	.568	.562	.522	.536	.564	.589	.683
40	.119	.347	.574	.569	.527	.544	.567	.595	.688
45	.099	.329	.561	.558	.515	.536	.549	.585	.686
50	.075	.295	.528	.530	.483	.512	.509	.557	.676
55	.049	.248	.474	.482	.431	.471	.443	.510	.657
60	.025	.193	.394	.410	.358	.410	.352	.437	.621
65	.006	.137	.293	.317	.269	.330	.243	.338	.557
70	−.007	.088	.186	.213	.177	.238	.136	.225	.449
75	−.012	.049	.094	.119	.098	.149	.055	.122	.296
80	−.012	.024	.035	.053	.044	.079	.010	.051	.140
85	−.007	.009	.009	.018	.015	.032	−.003	.015	.042
90	0	0	0	0	0	0	0	0	0

Table 31. Values of $\delta = \frac{D_{26}}{\left(D_{11} D_{22}^3\right)^{1/4}}$ for $[\pm\theta]_s$ Laminates (see ref. 5, fig. 27)

θ, deg	Material systems								
	Boron-Al	S-glass-epoxy	Kevlar 49-epoxy	IM7/5260	AS4/3502	AS4/3501-6	Boron-epoxy	IM7/PETI-5	P-100/3502
0	0	0	0	0	0	0	0	0	0
5	−.007	.009	.009	.018	.015	.032	−.003	.015	.042
10	−.012	.024	.035	.053	.044	.079	.010	.051	.140
15	−.012	.049	.094	.119	.098	.149	.055	.122	.296
20	−.007	.088	.186	.213	.177	.238	.136	.225	.449
25	.006	.137	.293	.317	.269	.330	.243	.338	.557
30	.025	.193	.394	.410	.358	.410	.352	.437	.621
35	.049	.248	.474	.482	.431	.471	.443	.510	.657
40	.075	.295	.528	.530	.483	.512	.509	.557	.676
45	.099	.329	.561	.558	.515	.536	.549	.585	.686
50	.119	.347	.574	.569	.527	.544	.567	.595	.688
55	.131	.348	.568	.562	.522	.536	.564	.589	.683
60	.133	.332	.543	.538	.497	.512	.538	.565	.670
65	.127	.300	.496	.493	.452	.469	.488	.519	.642
70	.112	.255	.425	.424	.386	.405	.414	.449	.589
75	.090	.199	.333	.335	.303	.322	.322	.355	.496
80	.063	.136	.228	.230	.208	.222	.219	.243	.356
85	.032	.069	.115	.116	.105	.113	.110	.123	.184
90	0	0	0	0	0	0	0	0	0

Table 32. Values of $\left(\frac{D_{11}}{D_{22}}\right)^{1/4}$ for $[(\pm\theta)_m]_s$ and $[(+\theta)_{2m}]_s$ Laminates (m = 1, 2, ...)

θ, deg	Material systems								
	Boron-Al	S-glass-epoxy	Kevlar 49-epoxy	IM7/5260	AS4/3502	AS4/3501-6	Boron-epoxy	IM7/PETI-5	P-100/3502
0	1.12	1.45	1.93	1.97	1.83	1.98	1.82	2.05	2.93
5	1.12	1.44	1.92	1.96	1.82	1.97	1.82	2.04	2.90
10	1.11	1.43	1.89	1.93	1.80	1.92	1.80	2.00	2.79
15	1.11	1.40	1.83	1.86	1.74	1.85	1.76	1.93	2.56
20	1.10	1.36	1.74	1.75	1.65	1.73	1.68	1.81	2.24
25	1.08	1.30	1.61	1.61	1.54	1.59	1.57	1.66	1.92
30	1.07	1.24	1.45	1.45	1.41	1.43	1.43	1.48	1.63
35	1.05	1.16	1.29	1.29	1.26	1.28	1.28	1.31	1.38
40	1.02	1.08	1.14	1.14	1.13	1.13	1.14	1.15	1.17
45	1.00	1.00	1.00	1.00	1.00	1.00	1.00	1.00	1.00
50	.977	.927	.878	.879	.888	.883	.881	.873	.852
55	.957	.863	.774	.775	.791	.782	.780	.765	.725
60	.939	.809	.689	.688	.712	.697	.698	.675	.615
65	.924	.767	.623	.620	.650	.629	.637	.604	.522
70	.912	.736	.576	.570	.604	.577	.595	.552	.446
75	.903	.714	.546	.538	.575	.542	.570	.519	.391
80	.898	.700	.529	.519	.557	.520	.556	.500	.359
85	.894	.692	.521	.509	.548	.508	.550	.491	.345
90	.893	.690	.519	.507	.546	.505	.549	.489	.342

Table 33. Values of $\gamma = \frac{D_{16}}{\left(D_{11}^3 D_{22}\right)^{1/4}}$ for $[(+\theta)_{2m}]_s$ Laminates With m = 1, 2, ... (see fig. 22)

θ, deg	Material systems								
	Boron-Al	S-glass-epoxy	Kevlar 49-epoxy	IM7/5260	AS4/3502	AS4/3501-6	Boron-epoxy	IM7/PETI-5	P-100/3502
0	0	0	0	0	0	0	0	0	0
5	.043	.092	.154	.155	.140	.151	.147	.164	.245
10	.084	.182	.304	.306	.277	.296	.292	.325	.475
15	.120	.266	.445	.446	.404	.429	.429	.473	.661
20	.149	.340	.567	.566	.515	.540	.552	.598	.785
25	.169	.400	.661	.657	.603	.625	.650	.692	.856
30	.178	.443	.724	.717	.663	.682	.717	.753	.893
35	.174	.464	.758	.750	.696	.715	.752	.785	.911
40	.158	.463	.765	.758	.703	.725	.757	.793	.917
45	.132	.439	.747	.744	.686	.715	.733	.780	.914
50	.099	.394	.704	.707	.644	.683	.679	.743	.902
55	.065	.331	.631	.642	.574	.628	.591	.679	.876
60	.033	.258	.526	.547	.477	.547	.469	.582	.828
65	.008	.183	.391	.422	.359	.440	.323	.451	.743
70	−.009	.117	.248	.284	.236	.317	.181	.300	.599
75	−.016	.066	.126	.159	.131	.199	.073	.163	.394
80	−.016	.032	.047	.071	.059	.105	.014	.067	.187
85	−.009	.012	.011	.023	.020	.042	−.004	.019	.056
90	0	0	0	0	0	0	0	0	0

Table 34. Values of $\delta = \frac{D_{26}}{\left(D_{11}D_{22}^3\right)^{1/4}}$ for $[(+\theta)_{2m}]_s$ Laminates With m = 1, 2, ... (see fig. 23)

θ, deg	Material systems								
	Boron-Al	S-glass-epoxy	Kevlar 49-epoxy	IM7/ 5260	AS4/ 3502	AS4/ 3501-6	Boron-epoxy	IM7/ PETI-5	P-100/ 3502
0	0	0	0	0	0	0	0	0	0
5	−.009	.012	.011	.023	.020	.042	−.004	.019	.056
10	−.016	.032	.047	.071	.059	.105	.014	.067	.187
15	−.016	.066	.126	.159	.131	.199	.073	.163	.394
20	−.009	.117	.248	.284	.236	.317	.181	.300	.599
25	.008	.183	.391	.422	.359	.440	.323	.451	.743
30	.033	.258	.526	.547	.477	.547	.469	.582	.828
35	.065	.331	.631	.642	.574	.628	.591	.679	.876
40	.099	.394	.704	.707	.644	.683	.679	.743	.902
45	.132	.439	.747	.744	.686	.715	.733	.780	.914
50	.158	.463	.765	.758	.703	.725	.757	.793	.917
55	.174	.464	.758	.750	.696	.715	.752	.785	.911
60	.178	.443	.724	.717	.663	.682	.717	.753	.893
65	.169	.400	.661	.657	.603	.625	.650	.692	.856
70	.149	.340	.567	.566	.515	.540	.552	.598	.785
75	.120	.266	.445	.446	.404	.429	.429	.473	.661
80	.084	.182	.304	.306	.277	.296	.292	.325	.475
85	.043	.092	.154	.155	.140	.151	.147	.164	.245
90	0	0	0	0	0	0	0	0	0

Table 35. Values of Buckling Coefficient K_x for Plates Subjected to Axial Compression and Transverse Tension or Compression Loads ($\gamma = \delta = 0$, see fig. 26)

Buckling coefficient, K_x												
*L_2	Simply supported edges						Clamped edges					
	Orthotropy parameter, β						Orthotropy parameter, β					
	0.5	1	1.5	2	2.5	3	0.5	1	1.5	2	2.5	3
−1.0	6.47	8.00	9.47	10.9	12.3	13.7	9.20	10.8	12.3	13.8	15.2	16.6
−0.9	6.09	7.60	9.05	10.5	11.8	13.2	8.84	10.4	11.9	13.3	14.8	16.1
−0.8	5.72	7.20	8.62	10.0	11.3	12.7	8.47	10.0	11.5	12.9	14.3	15.7
−0.7	5.36	6.80	8.19	9.54	10.9	12.2	8.12	9.61	11.1	12.5	13.8	15.2
−0.6	5.00	6.40	7.76	9.08	10.4	11.7	7.76	9.23	10.6	12.0	13.4	14.7
−0.5	4.65	6.00	7.32	8.61	9.87	11.1	7.41	8.84	10.2	11.6	12.9	14.2
−0.4	4.30	5.60	6.87	8.12	9.36	10.6	7.07	8.46	9.82	11.1	12.5	13.7
−0.3	3.96	5.20	6.42	7.63	8.82	10.0	6.73	8.08	9.41	10.7	12.0	13.2
−0.2	3.63	4.80	5.96	7.11	8.26	9.39	6.40	7.71	8.99	10.3	11.5	12.7
−0.1	3.31	4.40	5.49	6.57	7.66	8.74	6.08	7.34	8.58	9.80	11.0	12.2
0	3.00	4.00	5.00	6.00	7.00	8.00	5.77	6.97	8.16	9.33	10.5	11.6
0.1	2.71	3.60	4.49	5.36	6.23	7.08	5.46	6.61	7.74	8.86	9.97	11.1
0.2	2.43	3.20	3.93	4.58	5.00	5.00	5.17	6.26	7.33	8.38	9.43	10.5
0.3	2.18	2.80	3.27	3.33	3.33	3.33	4.89	5.91	6.91	7.89	8.86	9.80
0.4	1.94	2.40	2.50	2.50	2.50	2.5	4.62	5.57	6.49	7.38	8.24	9.05
0.5	1.73	2.00	2.00	2.00	2.00	2.00	4.36	5.23	6.07	6.85	7.55	8.00
0.6	1.54	1.67	1.67	1.67	1.67	1.67	4.11	4.91	5.65	6.29	6.67	6.67
0.7	1.38	1.43	1.43	1.43	1.43	1.43	3.88	4.60	5.23	5.67	5.71	5.71
0.8	1.23	1.25	1.25	1.25	1.25	1.25	3.66	4.31	4.82	5.00	5.00	5.00
0.9	1.11	1.11	1.11	1.11	1.11	1.11	3.46	4.02	4.40	4.44	4.44	4.44
1.0	1.00	1.00	1.00	1.00	1.00	1.00	3.27	3.76	4.00	4.00	4.00	4.00
1.1	0.91	0.91	0.91	0.91	0.91	0.91	3.09	3.51	3.64	3.64	3.64	3.64
1.2	0.83	0.83	0.83	0.83	0.83	0.83	2.92	3.27	3.33	3.33	3.33	3.33
1.3	0.77	0.77	0.77	0.77	0.77	0.77	2.77	3.05	3.08	3.08	3.08	3.08
1.4	0.71	0.71	0.71	0.71	0.71	0.71	2.63	2.85	2.86	2.86	2.86	2.86
1.5	0.67	0.67	0.67	0.67	0.67	0.67	2.49	2.67	2.67	2.67	2.67	2.67

* $L_2 = \frac{N_{y1}}{N^c_{x1}}\left(\frac{D_{11}}{D_{22}}\right)^{1/2}$ and $K_y = L_2 K_x$.

Table 36. Values of Buckling Coefficient K_x for Plates Subjected to Axial Compression and Transverse Tension or Compression Loads ($\gamma = \delta = 0$, see fig. 27)

Buckling coefficient, K_x												
*L_2	Simply supported edges						Clamped edges					
	Orthotropy parameter, β						Orthotropy parameter, β					
	0.5	1	1.5	2	2.5	3	0.5	1	1.5	2	2.5	3
−10	42.1	44.0	45.9	47.8	49.6	51.4	45.0	46.9	48.8	50.7	52.6	54.4
−9	38.1	40.0	41.9	43.8	45.6	47.3	40.9	42.8	44.7	46.6	48.5	50.3
−8	34.1	36.0	37.9	39.7	41.5	43.3	36.9	38.8	40.7	42.5	44.4	46.2
−7	30.1	32.0	33.9	35.7	37.4	39.2	32.8	34.7	36.6	38.4	40.2	42.0
−6	26.1	28.0	29.8	31.6	33.4	35.1	28.8	30.7	32.6	34.4	36.2	37.9
−5	22.1	24.0	25.8	27.6	29.3	31.0	24.8	26.7	28.5	30.3	32.0	33.7
−4	18.2	20.0	21.8	23.5	25.2	26.8	20.8	22.7	24.5	26.2	27.9	29.6
−3	14.2	16.0	17.7	19.4	21.0	22.6	16.9	18.7	20.4	22.1	23.7	25.4
−2	10.3	12.0	13.6	15.2	16.7	18.2	13.0	14.7	16.4	18.0	19.5	21.0
−1	6.47	8.00	9.47	10.9	12.3	13.7	9.20	10.8	12.3	13.7	15.2	16.6

* $L_2 = \frac{N_{y1}}{N^c_{x1}}\left(\frac{D_{11}}{D_{22}}\right)^{1/2}$ and $K_y = L_2 K_x$.

Table 37. Buckling Coefficient Ratio for Simply Supported Plates Subjected to Axial Compression and Transverse Tension or Compression Loads and With $\gamma = \delta = 0.1$ or 0.2 (see figs. 28 and 29)

Buckling coefficient ratio, $\frac{K_x}{K_x\vert_{\gamma=\delta=0}}$														
β	$\gamma = \delta = 0.1$							$\gamma = \delta = 0.2$						
	Load factor, L_2							Load factor, L_2						
	−10	−4	−2	−1	−0.5	0	0.1	−10	−4	−2	−1	−0.5	0	0.1
3	.999	.997	.996	.996	.995	.993	.993	.994	.990	.986	.982	.979	.974	.972
2.8	.999	.997	.996	.995	.994	.993	.993	.994	.989	.985	.980	.977	.971	.970
2.6	.998	.997	.996	.995	.994	.992	.992	.994	.988	.983	.979	.975	.969	.968
2.4	.998	.997	.996	.994	.993	.991	.991	.994	.988	.982	.977	.972	.966	.965
2.2	.998	.997	.995	.994	.992	.991	.990	.994	.987	.981	.974	.969	.962	.961
2	.998	.997	.995	.993	.991	.990	.989	.993	.986	.979	.971	.965	.958	.957
1.8	.998	.996	.994	.992	.990	.988	.988	.993	.985	.977	.968	.961	.953	.953
1.6	.998	.996	.994	.991	.989	.987	.987	.993	.984	.974	.964	.955	.947	.947
1.4	.998	.996	.993	.990	.987	.985	.985	.992	.983	.971	.959	.949	.940	.940
1.2	.998	.995	.992	.988	.985	.983	.983	.992	.981	.967	.952	.941	.931	.932
1	.998	.995	.991	.986	.983	.980	.981	.992	.979	.963	.944	.930	.920	.921
0.8	.998	.994	.990	.984	.980	.977	.977	.991	.978	.957	.934	.917	.906	.907
0.6	.998	.994	.988	.981	.975	.973	.973	.991	.975	.951	.920	.899	.887	.889
0.4	.998	.993	.986	.976	.970	.967	.967	.990	.972	.942	.901	.873	.862	.864
0.2	.997	.992	.983	.970	.961	.958	.959	.990	.969	.929	.873	.837	.827	.830

Table 38. Buckling Coefficient Ratio for Simply Supported Plates Subjected to Axial Compression and Transverse Tension or Compression Loads and With $\gamma = \delta = 0.3$ or 0.4 (see figs. 28 and 29)

Buckling coefficient ratio, $\frac{K_x}{K_x\vert_{\gamma=\delta=0}}$														
β	$\gamma = \delta = 0.3$							$\gamma = \delta = 0.4$						
	Load factor, L_2							Load factor, L_2						
	−10	−4	−2	−1	−0.5	0	0.1	−10	−4	−2	−1	−0.5	0	0.1
3	.987	.977	.967	.959	.952	.940	.937	.977	.958	.941	.926	.913	.892	.888
2.8	.987	.975	.965	.955	.947	.935	.932	.976	.955	.937	.919	.905	.882	.878
2.6	.986	.973	.962	.951	.942	.929	.927	.975	.952	.932	.911	.895	.871	.868
2.4	.985	.972	.959	.946	.936	.922	.920	.974	.949	.925	.902	.883	.858	.855
2.2	.985	.970	.955	.940	.929	.913	.912	.973	.946	.918	.891	.869	.843	.841
2	.985	.968	.951	.934	.920	.904	.903	.972	.942	.910	.878	.853	.825	.824
1.8	.984	.965	.946	.925	.909	.892	.892	.971	.937	.900	.862	.833	.804	.803
1.6	.983	.963	.940	.916	.897	.878	.879	.970	.931	.889	.843	.808	.778	.778
1.4	.982	.960	.933	.903	.881	.862	.862	.968	.926	.874	.818	.777	.745	.747
1.2	.982	.956	.924	.888	.861	.841	.842	.967	.920	.857	.786	.736	.705	.707
1	.981	.952	.913	.868	.835	.814	.816	.965	.911	.834	.743	.682	.651	.655
0.8	.980	.947	.899	.842	.801	.780	.783	.964	.901	.804	.682	.606	.578	.583
0.6	.979	.942	.882	.805	.754	.734	.737	.962	.890	.762	.583	.484	.465	.471
0.4	.978	.934	.857	.751	.687	.669	.673							
0.2	.977	.926	.822	.664	.579	.568	.574							

Table 39. Buckling Coefficient Ratio for Simply Supported Plates Subjected to Axial Compression and Transverse Tension or Compression Loads and With $\gamma = \delta = 0.5$ or 0.6 (see figs. 28 and 29)

Buckling coefficient ratio, $\frac{K_x}{K_x\vert_{\gamma=\delta=0}}$														
β	$\gamma = \delta = 0.5$							$\gamma = \delta = 0.6$						
	Load factor, L_2							Load factor, L_2						
	−10	−4	−2	−1	−0.5	0	0.1	−10	−4	−2	−1	−0.5	0	0.1
3	.963	.933	.906	.881	.861	.828	.822	.946	.900	.859	.822	.792	.747	.739
2.8	.962	.929	.898	.869	.847	.812	.807	.944	.894	.848	.804	.770	.723	.716
2.6	.960	.923	.889	.856	.830	.794	.790	.942	.886	.833	.783	.744	.695	.690
2.4	.959	.918	.879	.841	.810	.773	.770	.939	.878	.816	.758	.713	.662	.658
2.2	.957	.913	.867	.822	.787	.748	.746	.937	.868	.797	.726	.674	.622	.620
2	.956	.906	.853	.799	.759	.718	.717	.934	.857	.773	.687	.626	.574	.573
1.8	.954	.898	.836	.771	.723	.681	.681	.932	.845	.742	.635	.562	.512	.513
1.6	.952	.889	.814	.735	.678	.636	.637	.929	.829	.703	.562	.474	.429	.432
1.4	.950	.879	.788	.687	.619	.578	.581	.926	.812	.646	.436	.319	.285	.289
1.2	.947	.867	.753	.620	.536	.499	.503							
1	.945	.852	.703	.508	.399	.371	.376							

Table 40. Values of Buckling Coefficient K_x for Simply Supported Plates Subjected to Axial Compression, Transverse Tension or Compression, and Shear Loads ($\gamma = \delta = 0$, see figs. 31 and 32)

Buckling coefficient, K_x*												
L_2	Shear load factor, $L_3 = \pm 0.5$						Shear load factor, $L_3 = \pm 1$					
	Orthotropy parameter, β						Orthotropy parameter, β					
	0.5	1	1.5	2	2.5	3	0.5	1	1.5	2	2.5	3
−1.0	5.55	6.97	8.35	9.70	11.0	12.3	4.09	5.23	6.35	7.47	8.58	9.68
−0.9	5.23	6.61	7.96	9.28	10.6	11.9	3.87	4.97	6.05	7.13	8.20	9.27
−0.8	4.92	6.26	7.57	8.85	10.1	11.4	3.66	4.71	5.75	6.79	7.82	8.85
−0.7	4.61	5.91	7.18	8.43	9.66	10.9	3.46	4.46	5.46	6.45	7.44	8.43
−0.6	4.31	5.56	6.79	8.00	9.19	10.4	3.26	4.22	5.16	6.11	7.06	8.00
−0.5	4.02	5.22	6.39	7.56	8.72	9.87	3.07	3.98	4.88	5.78	6.67	7.57
−0.4	3.74	4.88	6.00	7.12	8.23	9.33	2.89	3.74	4.59	5.44	6.28	7.13
−0.3	3.47	4.54	5.61	6.67	7.72	8.78	2.71	3.51	4.31	5.10	5.89	6.67
−0.2	3.20	4.21	5.21	6.21	7.20	8.20	2.54	3.29	4.03	4.76	5.49	6.21
−0.1	2.95	3.88	4.81	5.73	6.65	7.57	2.37	3.07	3.76	4.43	5.08	5.73
0	2.70	3.56	4.40	5.24	6.06	6.88	2.21	2.86	3.48	4.08	4.66	5.23
0.1	2.47	3.24	3.99	4.71	5.40	6.07	2.06	2.65	3.21	3.73	4.23	4.69
0.2	2.25	2.92	3.55	4.12	4.60	4.93	1.92	2.45	2.93	3.37	3.76	4.10
0.3	2.04	2.61	3.08				1.78	2.24	2.65	2.98	3.22	
0.4	1.85	2.30					1.64	2.04	2.35	2.50		
0.5	1.67	1.98					1.52	1.84				
0.6	1.50						1.40	1.64				
0.7	1.35						1.28					
0.8	1.22						1.18					
0.9	1.10						1.08					
1.0	.999						.988					

*Unfilled entries in the table are given by the wide-column buckling formula, $K_x = 1/L_2$.

Table 41. Values of Buckling Coefficient K_x for Simply Supported Plates Subjected to Axial Compression, Transverse Tension or Compression, and Shear Loads ($\gamma = \delta = 0$, see figs. 31 and 32)

Buckling coefficient, K_x*												
L_2	Shear load factor, $L_3 = \pm 1.5$						Shear load factor, $L_3 = \pm 2$					
	Orthotropy parameter, β						Orthotropy parameter, β					
	0.5	1	1.5	2	2.5	3	0.5	1	1.5	2	2.5	3
−1.0	3.04	3.91	4.77	5.62	6.48	7.34	2.36	3.03	3.69	4.35	5.01	5.67
−0.9	2.90	3.73	4.55	5.37	6.20	7.02	2.26	2.90	3.54	4.17	4.80	5.42
−0.8	2.76	3.55	4.34	5.13	5.91	6.69	2.17	2.78	3.39	3.99	4.59	5.18
−0.7	2.63	3.38	4.13	4.88	5.63	6.37	2.08	2.67	3.24	3.82	4.38	4.95
−0.6	2.50	3.22	3.93	4.64	5.34	6.05	1.99	2.55	3.10	3.64	4.18	4.71
−0.5	2.38	3.06	3.73	4.40	5.06	5.72	1.91	2.44	2.96	3.47	3.98	4.47
−0.4	2.26	2.90	3.54	4.16	4.78	5.40	1.83	2.33	2.82	3.31	3.78	4.24
−0.3	2.14	2.75	3.34	3.93	4.50	5.07	1.75	2.23	2.69	3.14	3.58	4.00
−0.2	2.03	2.60	3.16	3.70	4.23	4.74	1.67	2.12	2.56	2.98	3.38	3.77
−0.1	1.92	2.46	2.97	3.47	3.95	4.41	1.60	2.02	2.43	2.82	3.19	3.54
0	1.82	2.31	2.79	3.24	3.67	4.07	1.52	1.93	2.30	2.66	2.99	3.31
0.1	1.72	2.18	2.61	3.01	3.38	3.73	1.45	1.83	2.18	2.50	2.80	3.07
0.2	1.62	2.04	2.43	2.78	3.09	3.37	1.38	1.74	2.05	2.34	2.60	2.84
0.3	1.52	1.91	2.25	2.54	2.79	2.99	1.32	1.64	1.93	2.18	2.40	2.59
0.4	1.43	1.78	2.07	2.29	2.44		1.25	1.55	1.81	2.02	2.19	2.33
0.5	1.34	1.65	1.87	2.00			1.19	1.46	1.68	1.85	1.96	
0.6	1.26	1.52	1.66				1.13	1.37	1.55	1.66		
0.7	1.18	1.39					1.07	1.28	1.41			
0.8	1.10	1.25					1.01	1.19				
0.9	1.03						.958	1.10				
1.0	.955						.904					

*Unfilled entries in the table are given by the wide-column buckling formula, $K_x = 1/L_2$.

Table 42. Values of Buckling Coefficient K_x for Simply Supported Plates Subjected to Axial Compression, Transverse Tension or Compression, and Shear Loads ($\gamma = \delta = 0.2$, see figs. 34 and 36)

Buckling coefficient, K_x*												
L_2	Shear load factor, $L_3 = -2$						Shear load factor, $L_3 = -1.5$					
	Orthotropy parameter, β						Orthotropy parameter, β					
	0.5	1	1.5	2	2.5	3	0.5	1	1.5	2	2.5	3
−1.0	3.17	3.86	4.54	5.21	5.88	6.54	4.02	4.90	5.78	6.65	7.52	8.39
−0.9	3.03	3.69	4.35	4.99	5.63	6.27	3.82	4.68	5.52	6.36	7.20	8.03
−0.8	2.90	3.54	4.16	4.78	5.39	5.99	3.64	4.46	5.27	6.07	6.87	7.66
−0.7	2.77	3.38	3.98	4.56	5.14	5.72	3.46	4.24	5.02	5.78	6.54	7.30
−0.6	2.65	3.23	3.80	4.35	4.90	5.44	3.28	4.03	4.77	5.50	6.22	6.94
−0.5	2.53	3.08	3.62	4.15	4.66	5.17	3.11	3.82	4.52	5.21	5.89	6.57
−0.4	2.41	2.94	3.45	3.94	4.42	4.90	2.94	3.62	4.28	4.93	5.57	6.20
−0.3	2.29	2.80	3.28	3.74	4.19	4.62	2.77	3.42	4.04	4.65	5.24	5.82
−0.2	2.18	2.66	3.11	3.53	3.95	4.35	2.61	3.22	3.80	4.36	4.91	5.44
−0.1	2.07	2.52	2.94	3.33	3.71	4.07	2.46	3.03	3.57	4.08	4.57	5.05
0	1.96	2.38	2.77	3.13	3.47	3.79	2.30	2.83	3.33	3.79	4.23	4.65
0.1	1.86	2.25	2.60	2.93	3.23	3.50	2.15	2.64	3.09	3.50	3.88	4.23
0.2	1.75	2.11	2.44	2.72	2.98	3.21	2.01	2.46	2.85	3.20	3.51	3.78
0.3	1.65	1.98	2.27	2.51	2.71	2.89	1.86	2.27	2.60	2.88	3.09	3.25
0.4	1.55	1.85	2.09	2.28	2.41	2.49	1.72	2.07	2.33	2.49		
0.5	1.45	1.71	1.90	2.00			1.59	1.87				
0.6	1.35	1.57					1.46	1.66				
0.7	1.26	1.42					1.33					
0.8	1.17						1.21					
0.9	1.08						1.10					
1.0	.989						.998					

*Unfilled entries in the table are given by the wide-column buckling formula, $K_x = 1/L_2$.

Table 43. Values of Buckling Coefficient K_x for Simply Supported Plates Subjected to Axial Compression, Transverse Tension or Compression, and Shear Loads ($\gamma = \delta = 0.2$, see figs. 34 and 36)

Buckling coefficient, K_x*												
L_2	Shear load factor, $L_3 = -1$						Shear load factor, $L_3 = -0.5$					
	Orthotropy parameter, β						Orthotropy parameter, β					
	0.5	1	1.5	2	2.5	3	0.5	1	1.5	2	2.5	3
−1.0	5.18	6.34	7.47	8.59	9.70	10.8	6.31	7.76	9.14	10.5	11.8	13.1
−0.9	4.91	6.03	7.13	8.21	9.29	10.4	5.96	7.37	8.73	10.0	11.3	12.6
−0.8	4.64	5.73	6.79	7.84	8.88	9.91	5.60	6.99	8.31	9.60	10.9	12.1
−0.7	4.38	5.42	6.45	7.46	8.46	9.46	5.25	6.60	7.90	9.16	10.4	11.6
−0.6	4.13	5.13	6.11	7.07	8.04	8.99	4.91	6.22	7.48	8.70	9.91	11.1
−0.5	3.87	4.83	5.77	6.69	7.61	8.52	4.57	5.84	7.06	8.24	9.42	10.6
−0.4	3.63	4.54	5.43	6.31	7.17	8.04	4.24	5.46	6.63	7.78	8.91	10.0
−0.3	3.39	4.26	5.09	5.92	6.73	7.54	3.91	5.08	6.20	7.30	8.38	9.46
−0.2	3.16	3.97	4.76	5.52	6.28	7.02	3.59	4.70	5.76	6.80	7.83	8.85
−0.1	2.93	3.69	4.42	5.12	5.81	6.48	3.27	4.31	5.31	6.29	7.25	8.20
0	2.70	3.41	4.08	4.71	5.32	5.90	2.97	3.93	4.85	5.74	6.62	7.47
0.1	2.49	3.13	3.73	4.28	4.79	5.27	2.68	3.55	4.37	5.15	5.89	6.59
0.2	2.28	2.86	3.37	3.82	4.20	4.52	2.41	3.17	3.85	4.44	4.89	
0.3	2.07	2.57	2.98	3.26			2.15	2.78	3.24			
0.4	1.88	2.28	2.50				1.92	2.39				
0.5	1.70	1.98					1.71	2.00				
0.6	1.52						1.52					
0.7	1.37						1.36					
0.8	1.23						1.22					
0.9	1.11						1.10					
1.0	1.00						.998					

*Unfilled entries in the table are given by the wide-column buckling formula, $K_x = 1/L_2$.

Table 44. Values of Buckling Coefficient K_x for Simply Supported Plates Subjected to Axial Compression, Transverse Tension or Compression, and Shear Loads ($\gamma = \delta = 0.2$, see figs. 33 and 35)

Buckling coefficient, K_x*												
L_2	Shear load factor, $L_3 = 0.5$						Shear load factor, $L_3 = 1$					
	Orthotropy parameter, β						Orthotropy parameter, β					
	0.5	1	1.5	2	2.5	3	0.5	1	1.5	2	2.5	3
−1.0	4.04	5.59	7.06	8.47	9.85	11.2	2.68	3.84	5.00	6.13	7.26	8.38
−0.9	3.78	5.27	6.70	8.08	9.42	10.7	2.53	3.64	4.75	5.84	6.92	8.00
−0.8	3.54	4.97	6.34	7.68	8.99	10.3	2.39	3.45	4.50	5.55	6.59	7.63
−0.7	3.31	4.67	5.99	7.29	8.56	9.81	2.26	3.27	4.27	5.26	6.26	7.25
−0.6	3.08	4.38	5.65	6.89	8.12	9.33	2.14	3.09	4.03	4.98	5.92	6.86
−0.5	2.87	4.10	5.30	6.49	7.67	8.84	2.02	2.91	3.81	4.70	5.59	6.48
−0.4	2.67	3.82	4.96	6.09	7.22	8.34	1.91	2.75	3.59	4.42	5.25	6.09
−0.3	2.48	3.56	4.63	5.69	6.76	7.82	1.80	2.59	3.37	4.15	4.92	5.69
−0.2	2.31	3.30	4.30	5.29	6.28	7.27	1.70	2.43	3.16	3.88	4.59	5.29
−0.1	2.14	3.06	3.97	4.88	5.78	6.69	1.61	2.29	2.96	3.61	4.25	4.88
0	1.98	2.82	3.65	4.46	5.27	6.06	1.52	2.15	2.76	3.35	3.92	4.46
0.1	1.84	2.59	3.33	4.03	4.71	5.37	1.43	2.01	2.56	3.08	3.58	4.04
0.2	1.70	2.38	3.01	3.59	4.10	4.53	1.35	1.88	2.37	2.82	3.23	3.59
0.3	1.58	2.17	2.69	3.10	3.33		1.27	1.76	2.19	2.56	2.87	3.11
0.4	1.46	1.97	2.36				1.20	1.64	2.00	2.29	2.47	
0.5	1.35	1.78	2.00				1.13	1.52	1.82	1.99		
0.6	1.25	1.59					1.07	1.41	1.63			
0.7	1.16	1.42					1.01	1.30				
0.8	1.08						.953	1.20				
0.9	.999						.900	1.10				
1.0	.928						.850	1.00				

*Unfilled entries in the table are given by the wide-column buckling formula, $K_x = 1/L_2$.

Table 45. Values of Buckling Coefficient K_x for Simply Supported Plates Subjected to Axial Compression, Transverse Tension or Compression, and Shear Loads ($\gamma = \delta = 0.2$, see figs. 33 and 35)

Buckling coefficient, K_x*												
L_2	Shear load factor, $L_3 = 1.5$						Shear load factor, $L_3 = 2$					
	Orthotropy parameter, β						Orthotropy parameter, β					
	0.5	1	1.5	2	2.5	3	0.5	1	1.5	2	2.5	3
−1.0	1.91	2.77	3.63	4.49	5.35	6.20	1.47	2.12	2.78	3.43	4.08	4.73
−0.9	1.83	2.65	3.47	4.29	5.10	5.92	1.41	2.04	2.67	3.29	3.91	4.53
−0.8	1.75	2.53	3.31	4.09	4.86	5.64	1.36	1.96	2.56	3.15	3.74	4.33
−0.7	1.67	2.41	3.15	3.89	4.63	5.36	1.31	1.88	2.45	3.01	3.57	4.13
−0.6	1.59	2.30	3.00	3.70	4.39	5.09	1.26	1.81	2.35	2.88	3.41	3.93
−0.5	1.52	2.19	2.85	3.51	4.16	4.81	1.21	1.73	2.25	2.75	3.25	3.73
−0.4	1.45	2.09	2.71	3.32	3.93	4.54	1.17	1.66	2.15	2.62	3.09	3.54
−0.3	1.39	1.99	2.57	3.14	3.71	4.26	1.12	1.60	2.06	2.50	2.93	3.35
−0.2	1.33	1.89	2.43	2.97	3.48	3.99	1.08	1.53	1.96	2.38	2.78	3.16
−0.1	1.27	1.79	2.30	2.79	3.26	3.72	1.04	1.47	1.87	2.26	2.62	2.97
0	1.21	1.70	2.18	2.62	3.05	3.45	1.00	1.41	1.79	2.14	2.48	2.79
0.1	1.16	1.62	2.05	2.45	2.83	3.18	.965	1.35	1.70	2.03	2.33	2.61
0.2	1.10	1.53	1.93	2.29	2.61	2.91	.930	1.29	1.62	1.91	2.18	2.43
0.3	1.05	1.45	1.81	2.13	2.40	2.63	.895	1.23	1.54	1.80	2.04	2.25
0.4	1.01	1.38	1.70	1.96	2.18	2.34	.862	1.18	1.46	1.69	1.90	2.07
0.5	.962	1.30	1.58	1.80	1.94		.830	1.13	1.38	1.59	1.75	1.87
0.6	.919	1.23	1.47	1.62			.799	1.08	1.30	1.48	1.60	1.66
0.7	.878	1.16	1.36				.770	1.03	1.23	1.36		
0.8	.838	1.09	1.24				.741	.978	1.15	1.24		
0.9	.801	1.02					.714	.931	1.07			
1.0	.765	.958					.687	.885	.994			

*Unfilled entries in the table are given by the wide-column buckling formula, $K_x = 1/L_2$.

Table 46. Values of Buckling Coefficient K_x for Simply Supported Plates Subjected to Axial Compression, Transverse Tension or Compression, and Shear Loads ($\gamma = \delta = 0.4$, see figs. 38 and 40)

Buckling coefficient, K_x*												
L_2	Shear load factor, $L_3 = -2$						Shear load factor, $L_3 = -1.5$					
	Orthotropy parameter, β						Orthotropy parameter, β					
	0.6	1	1.5	2	2.5	3	0.6	1	1.5	2	2.5	3
−1.0	4.03	4.61	5.31	6.01	6.69	7.37	5.02	5.77	6.68	7.58	8.47	9.35
−0.9	3.86	4.41	5.09	5.76	6.41	7.06	4.78	5.51	6.39	7.25	8.11	8.95
−0.8	3.68	4.22	4.87	5.51	6.14	6.76	4.55	5.24	6.09	6.92	7.74	8.56
−0.7	3.52	4.03	4.65	5.26	5.86	6.45	4.31	4.99	5.80	6.60	7.38	8.16
−0.6	3.35	3.84	4.44	5.02	5.58	6.14	4.08	4.73	5.51	6.27	7.02	7.75
−0.5	3.19	3.66	4.23	4.77	5.31	5.83	3.86	4.48	5.22	5.94	6.65	7.34
−0.4	3.03	3.48	4.02	4.53	5.03	5.52	3.64	4.23	4.93	5.62	6.28	6.93
−0.3	2.87	3.30	3.81	4.29	4.75	5.20	3.42	3.98	4.65	5.29	5.91	6.51
−0.2	2.72	3.12	3.60	4.05	4.48	4.89	3.20	3.74	4.36	4.96	5.53	6.08
−0.1	2.57	2.95	3.39	3.81	4.20	4.57	2.99	3.50	4.08	4.62	5.14	5.64
0	2.42	2.78	3.19	3.56	3.91	4.24	2.78	3.26	3.79	4.28	4.74	5.18
0.1	2.27	2.60	2.98	3.31	3.62	3.90	2.57	3.01	3.50	3.93	4.33	4.69
0.2	2.12	2.43	2.77	3.06	3.32	3.54	2.37	2.77	3.20	3.56	3.87	4.14
0.3	1.97	2.25	2.54	2.78	2.98	3.13	2.16	2.52	2.87	3.13	3.30	
0.4	1.82	2.07	2.30	2.46			1.96	2.26	2.48			
0.5	1.68	1.88	2.00				1.76	1.97				
0.6	1.53	1.66					1.57					
0.7	1.38						1.39					
0.8	1.24						1.24					
0.9	1.11						1.11					
1.0												

*Unfilled entries in the table are given by the wide-column buckling formula, $K_x = 1/L_2$.

Table 47. Values of Buckling Coefficient K_x for Simply Supported Plates Subjected to Axial Compression, Transverse Tension or Compression, and Shear Loads ($\gamma = \delta = 0.4$, see figs. 38 and 40)

Buckling coefficient, K_x*												
L_2	Shear load factor, $L_3 = -1$						Shear load factor, $L_3 = -0.5$					
	Orthotropy parameter, β						Orthotropy parameter, β					
	0.6	1	1.5	2	2.5	3	0.6	1	1.5	2	2.5	3
−1.0	6.18	7.17	8.35	9.50	10.6	11.8	6.51	7.85	9.36	10.8	12.2	13.5
–0.9	5.86	6.82	7.97	9.09	10.2	11.3	6.11	7.44	8.94	10.3	11.7	13.0
–0.8	5.54	6.47	7.59	8.68	9.75	10.8	5.71	7.03	8.51	9.89	11.2	12.5
–0.7	5.22	6.13	7.22	8.27	9.30	10.3	5.31	6.62	8.07	9.43	10.7	12.0
–0.6	4.90	5.79	6.84	7.85	8.85	9.83	4.91	6.21	7.64	8.97	10.2	11.5
–0.5	4.59	5.45	6.46	7.43	8.39	9.33	4.51	5.80	7.20	8.49	9.74	10.9
–0.4	4.28	5.11	6.08	7.01	7.92	8.81	4.12	5.39	6.75	8.01	9.22	10.4
–0.3	3.98	4.77	5.70	6.58	7.44	8.28	3.73	4.97	6.30	7.51	8.68	9.81
–0.2	3.67	4.44	5.31	6.14	6.94	7.72	3.35	4.56	5.83	7.00	8.12	9.20
–0.1	3.37	4.10	4.92	5.68	6.42	7.13	2.99	4.15	5.36	6.47	7.52	8.54
0	3.08	3.76	4.52	5.21	5.87	6.49	2.66	3.74	4.87	5.90	6.87	7.80
0.1	2.79	3.42	4.10	4.71	5.26	5.77	2.35	3.34	4.36	5.27	6.11	6.89
0.2	2.50	3.08	3.66	4.15	4.54	4.83	2.07	2.95	3.81	4.51	4.98	
0.3	2.22	2.72	3.16				1.83	2.58	3.20			
0.4	1.97	2.36					1.63	2.23				
0.5	1.73	1.99					1.45	1.92				
0.6	1.53						1.31	1.66				
0.7	1.36						1.18					
0.8	1.21						1.07					
0.9	1.09						.983					
1.0	.988						.904					

*Unfilled entries in the table are given by the wide-column buckling formula, $K_x = 1/L_2$.

Table 48. Values of Buckling Coefficient K_x for Simply Supported Plates Subjected to Axial Compression, Transverse Tension or Compression, and Shear Loads ($\gamma = \delta = 0.4$, see figs. 37 and 39)

Buckling coefficient, K_x*												
L_2	Shear load factor, $L_3 = 0.5$						Shear load factor, $L_3 = 1$					
	Orthotropy parameter, β						Orthotropy parameter, β					
	0.6	1	1.5	2	2.5	3	0.6	1	1.5	2	2.5	3
–1.0	1.69	3.42	5.17	6.76	8.26	9.71	.955	2.11	3.36	4.56	5.74	6.90
–0.9	1.57	3.20	4.87	6.41	7.87	9.28	.911	2.00	3.18	4.33	5.46	6.57
–0.8	1.46	2.99	4.58	6.06	7.48	8.85	.871	1.89	3.01	4.10	5.18	6.24
–0.7	1.36	2.79	4.30	5.72	7.09	8.41	.833	1.79	2.85	3.88	4.90	5.91
–0.6	1.28	2.60	4.03	5.38	6.69	7.97	.798	1.70	2.69	3.67	4.63	5.58
–0.5	1.20	2.43	3.76	5.05	6.29	7.52	.765	1.61	2.55	3.46	4.36	5.26
–0.4	1.13	2.26	3.51	4.71	5.89	7.06	.735	1.53	2.40	3.25	4.09	4.93
–0.3	1.06	2.11	3.27	4.39	5.49	6.58	.707	1.45	2.27	3.06	3.83	4.60
–0.2	1.00	1.97	3.04	4.07	5.08	6.09	.680	1.38	2.14	2.86	3.57	4.27
–0.1	.949	1.84	2.81	3.75	4.67	5.59	.655	1.31	2.01	2.68	3.32	3.95
0	.900	1.72	2.60	3.44	4.26	5.06	.632	1.25	1.89	2.50	3.08	3.62
0.1	.855	1.61	2.40	3.14	3.84	4.50	.609	1.19	1.78	2.33	2.83	3.30
0.2	.813	1.50	2.21	2.84	3.41	3.90	.589	1.13	1.68	2.16	2.60	2.99
0.3	.775	1.40	2.03	2.55	2.96	3.25	.569	1.07	1.57	2.00	2.36	2.67
0.4	.739	1.31	1.86	2.26	2.49		.550	1.02	1.48	1.85	2.14	2.35
0.5	.706	1.23	1.69	1.97			.533	.975	1.38	1.70	1.91	2.00
0.6	.675	1.15	1.54				.516	.929	1.30	1.55	1.66	
0.7	.646	1.08	1.39				.500	.886	1.21	1.40		
0.8	.620	1.01	1.25				.484	.845	1.13			
0.9	.595	.952					.470	.807	1.05			
1.0	.571	.894					.456	.770	.979			

*Unfilled entries in the table are given by the wide-column buckling formula, $K_x = 1/L_2$.

Table 49. Values of Buckling Coefficient K_x for Simply Supported Plates Subjected to Axial Compression, Transverse Tension or Compression, and Shear Loads ($\gamma = \delta = 0.4$, see figs. 37 and 39)

Buckling coefficient, K_x*												
L_2	Shear load factor, $L_3 = 1.5$						Shear load factor, $L_3 = 2$					
	Orthotropy parameter, β						Orthotropy parameter, β					
	0.6	1	1.5	2	2.5	3	0.6	1	1.5	2	2.5	3
−1.0	.656	1.47	2.36	3.24	4.11	4.97	.498	1.11	1.79	2.45	3.10	3.75
−0.9	.634	1.41	2.26	3.09	3.92	4.74	.485	1.08	1.72	2.35	2.97	3.59
−0.8	.614	1.35	2.16	2.95	3.73	4.51	.473	1.04	1.65	2.25	2.84	3.42
−0.7	.595	1.29	2.06	2.81	3.55	4.28	.461	1.00	1.59	2.16	2.71	3.27
−0.6	.576	1.24	1.96	2.67	3.37	4.06	.450	.969	1.53	2.07	2.59	3.11
−0.5	.559	1.19	1.87	2.54	3.19	3.83	.439	.937	1.47	1.98	2.47	2.96
−0.4	.542	1.14	1.79	2.41	3.02	3.62	.429	.906	1.41	1.89	2.36	2.81
−0.3	.527	1.10	1.70	2.28	2.85	3.40	.419	.876	1.36	1.81	2.24	2.66
−0.2	.512	1.05	1.62	2.17	2.69	3.19	.410	.848	1.30	1.73	2.13	2.52
−0.1	.498	1.01	1.55	2.05	2.53	2.98	.401	.821	1.25	1.65	2.03	2.38
0	.484	.971	1.48	1.94	2.37	2.78	.392	.794	1.20	1.58	1.92	2.24
0.1	.471	.934	1.41	1.83	2.22	2.58	.384	.769	1.16	1.50	1.82	2.11
0.2	.459	.898	1.34	1.73	2.07	2.39	.375	.745	1.11	1.43	1.72	1.98
0.3	.447	.864	1.27	1.63	1.93	2.20	.368	.721	1.07	1.37	1.63	1.85
0.4	.436	.832	1.21	1.53	1.79	2.01	.360	.699	1.03	1.30	1.53	1.73
0.5	.425	.801	1.15	1.44	1.66	1.82	.353	.677	.984	1.24	1.44	1.61
0.6	.414	.771	1.10	1.35	1.52	1.63	.345	.657	.945	1.17	1.35	1.49
0.7	.404	.743	1.04	1.26	1.39		.339	.637	.907	1.11	1.27	1.37
0.8	.395	.715	.990	1.17	1.25		.332	.617	.870	1.05	1.18	1.24
0.9	.385	.690	.940	1.08			.326	.599	.834	.997	1.09	
1.0	.376	.665	.891	.997			.319	.581	.800	.940	.999	

*Unfilled entries in the table are given by the wide-column buckling formula, $K_x = 1/L_2$.

Table 50. Values of Buckling Coefficient K_x for Simply Supported Plates Subjected to Axial Compression, Transverse Tension or Compression, and Shear Loads ($\gamma = \delta = 0.6$, see figs. 42 and 44)

Buckling coefficient, K_x*								
L_2	Shear load factor, $L_3 = -2$				Shear load factor, $L_3 = -1.5$			
	Orthotropy parameter, β				Orthotropy parameter, β			
	1.5	2	2.5	3	1.5	2	2.5	3
−1.0	6.02	6.73	7.44	8.14	7.45	8.38	9.29	10.2
−0.9	5.76	6.45	7.13	7.80	7.12	8.01	8.90	9.78
−0.8	5.51	6.17	6.82	7.46	6.79	7.65	8.51	9.35
−0.7	5.26	5.89	6.51	7.12	6.46	7.29	8.11	8.91
−0.6	5.01	5.61	6.20	6.78	6.13	6.93	7.71	8.48
−0.5	4.76	5.33	5.89	6.43	5.80	6.56	7.31	8.03
−0.4	4.52	5.05	5.58	6.08	5.47	6.20	6.90	7.58
−0.3	4.27	4.78	5.27	5.73	5.15	5.83	6.49	7.12
−0.2	4.03	4.50	4.95	5.38	4.82	5.45	6.06	6.65
−0.1	3.79	4.22	4.63	5.02	4.49	5.08	5.63	6.16
0	3.54	3.94	4.31	4.65	4.15	4.69	5.18	5.64
0.1	3.29	3.65	3.97	4.26	3.81	4.28	4.71	5.09
0.2	3.04	3.34	3.61	3.84	3.45	3.84	4.17	4.44
0.3	2.76	3.00	3.18	3.30	3.04	3.29		
0.4	2.44							
0.5								
0.6								
0.7								
0.8								
0.9								
1.0								

*Unfilled entries in the table are given by the wide-column buckling formula, $K_x = 1/L_2$.

Table 51. Values of Buckling Coefficient K_x for Simply Supported Plates Subjected to Axial Compression, Transverse Tension or Compression, and Shear Loads ($\gamma = \delta = 0.6$, see figs. 42 and 44)

Buckling coefficient, K_x*								
L_2	Shear load factor, $L_3 = -1$				Shear load factor, $L_3 = -0.5$			
	Orthotropy parameter, β				Orthotropy parameter, β			
	1.5	2	2.5	3	1.5	2	2.5	3
−1.0	8.91	10.1	11.3	12.5	8.69	10.4	12.0	13.4
−0.9	8.51	9.69	10.9	12.0	8.23	9.94	11.5	12.9
−0.8	8.10	9.26	10.4	11.5	7.78	9.48	11.0	12.4
−0.7	7.69	8.82	9.92	11.0	7.31	9.01	10.5	11.9
−0.6	7.28	8.38	9.44	10.5	6.84	8.54	10.0	11.4
−0.5	6.86	7.93	8.96	9.95	6.37	8.05	9.51	10.9
−0.4	6.45	7.47	8.46	9.41	5.89	7.56	8.99	10.3
−0.3	6.02	7.01	7.95	8.85	5.40	7.06	8.45	9.73
−0.2	5.60	6.53	7.41	8.26	4.91	6.54	7.89	9.12
−0.1	5.16	6.04	6.86	7.63	4.42	6.00	7.29	8.47
0	4.71	5.52	6.26	6.94	3.93	5.43	6.65	7.74
0.1	4.24	4.97	5.60	6.15	3.45	4.82	5.91	6.85
0.2	3.74	4.33	4.75	4.99	2.99	4.15	4.89	
0.3	3.17				2.58	3.32		
0.4					2.22			
0.5					1.90			
0.6					1.64			
0.7					1.43			
0.8								
0.9								
1.0								

*Unfilled entries in the table are given by the wide-column buckling formula, $K_x = 1/L_2$.

Table 52. Values of Buckling Coefficient K_x for Simply Supported Plates Subjected to Axial Compression, Transverse Tension or Compression, and Shear Loads ($\gamma = \delta = 0.6$, see figs. 41 and 43)

Buckling coefficient, K_x*								
L_2	Shear load factor, $L_3 = 0.5$				Shear load factor, $L_3 = 1$			
	Orthotropy parameter, β				Orthotropy parameter, β			
	1.5	2	2.5	3	1.5	2	2.5	3
−1.0	2.11	4.32	6.12	7.76	1.20	2.65	3.94	5.18
−0.9	1.96	4.05	5.79	7.38	1.14	2.50	3.73	4.91
−0.8	1.82	3.80	5.46	6.99	1.08	2.37	3.53	4.65
−0.7	1.69	3.55	5.13	6.61	1.03	2.24	3.33	4.38
−0.6	1.58	3.31	4.81	6.22	.981	2.11	3.13	4.13
−0.5	1.48	3.09	4.49	5.83	.936	2.00	2.95	3.87
−0.4	1.38	2.87	4.18	5.44	.895	1.88	2.77	3.62
−0.3	1.30	2.67	3.88	5.04	.856	1.78	2.60	3.38
−0.2	1.22	2.47	3.58	4.64	.820	1.68	2.43	3.14
−0.1	1.15	2.29	3.29	4.24	.786	1.59	2.27	2.91
0	1.08	2.12	3.01	3.84	.754	1.50	2.12	2.69
0.1	1.02	1.96	2.74	3.45	.725	1.41	1.98	2.48
0.2	.969	1.82	2.49	3.06	.697	1.34	1.84	2.27
0.3	.919	1.68	2.25	2.69	.670	1.26	1.71	2.08
0.4	.872	1.56	2.02	2.33	.646	1.19	1.59	1.90
0.5	.830	1.44	1.81	1.99	.623	1.13	1.47	1.72
0.6	.790	1.33	1.61		.601	1.07	1.37	1.56
0.7	.754	1.23	1.42		.580	1.01	1.26	1.40
0.8	.720	1.14			.560	.955	1.17	1.25
0.9	.688	1.05			.542	.904	1.08	
1.0	.659	.975			.524	.856	.992	

*Unfilled entries in the table are given by the wide-column buckling formula, $K_x = 1/L_2$.

Table 53. Values of Buckling Coefficient K_x for Simply Supported Plates Subjected to Axial Compression, Transverse Tension or Compression, and Shear Loads ($\gamma = \delta = 0.6$, see figs. 41 and 43)

Buckling coefficient, K_x*								
L_2	Shear load factor, $L_3 = 1.5$				Shear load factor, $L_3 = 2$			
	Orthotropy parameter, β				Orthotropy parameter, β			
	1.5	2	2.5	3	1.5	2	2.5	3
−1.0	.816	1.82	2.73	3.62	.616	1.36	2.03	2.69
−0.9	.786	1.73	2.60	3.44	.598	1.31	1.95	2.58
−0.8	.757	1.66	2.47	3.27	.581	1.26	1.87	2.46
−0.7	.730	1.58	2.35	3.10	.564	1.21	1.79	2.35
−0.6	.705	1.51	2.23	2.94	.548	1.17	1.71	2.24
−0.5	.680	1.44	2.12	2.78	.533	1.12	1.64	2.13
−0.4	.658	1.38	2.01	2.62	.519	1.08	1.57	2.03
−0.3	.636	1.32	1.91	2.47	.505	1.04	1.50	1.93
−0.2	.615	1.26	1.81	2.32	.492	1.00	1.43	1.83
−0.1	.596	1.20	1.71	2.18	.479	.966	1.37	1.74
0	.577	1.15	1.62	2.05	.467	.931	1.31	1.65
0.1	.559	1.10	1.53	1.92	.455	.897	1.25	1.56
0.2	.543	1.05	1.45	1.80	.444	.865	1.19	1.48
0.3	.527	1.00	1.37	1.68	.433	.834	1.14	1.40
0.4	.512	.962	1.30	1.57	.423	.804	1.09	1.33
0.5	.497	.920	1.22	1.46	.413	.776	1.04	1.25
0.6	.483	.881	1.16	1.36	.404	.748	.994	1.18
0.7	.470	.844	1.09	1.26	.394	.722	.949	1.12
0.8	.457	.808	1.03	1.17	.386	.697	.905	1.05
0.9	.445	.775	.970	1.08	.377	.673	.864	.993
1.0	.433	.743	.914	.994	.369	.650	.824	.934

*Unfilled entries in the table are given by the wide-column buckling formula, $K_x = 1/L_2$.

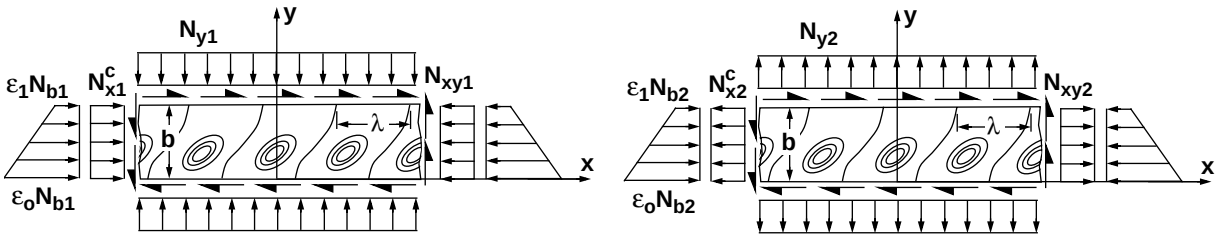

(a) Destabilizing loading system. (b) Subcritical loading system.

Figure 1. Sign convention for positive-valued stress resultants.

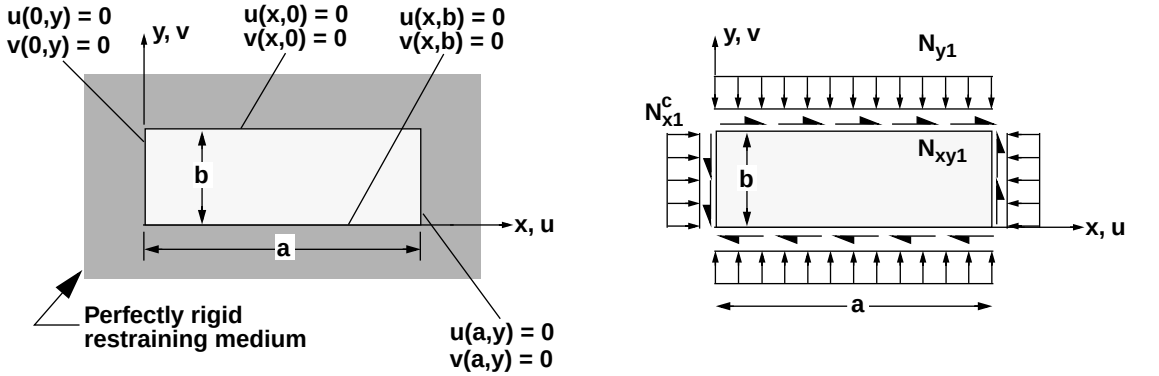

(a) Boundary conditions. (b) Positive values for equivalent mechanical loads.

Figure 2. Mechanical loads in a plate fully restrained against thermal expansion or contraction caused by uniform heating or cooling.

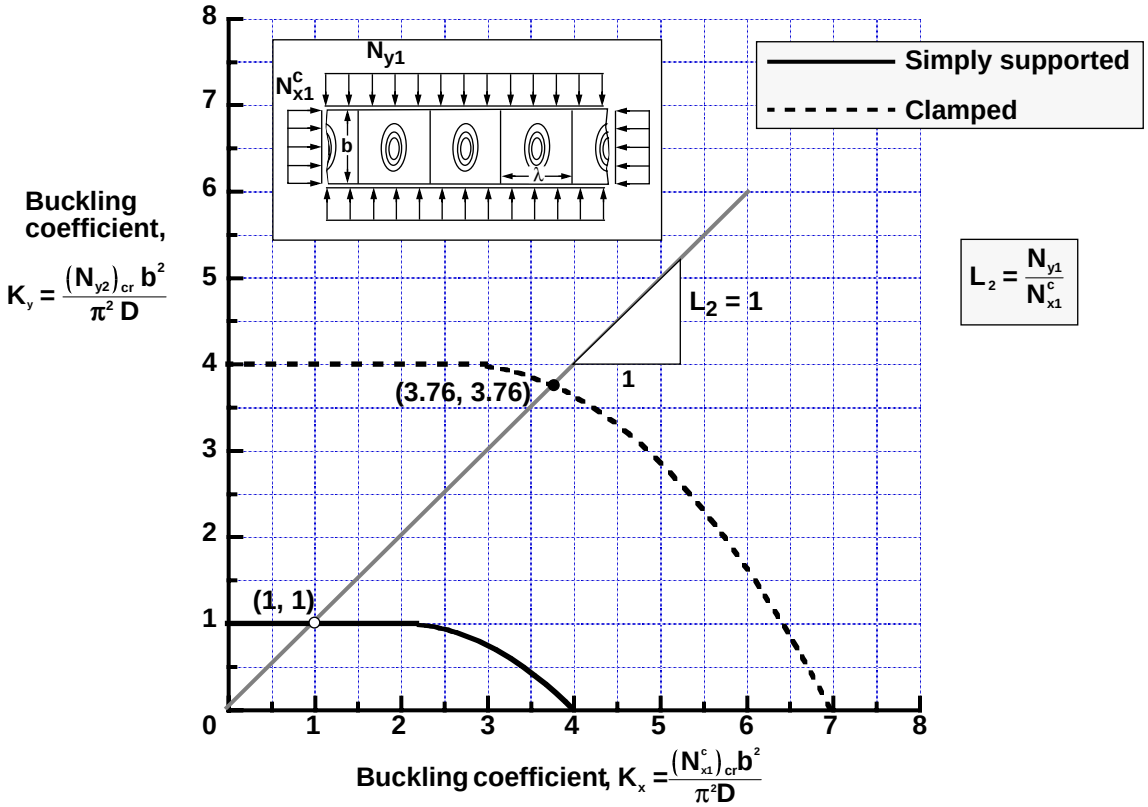

Figure 3. Buckling interaction curves for isotropic plates subjected to biaxial compression loads.

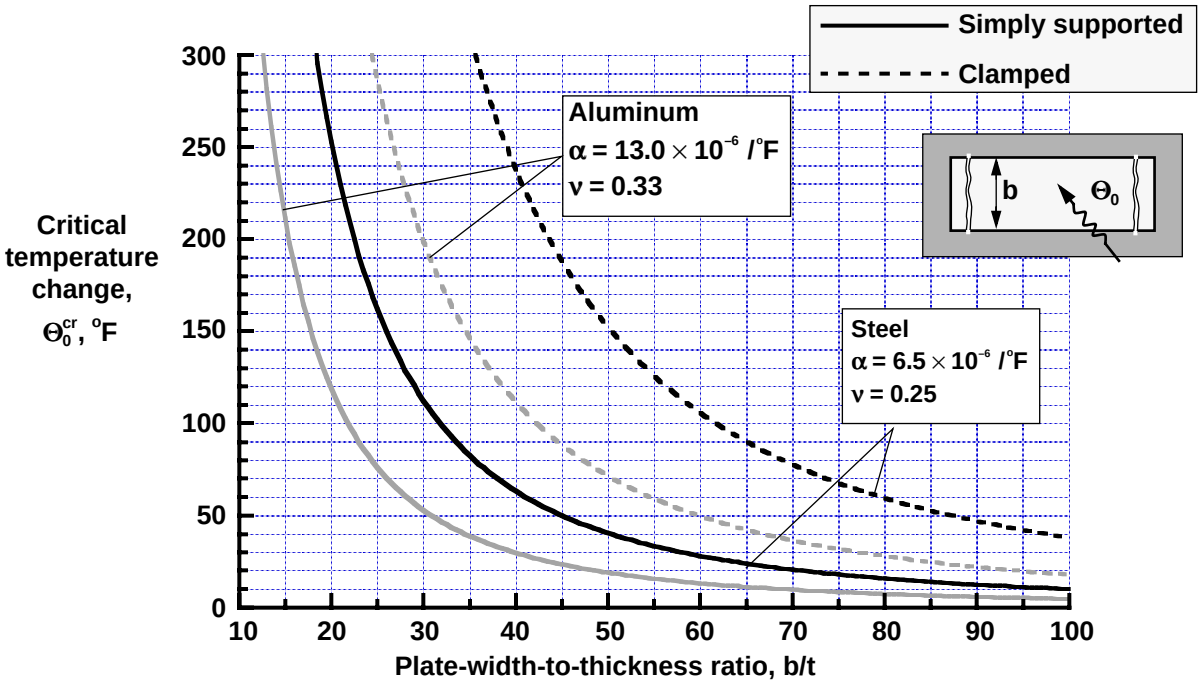

Figure 4. Critical temperature change versus plate-width-to-thickness ratio for simply supported and clamped plates made of steel or aluminum material, fully restrained against thermal expansion and contraction, and subjected to uniform heating.

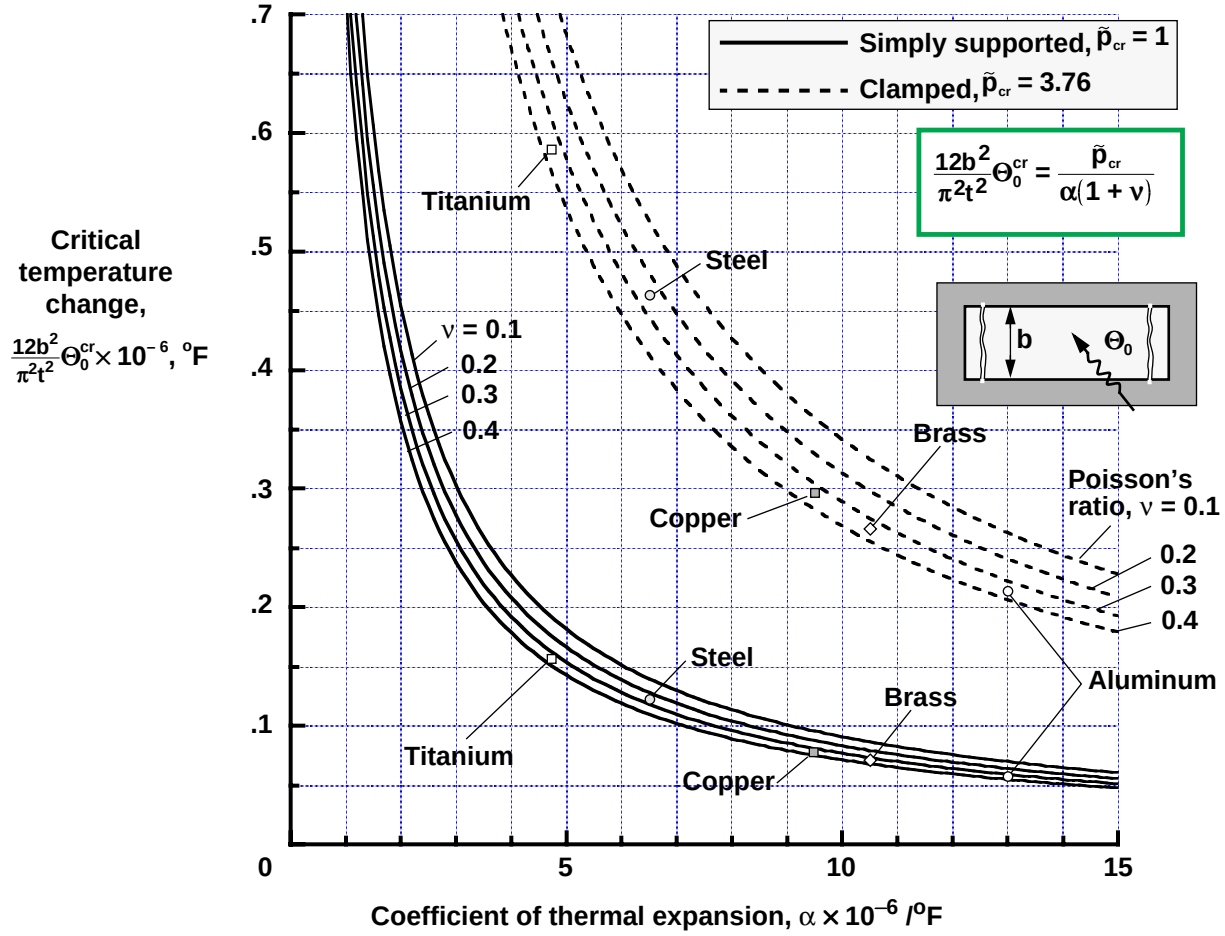

Figure 5. Critical temperature change for simply supported and clamped plates made of isotropic materials, fully restrained against thermal expansion and contraction, and subjected to uniform heating.

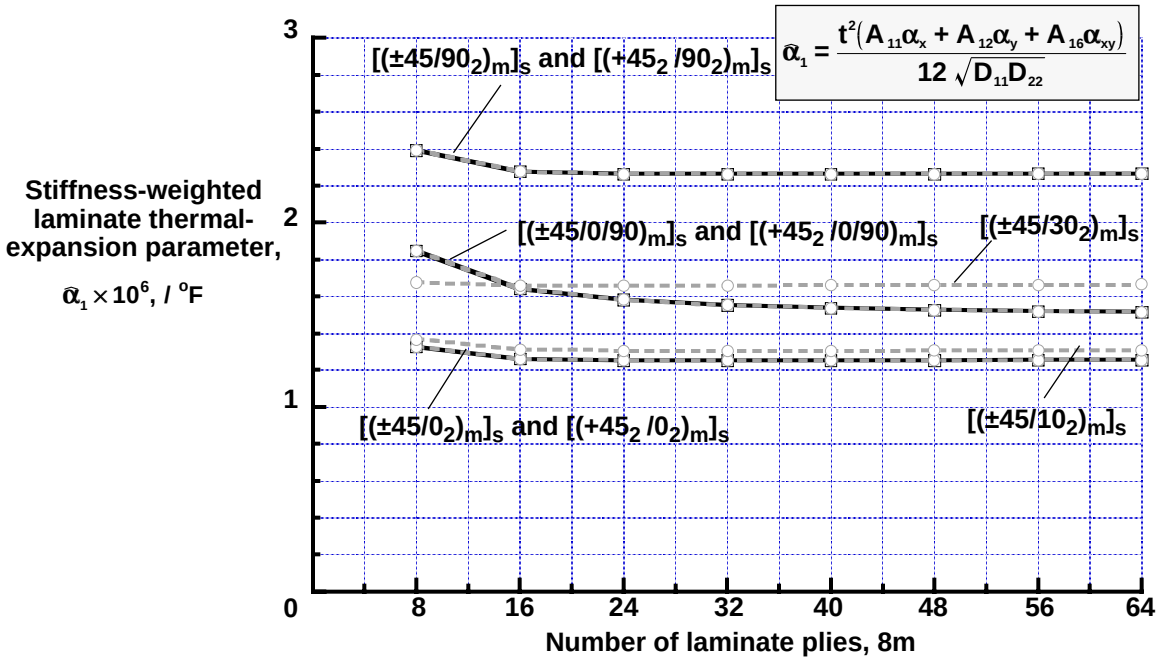

Figure 6. Stiffness-weighted laminate thermal-expansion parameter $\hat{\alpha}_1$ for laminates made of IM7/5260 material.

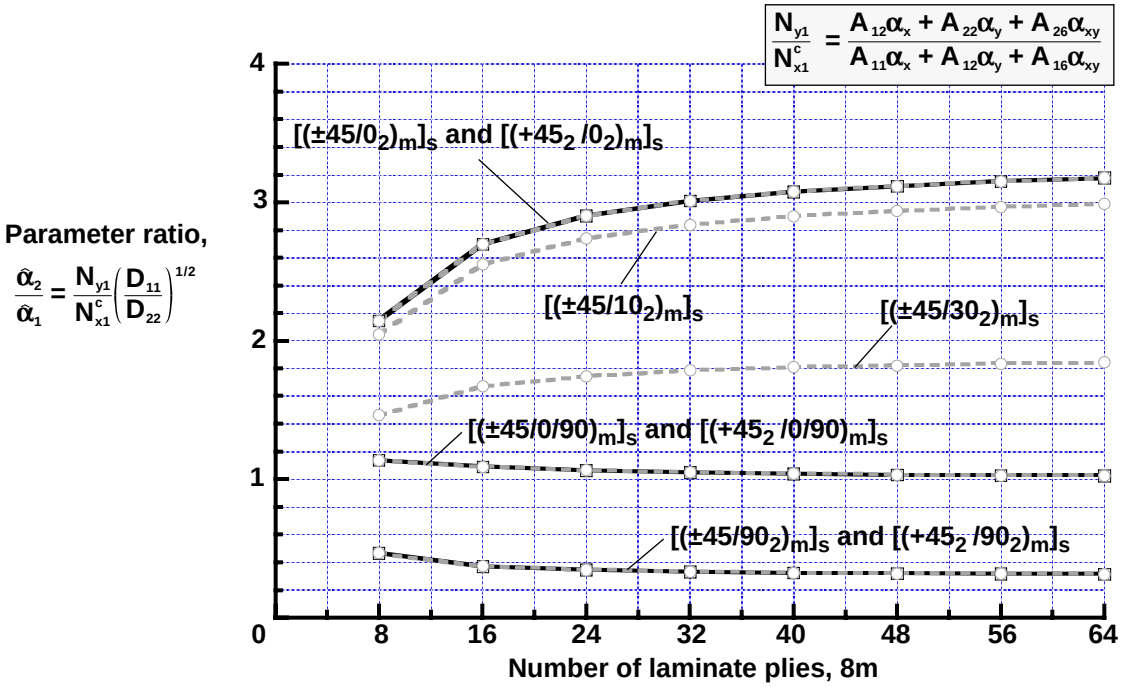

Figure 7. Ratio of stiffness-weighted thermal-expansion parameters $\hat{\alpha}_1$ and $\hat{\alpha}_2$ for laminates made of IM7/5260 material.

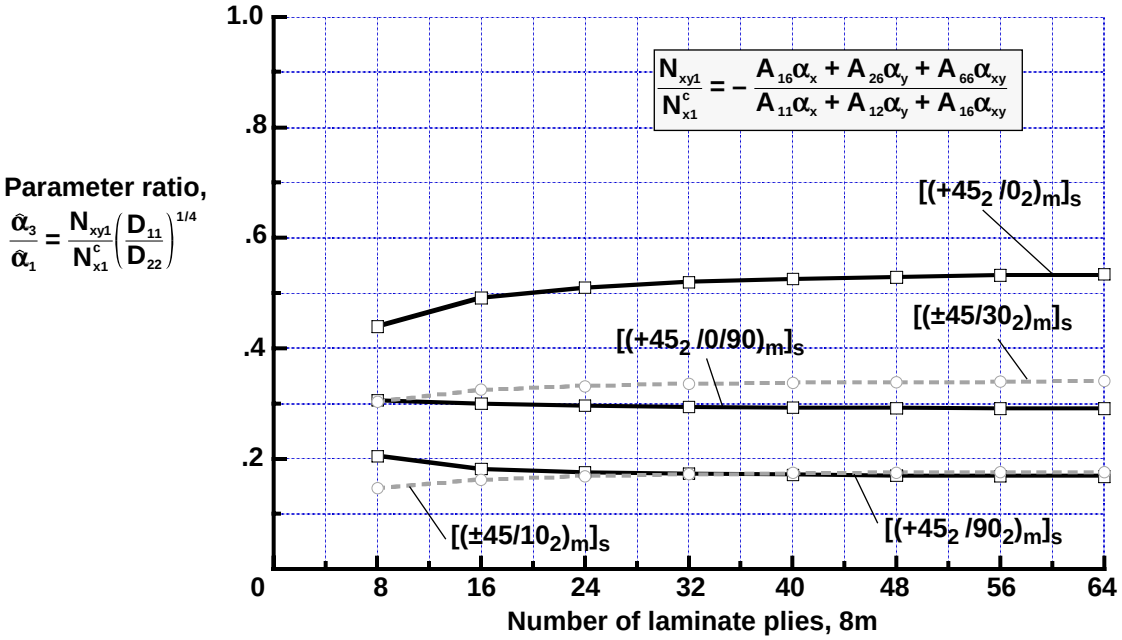

Figure 8. Ratio of stiffness-weighted thermal-expansion parameters $\hat{\alpha}_1$ and $\hat{\alpha}_3$ for laminates made of IM7/5260 material.

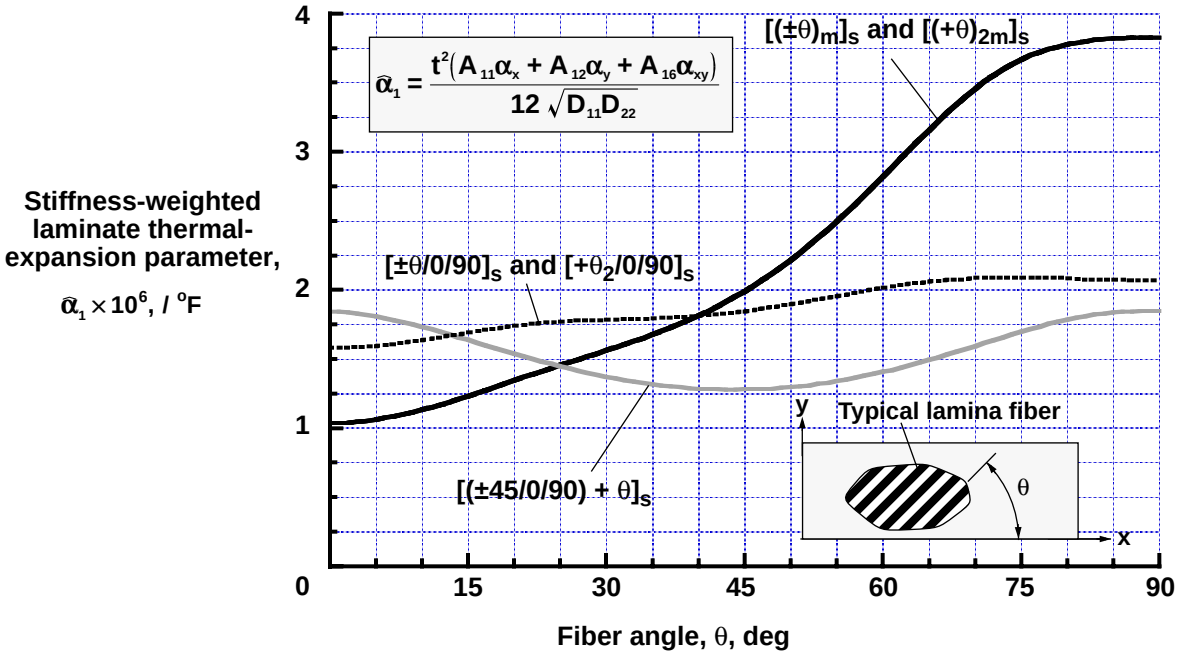

Figure 9. Stiffness-weighted laminate thermal-expansion parameter $\hat{\alpha}_1$ for balanced and unbalanced laminates with angle plies and unbalanced, unidirectional off-axis laminates made of IM7/5260 material (m = 1, 2, ...).

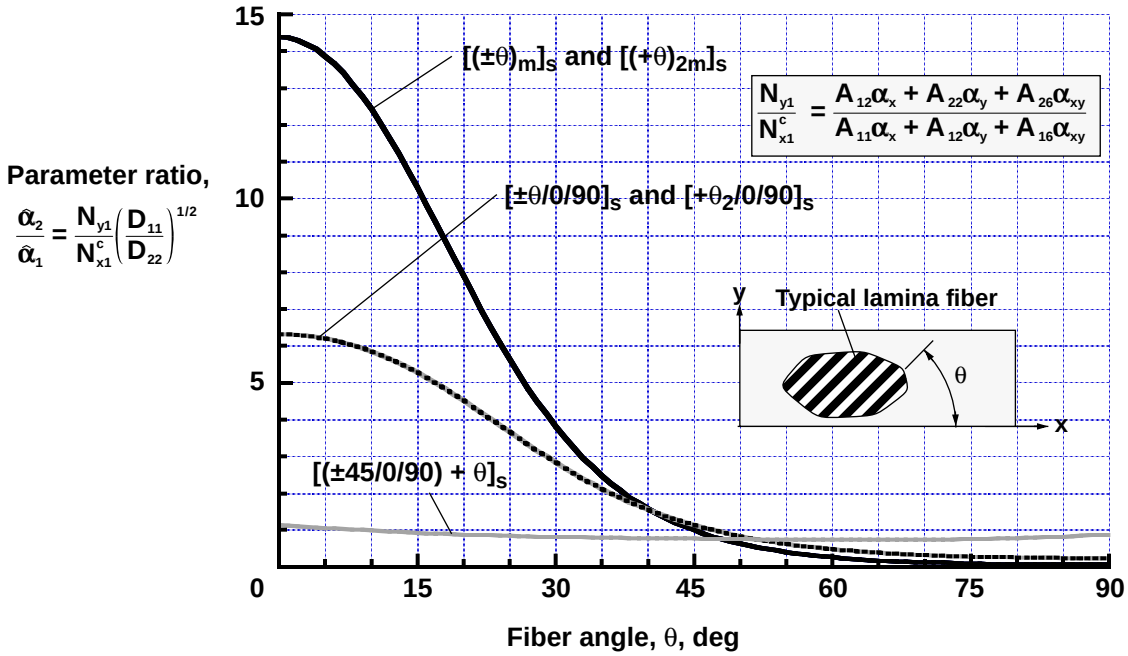

Figure 10. Ratio of stiffness-weighted thermal-expansion parameters $\hat{\alpha}_1$ and $\hat{\alpha}_2$ for balanced and unbalanced laminates with angle plies and unbalanced, unidirectional off-axis laminates made of IM7/5260 material (m = 1, 2, ...).

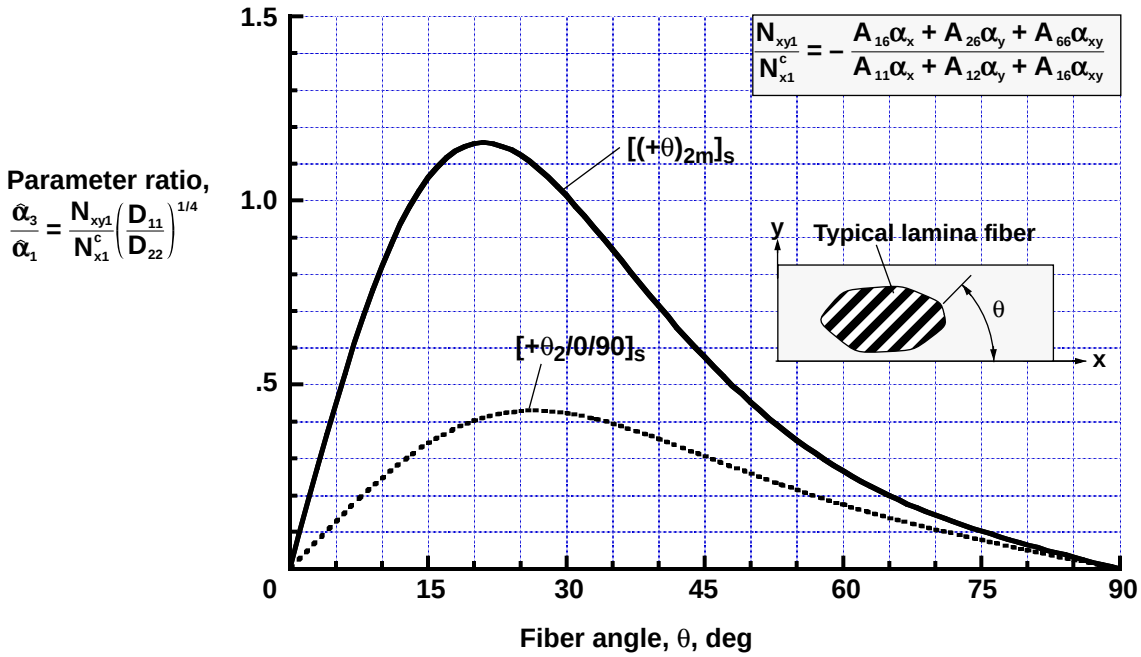

Figure 11. Ratio of stiffness-weighted thermal-expansion parameters $\hat{\alpha}_1$ and $\hat{\alpha}_3$ for $[(+\theta)_{2m}]_s$ and $[+\theta_2/0/90]_s$ unbalanced laminates made of IM7/5260 material (m = 1, 2, ...).

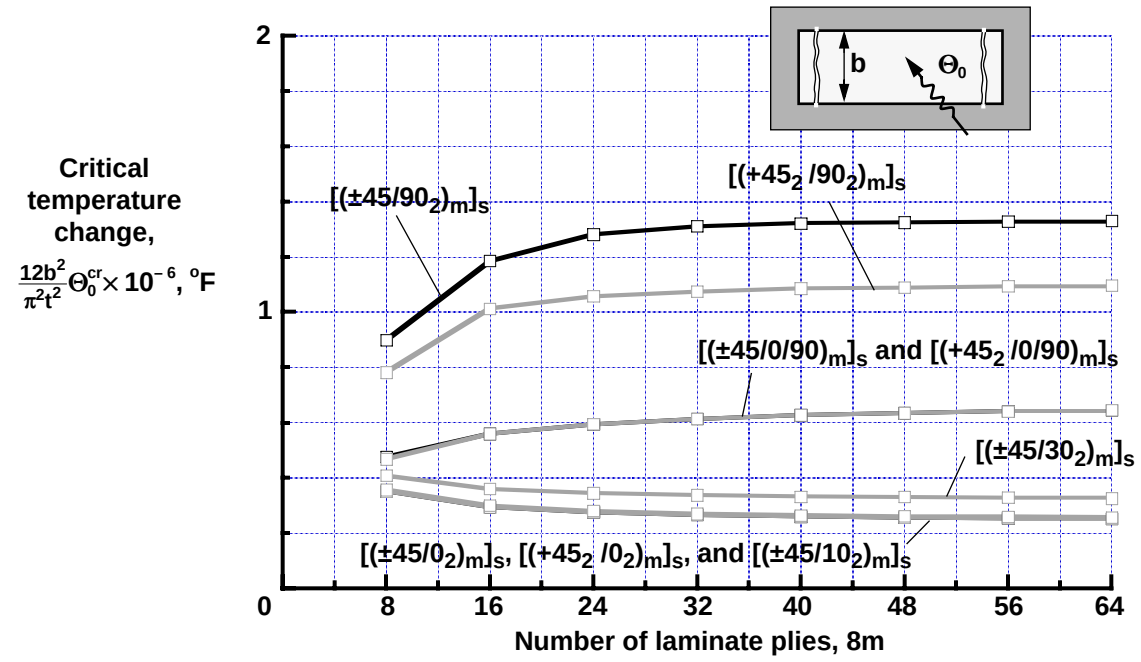

Figure 12. Critical temperature change for simply supported laminates made of IM7/5260 material, fully restrained against thermal expansion and contraction, and subjected to uniform heating.

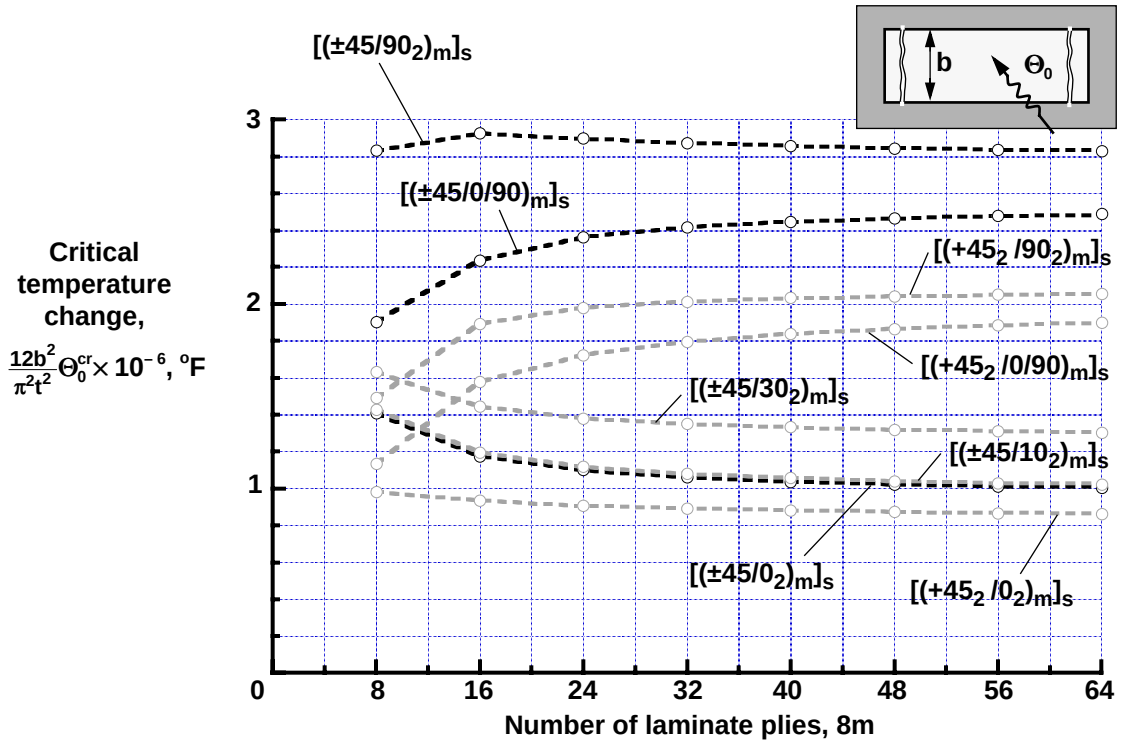

Figure 13. Critical temperature change for clamped laminates made of IM7/5260 material, fully restrained against thermal expansion or contraction, and subjected to uniform heating.

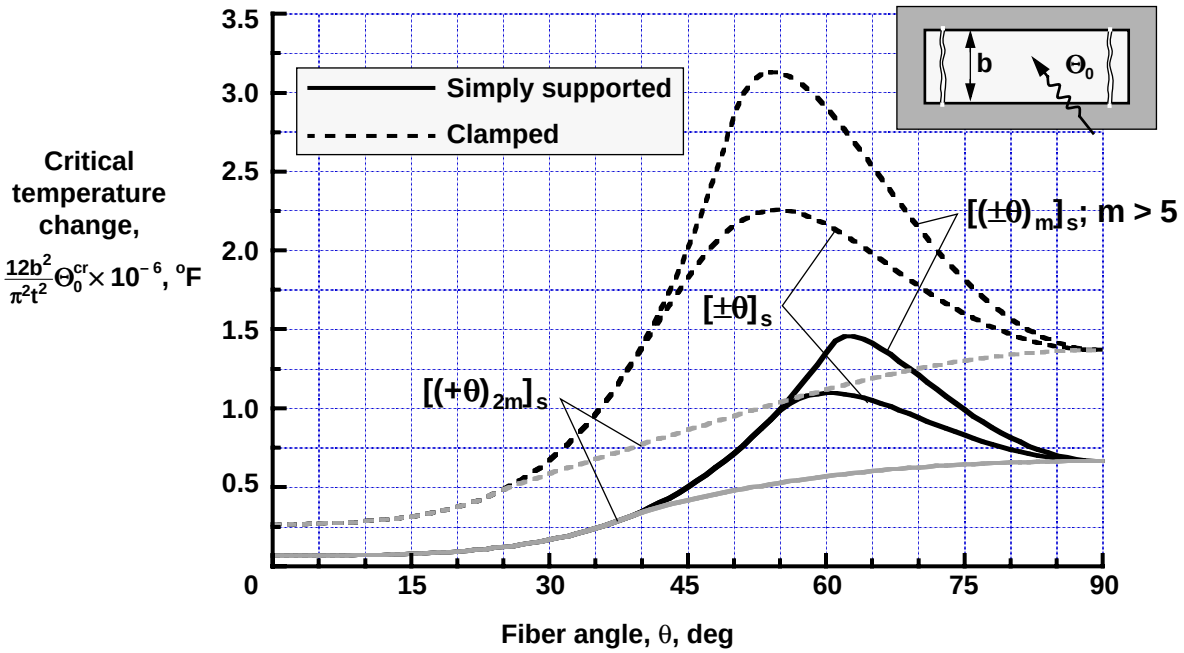

Figure 14. Critical temperature change for simply supported and clamped angle-ply laminates made of IM7/5260 material (m = 1, 2, ...).

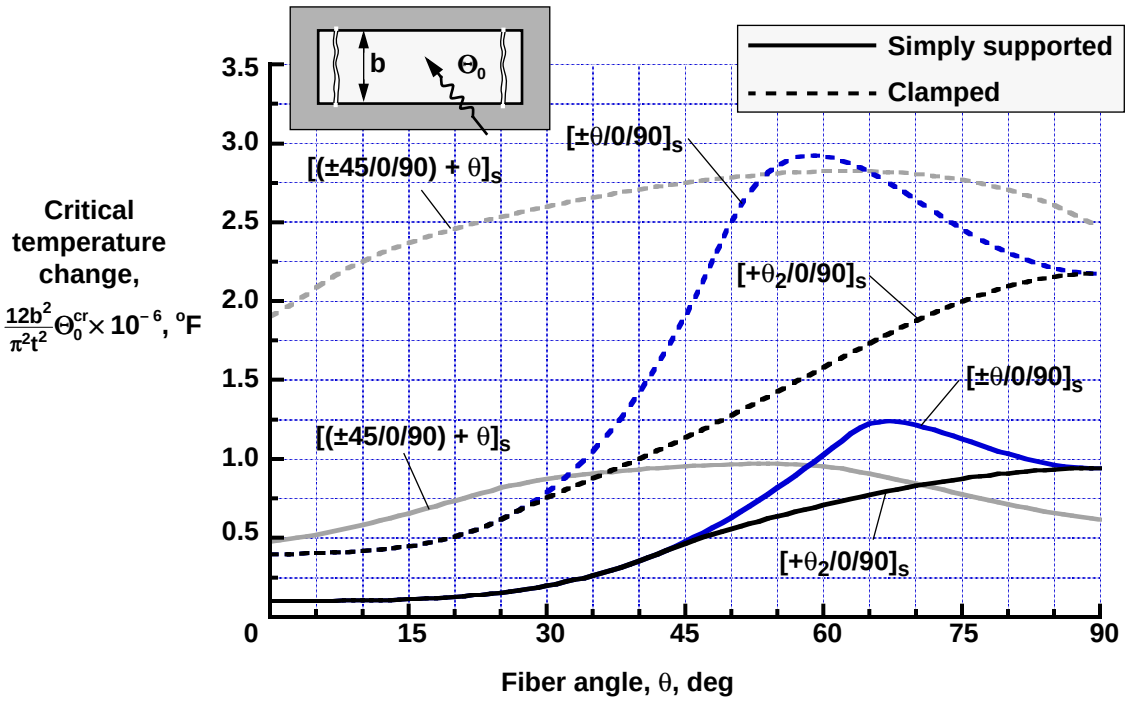

Figure 15. Critical temperature change for simply supported and clamped laminates with angle plies made of IM7/5260 material (m = 1, 2, ...).

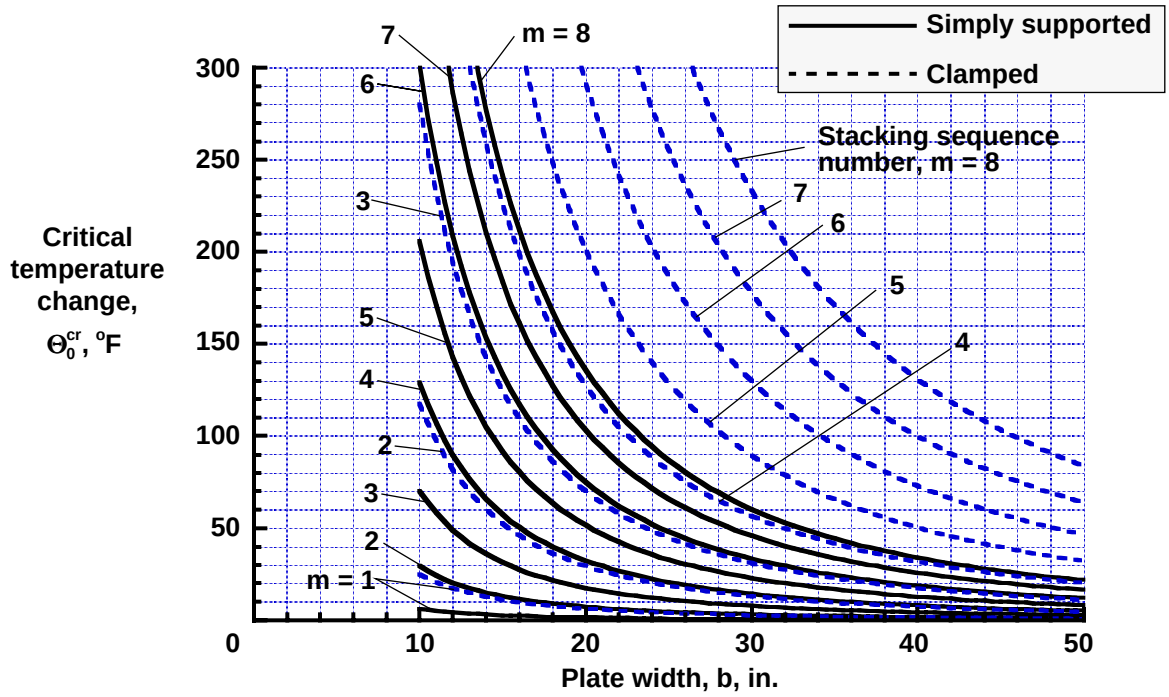

Figure 16. Critical temperature change versus plate width for simply supported and clamped $[(\pm45/0/90)_m]_s$ laminates made of IM7/5260 material, fully restrained against thermal expansion and contraction, and subjected to uniform heating.

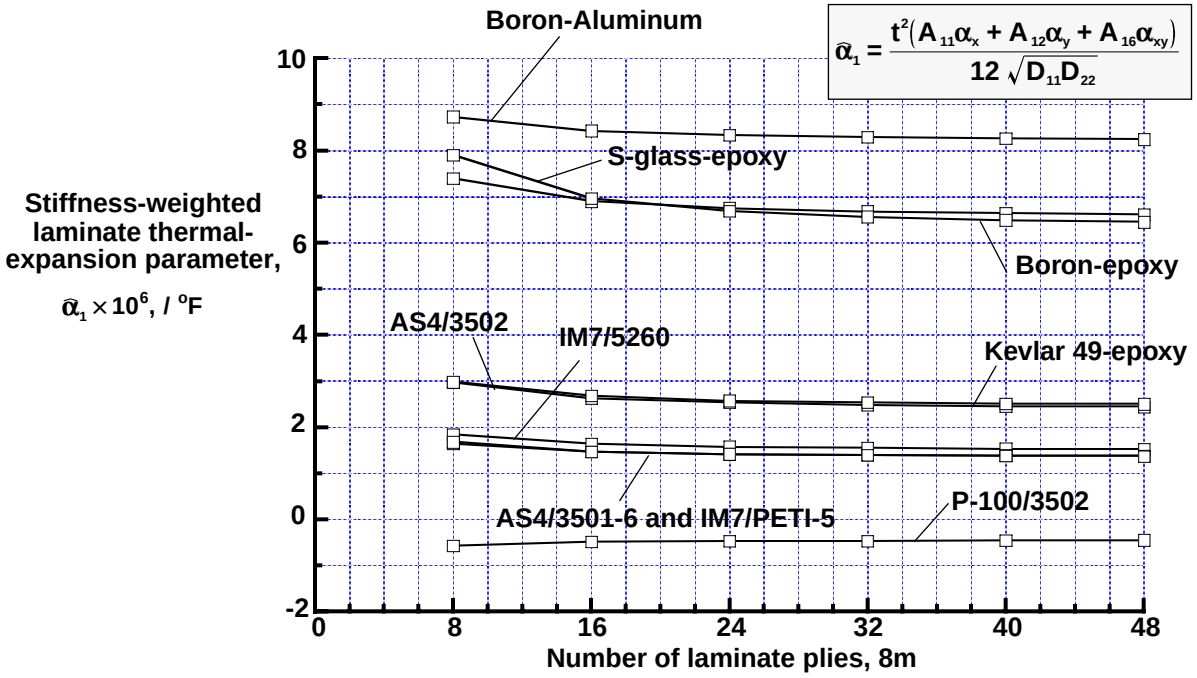

Figure 17. Effects of lamina material properties on stiffness-weighted laminate thermal-expansion parameter $\hat{\alpha}_1$ for $[(\pm 45/0/90)_m]_s$ laminates.

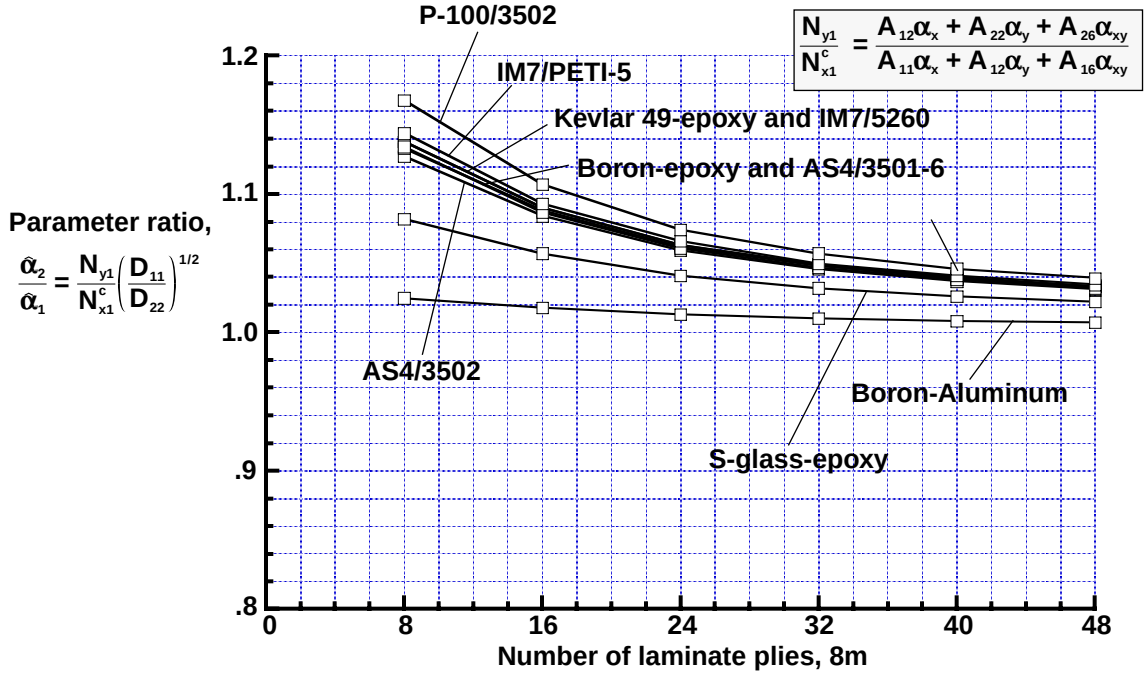

Figure 18. Effects of lamina material properties on parameter ratio $\hat{\alpha}_2/\hat{\alpha}_1$ for $[(\pm 45/0/90)_m]_s$ laminates.

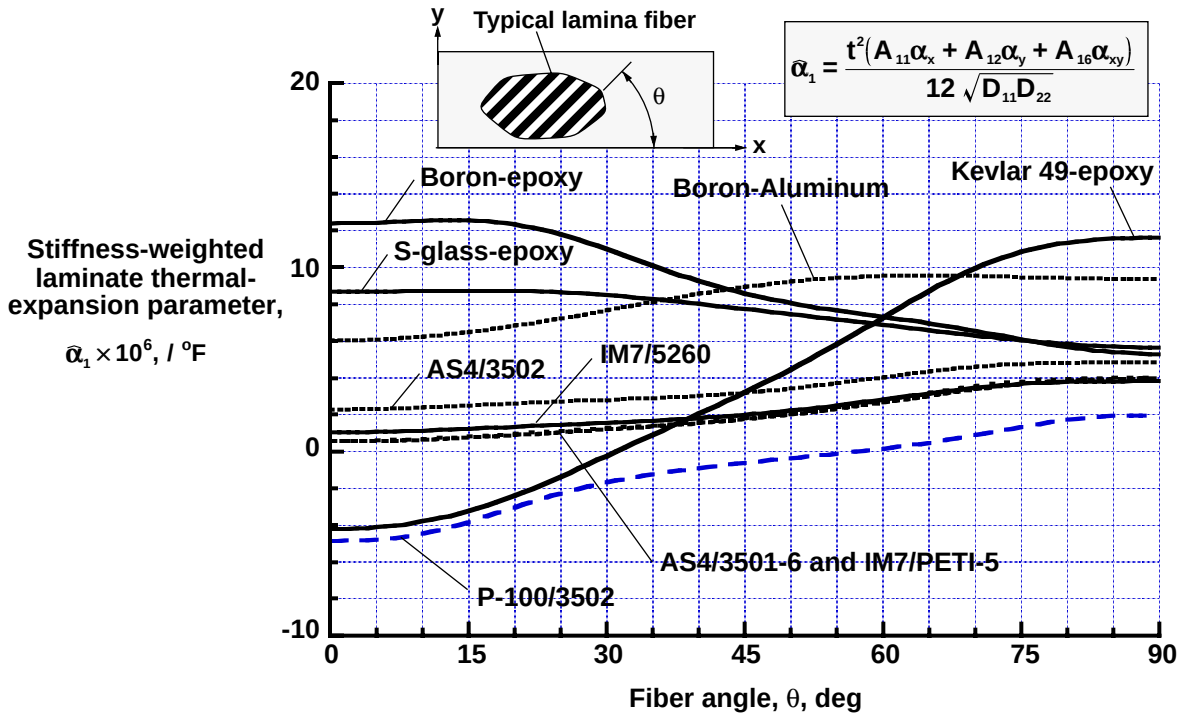

Figure 19. Effects of lamina material properties on stiffness-weighted laminate thermal-expansion parameter $\hat{\alpha}_1$ for $[(\pm\theta)_m]_s$ balanced, angle-ply laminates and $[(+\theta)_{2m}]_s$ unbalanced, unidirectional off-axis laminates.

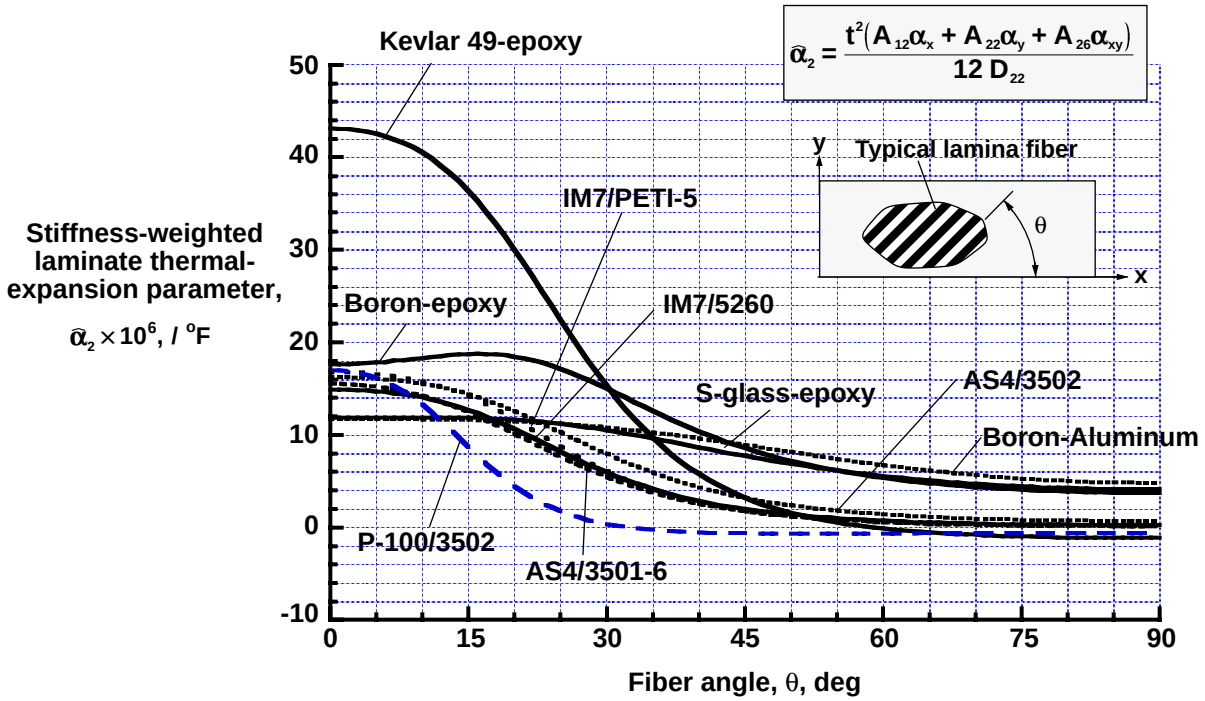

Figure 20. Effects of lamina material properties on stiffness-weighted laminate thermal-expansion parameter $\hat{\alpha}_2$ for $[(\pm\theta)_m]_s$ balanced, angle-ply laminates and $[(+\theta)_{2m}]_s$ unbalanced, unidirectional off-axis laminates.

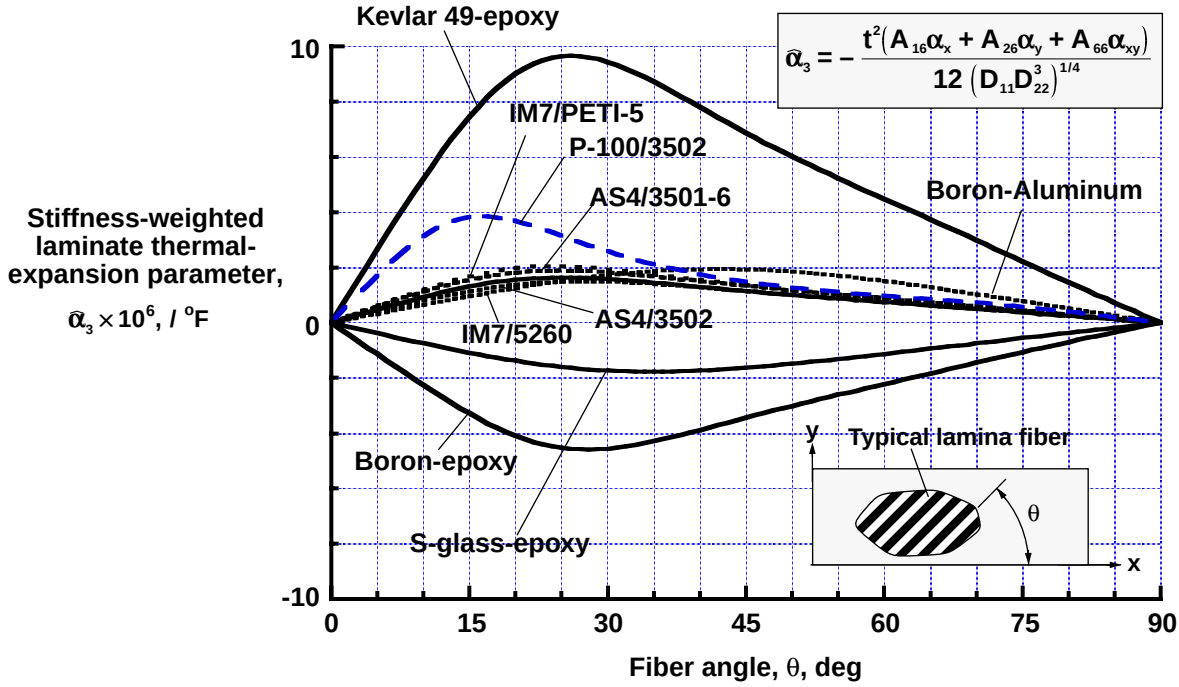

Figure 21. Effects of lamina material properties on stiffness-weighted laminate thermal-expansion parameter $\hat{\alpha}_3$ for $[(+\theta)_{2m}]_s$ unbalanced, unidirectional off-axis laminates.

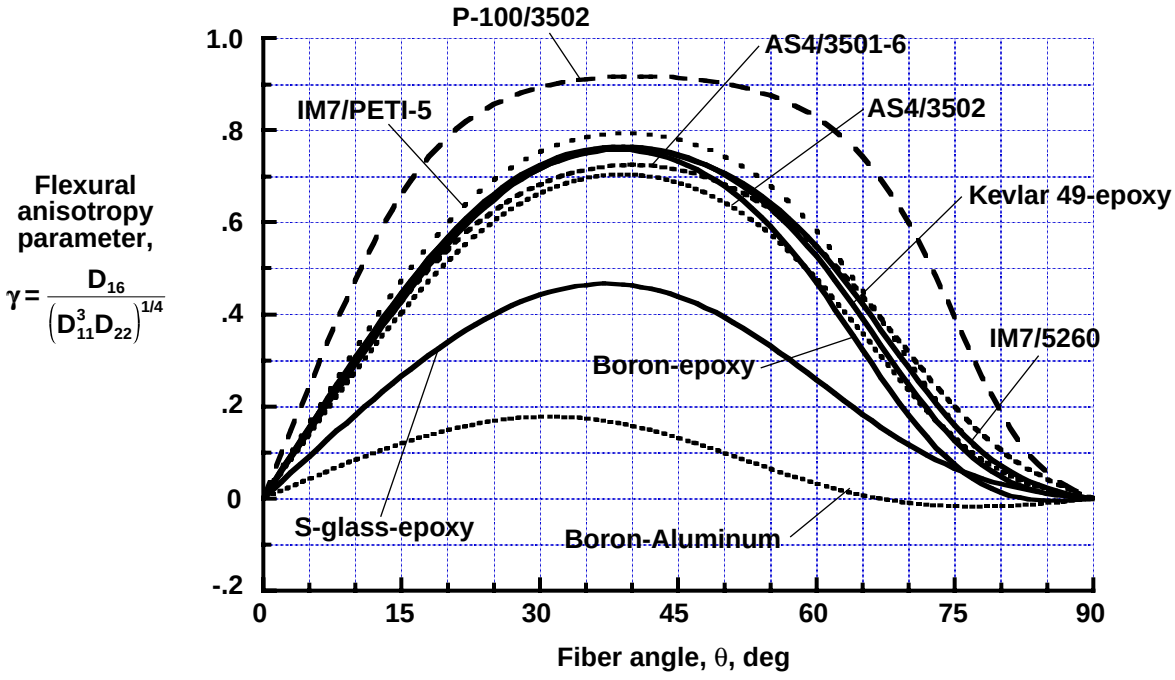

Figure 22. Effects of lamina material properties on nondimensional flexural anisotropy parameter γ for $[(+\theta)_{2m}]_s$ laminates (m = 1, 2, ...).

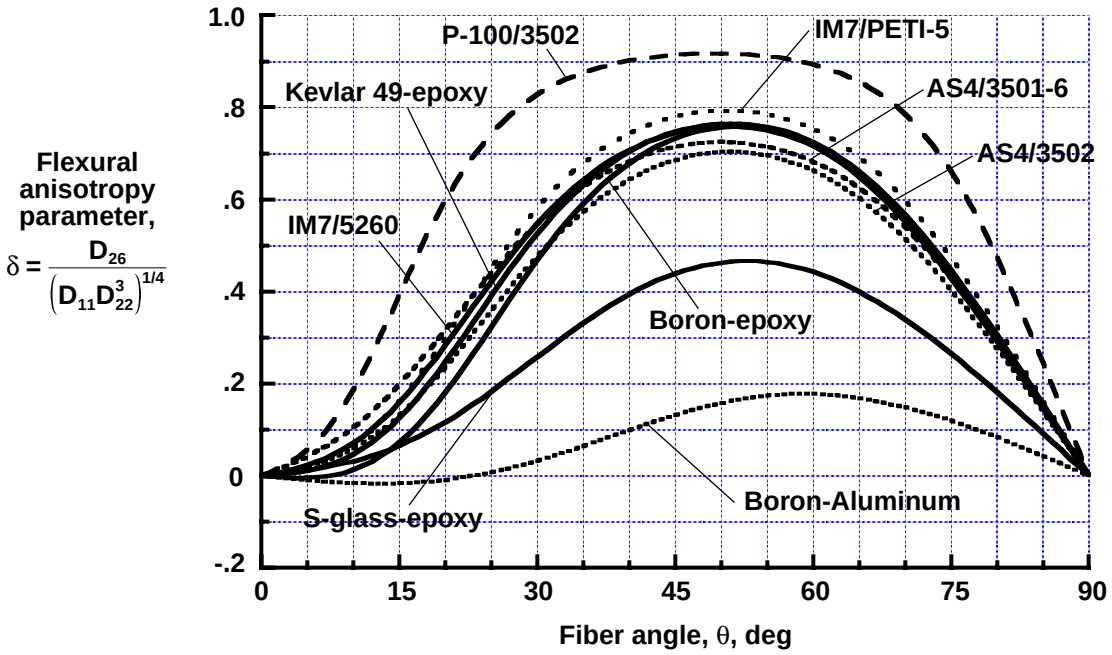

Figure 23. Effects of lamina material properties on nondimensional flexural anisotropy parameter δ for $[(+\theta)_{2m}]_s$ laminates (m = 1, 2, ...).

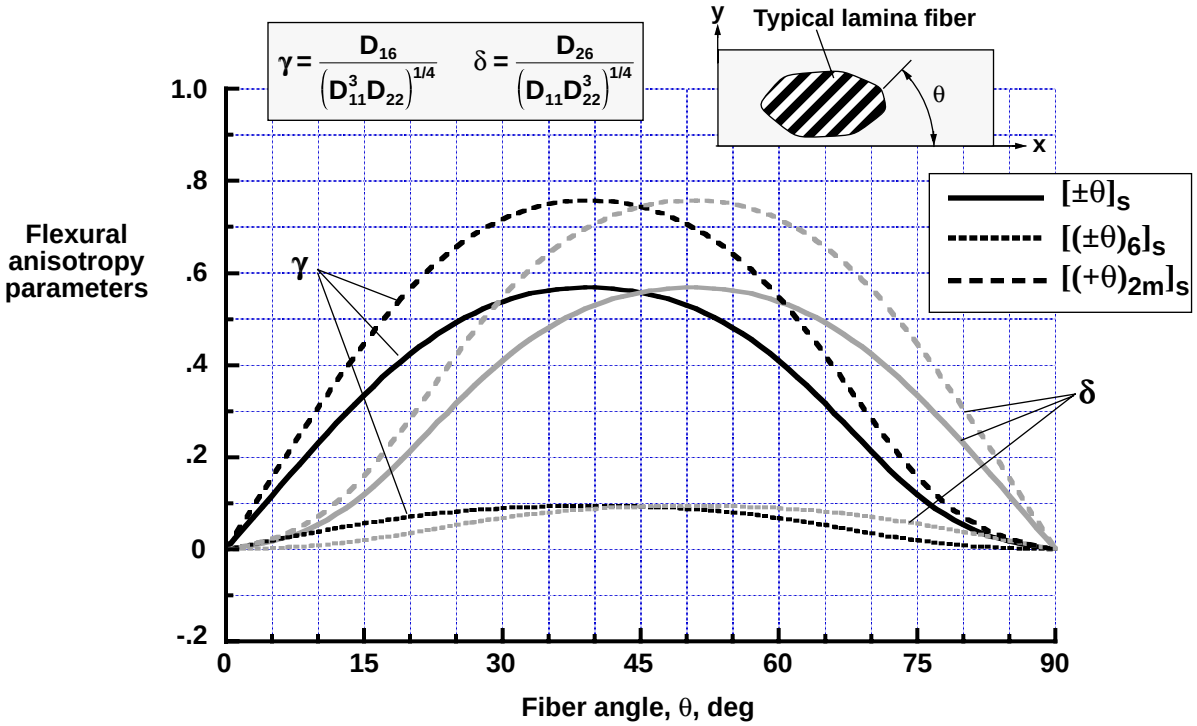

Figure 24. Flexural anisotropy parameters for angle-ply laminates made of IM7/5260 material.

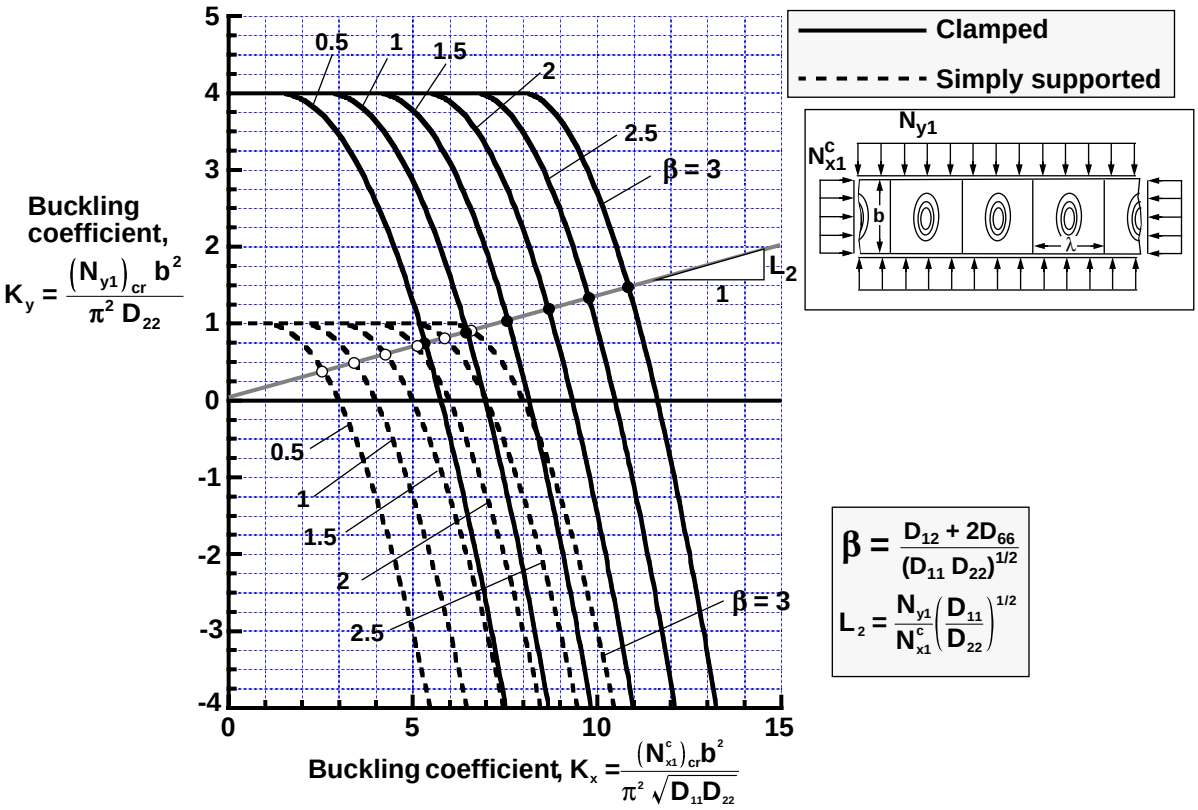

Figure 25. Effects of orthotropy parameter β on buckling interaction curves for specially orthotropic plates ($\gamma = \delta = 0$) subjected to axial compression and transverse tension or compression loads.

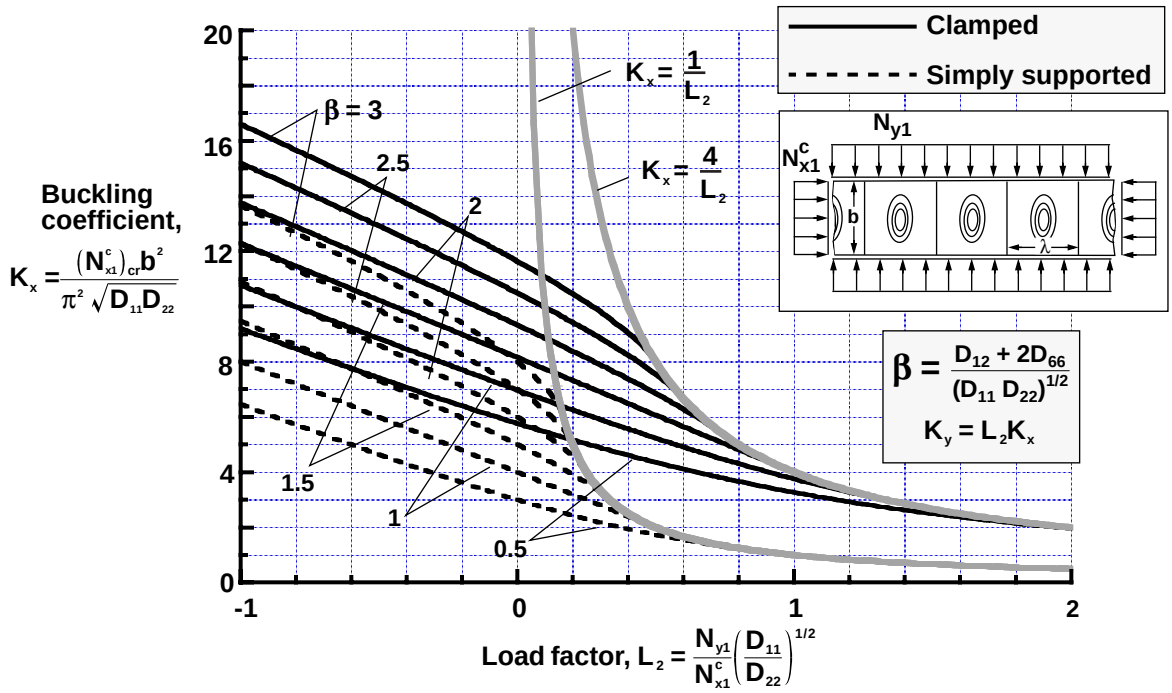

Figure 26. Effects of orthotropy parameter β and load factor on buckling coefficient for specially orthotropic plates ($\gamma = \delta = 0$) subjected to axial compression and transverse tension or compression loads.

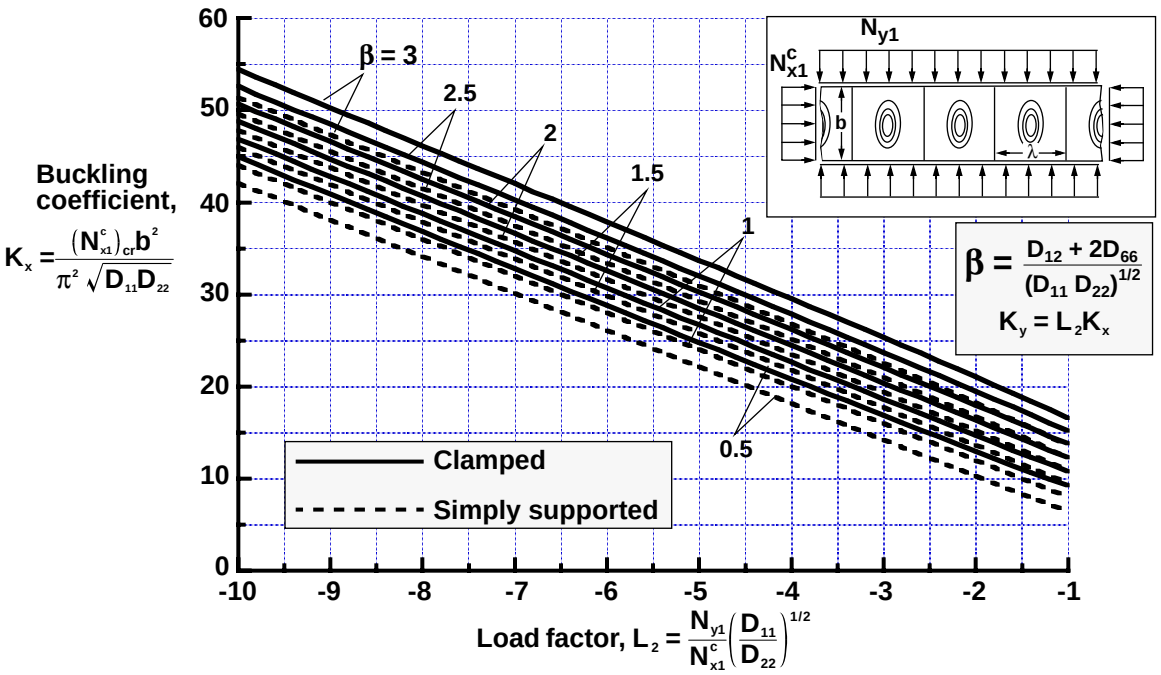

Figure 27. Effects of orthotropy parameter β and load factor on buckling coefficient for specially orthotropic plates (γ = δ = 0) subjected to axial compression and transverse tension or compression loads.

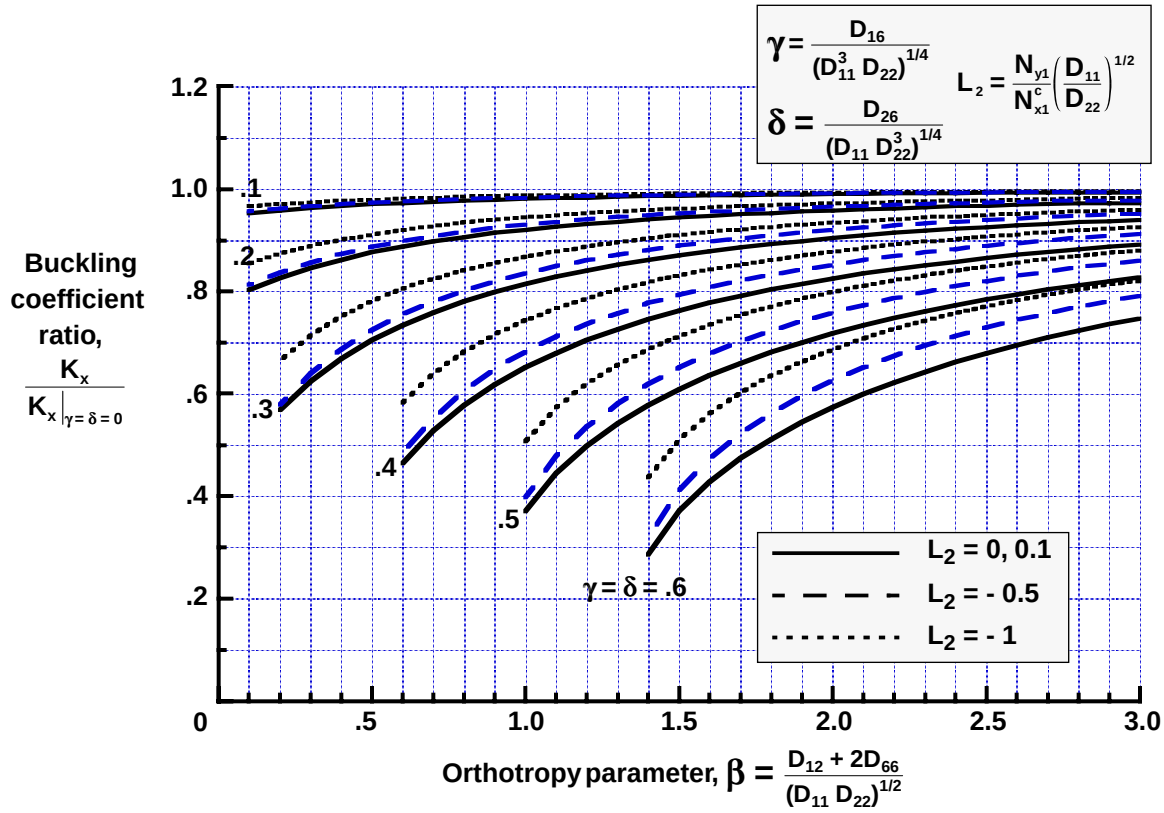

Figure 28. Effects of flexural orthotropy parameter β and flexural anisotropy parameters γ and δ on buckling coefficients for simply supported plates subjected to axial compression and transverse tension or compression loads.

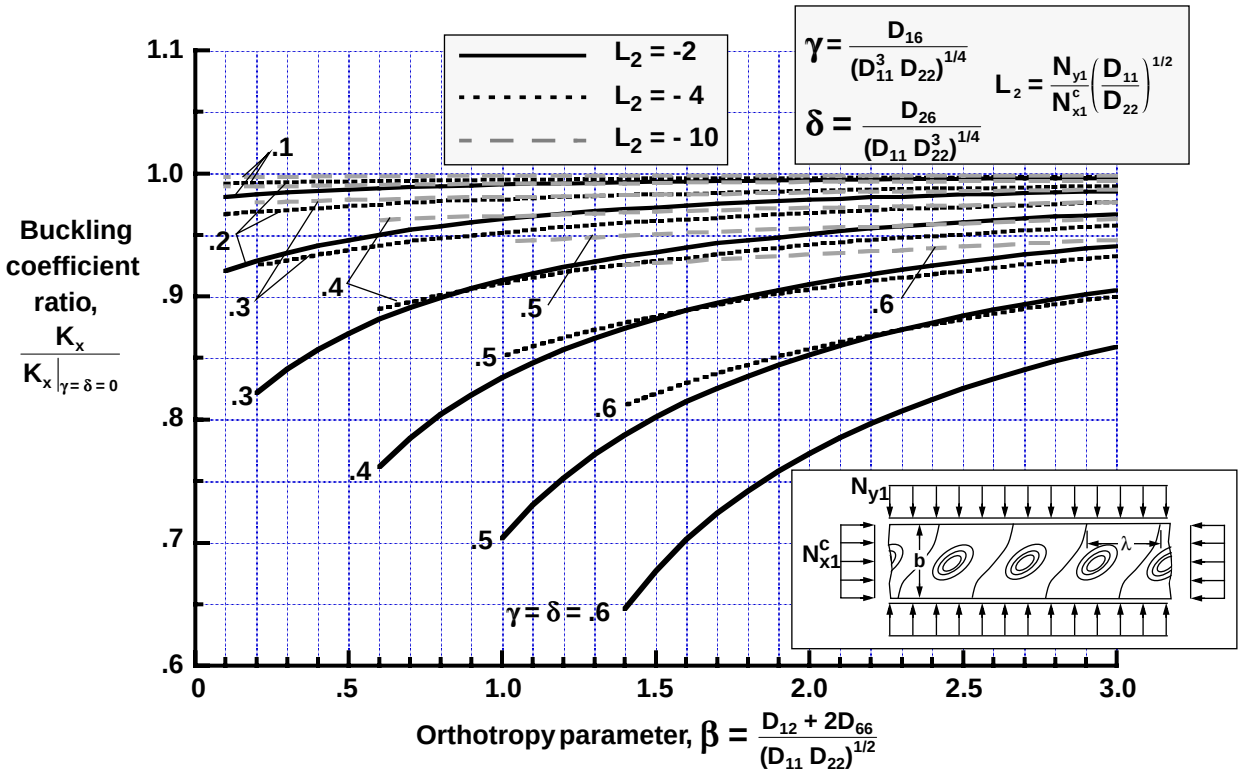

Figure 29. Effects of flexural orthotropy parameter β and flexural anisotropy parameters γ and δ on buckling coefficients for simply supported plates subjected to axial compression and transverse tension or compression loads.

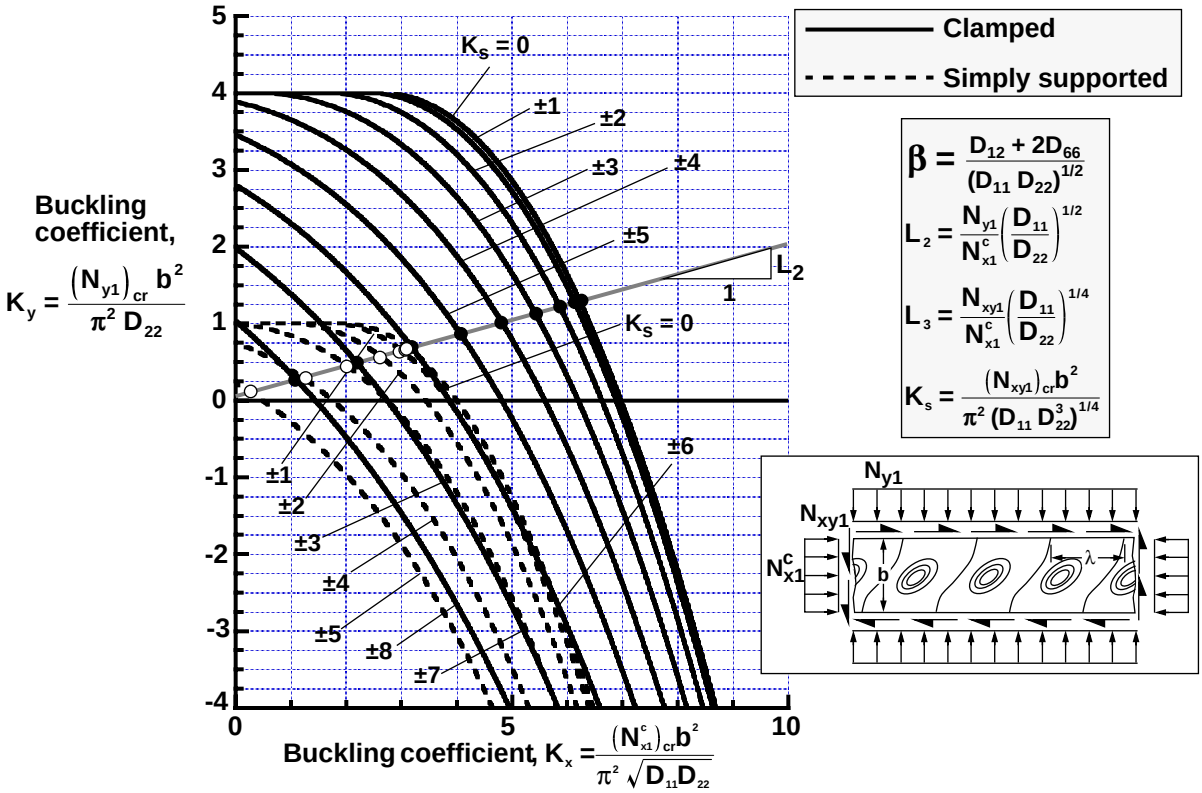

Figure 30. Buckling interaction curves for specially orthotropic plates (γ = δ = 0) with β = 1 and subjected to axial compression, transverse tension or compression, and shear loads.

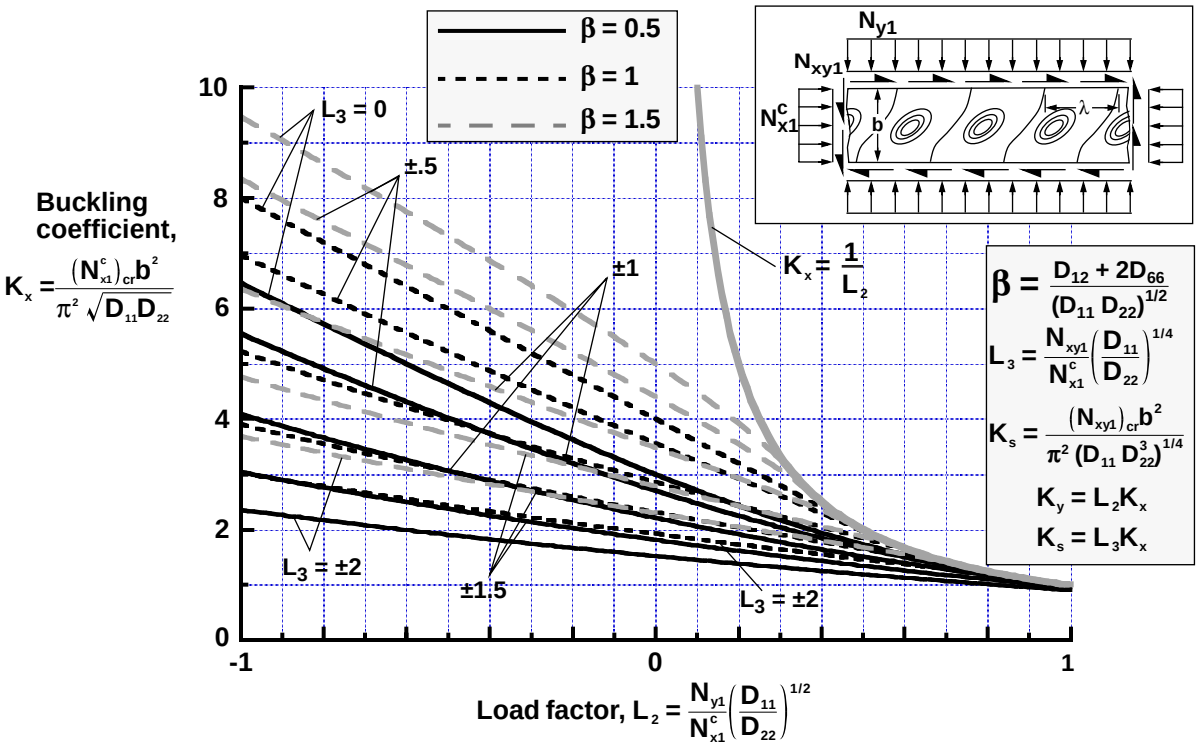

Figure 31. Effects of orthotropy parameter β and load factors on buckling coefficient for simply supported, specially orthotropic plates (γ = δ = 0) subjected to axial compression, transverse tension or compression, and shear loads.

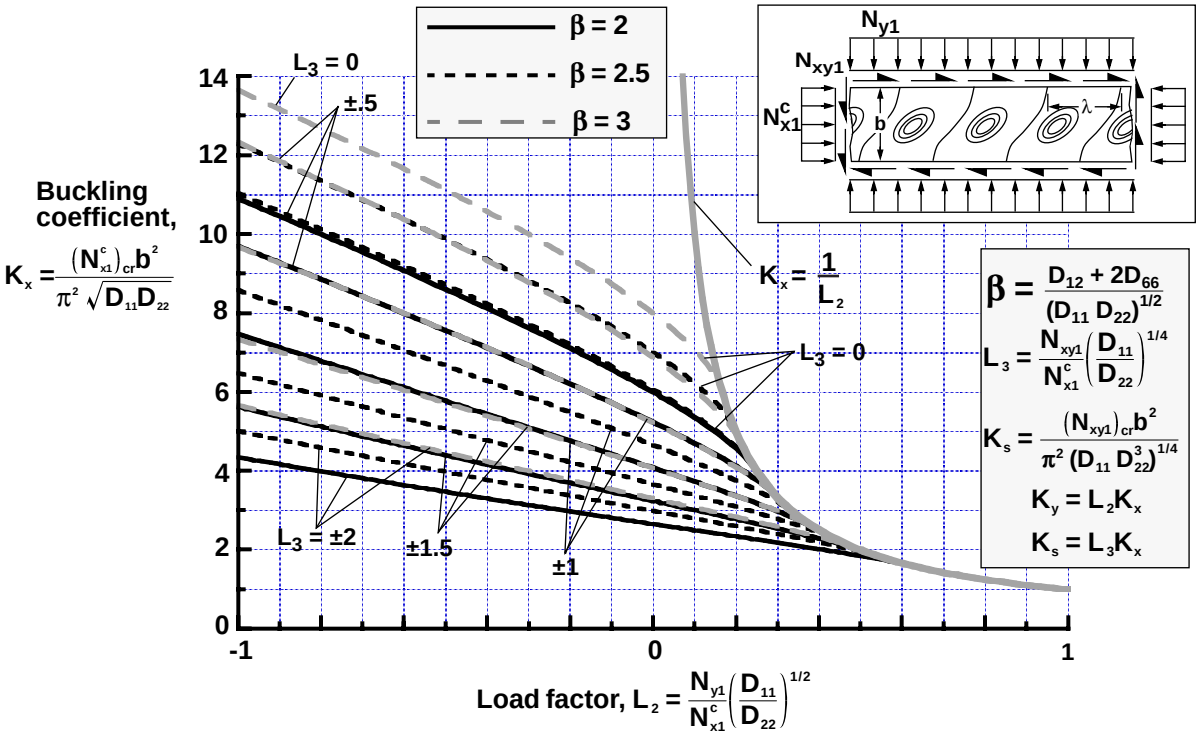

Figure 32. Effects of orthotropy parameter β and load factors on buckling coefficient for simply supported, specially orthotropic plates (γ = δ = 0) subjected to axial compression, transverse tension or compression, and shear loads.

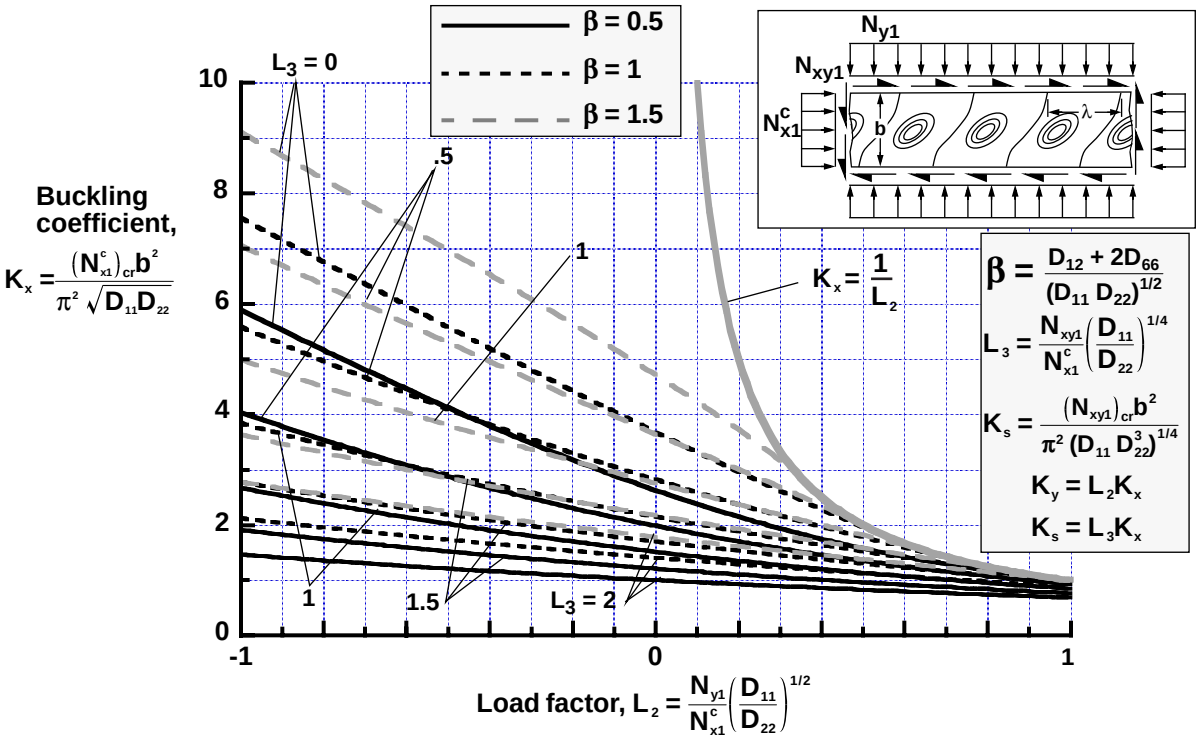

Figure 33. Effects of orthotropy parameter β and load factors on buckling coefficient for simply supported, specially orthotropic plates (γ = δ = 0.2) subjected to axial compression, transverse tension or compression, and shear loads.

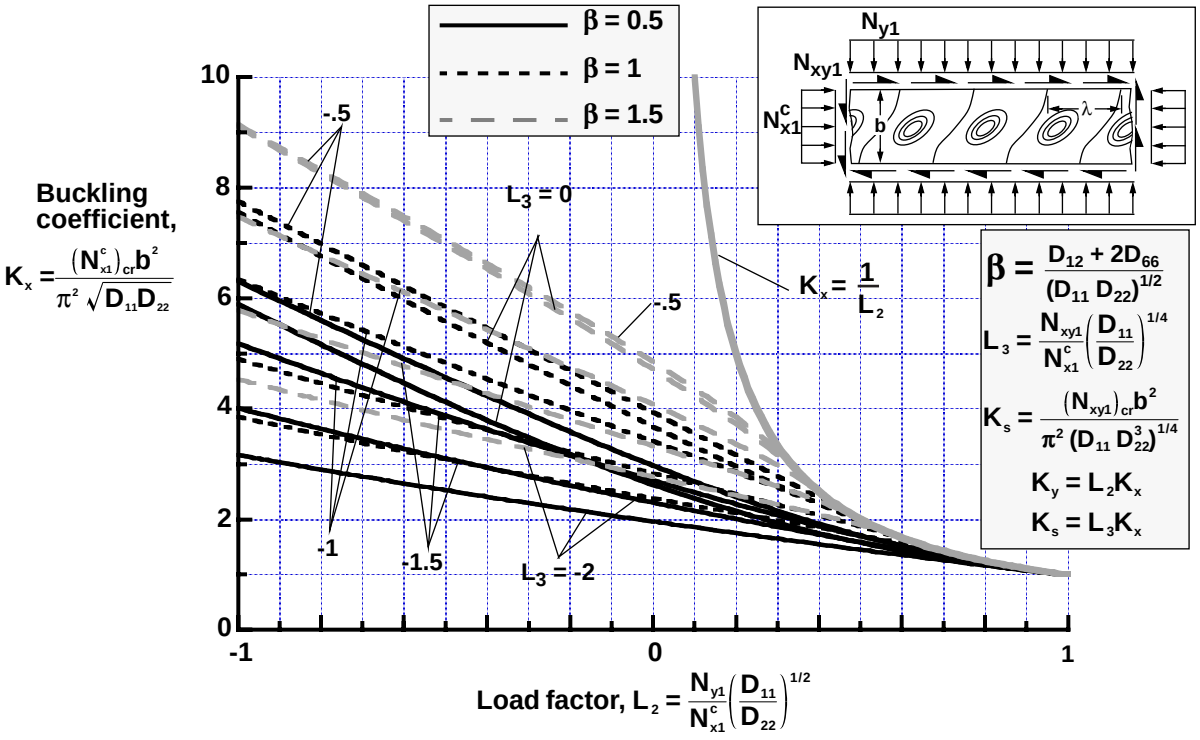

Figure 34. Effects of orthotropy parameter β and load factors on buckling coefficient for simply supported, specially orthotropic plates (γ = δ = 0.2) subjected to axial compression, transverse tension or compression, and shear loads.

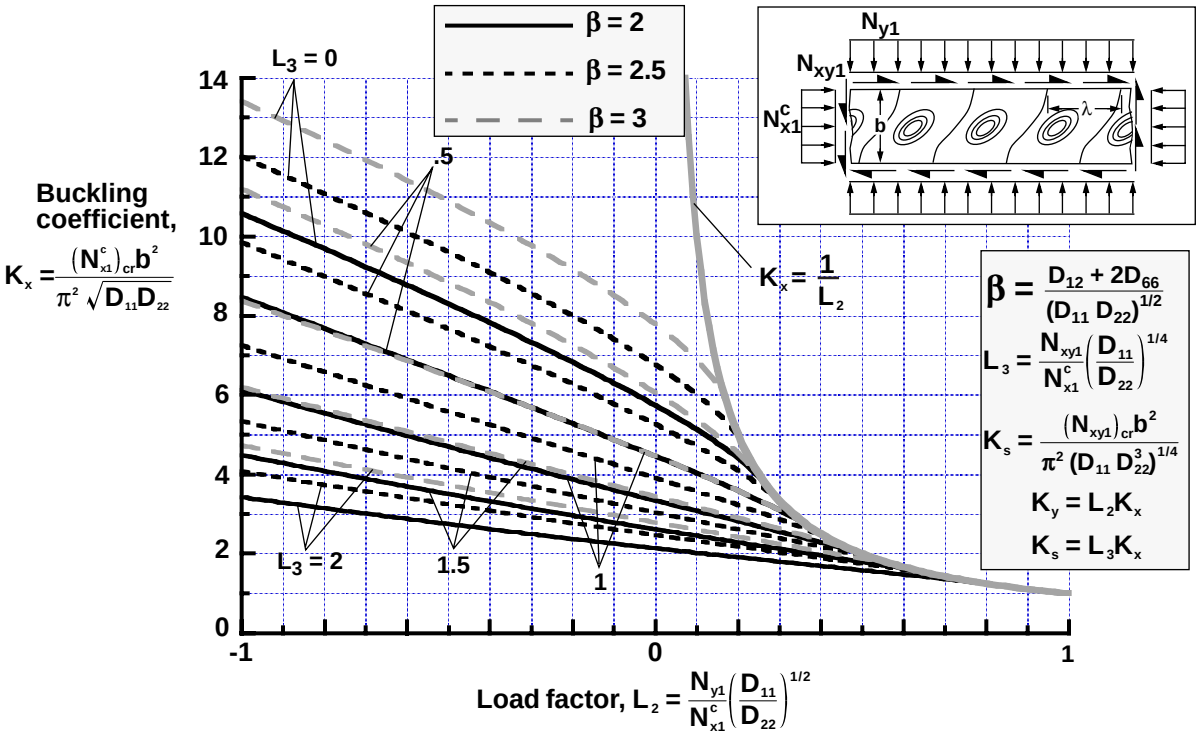

Figure 35. Effects of orthotropy parameter β and load factors on buckling coefficient for simply supported, specially orthotropic plates (γ = δ = 0.2) subjected to axial compression, transverse tension or compression, and shear loads.

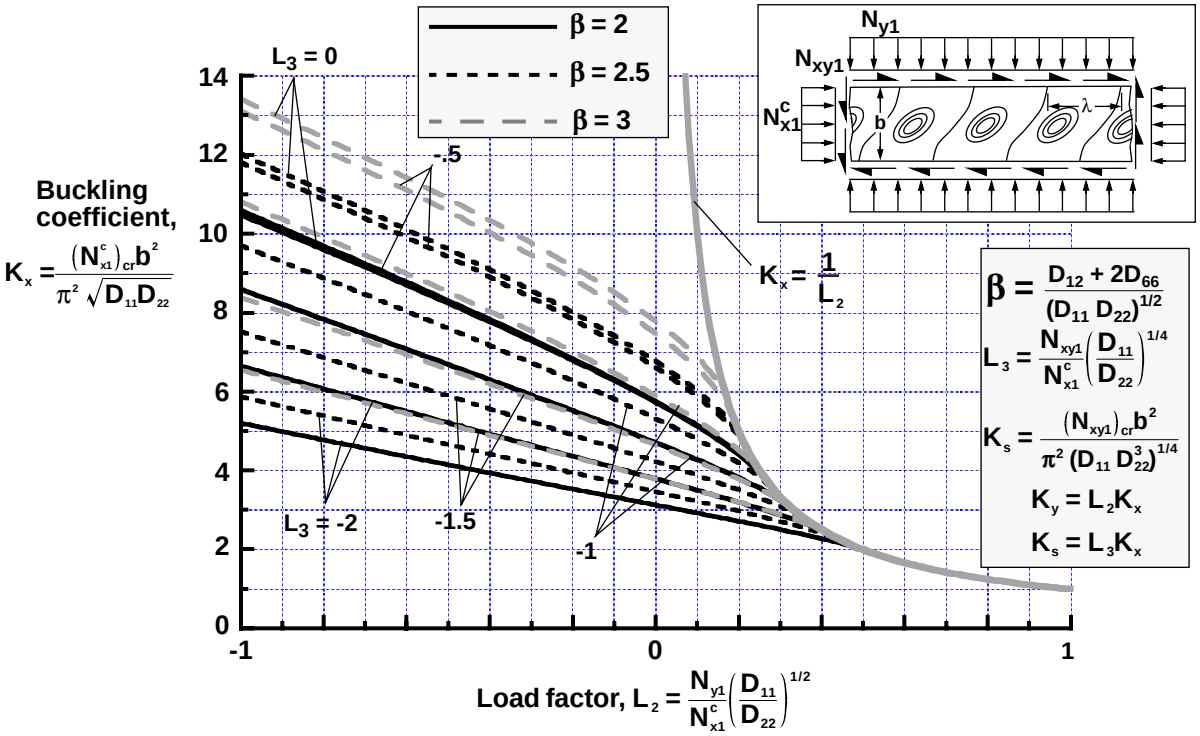

Figure 36. Effects of orthotropy parameter β and load factors on buckling coefficient for simply supported, specially orthotropic plates (γ = δ = 0.2) subjected to axial compression, transverse tension or compression, and shear loads.

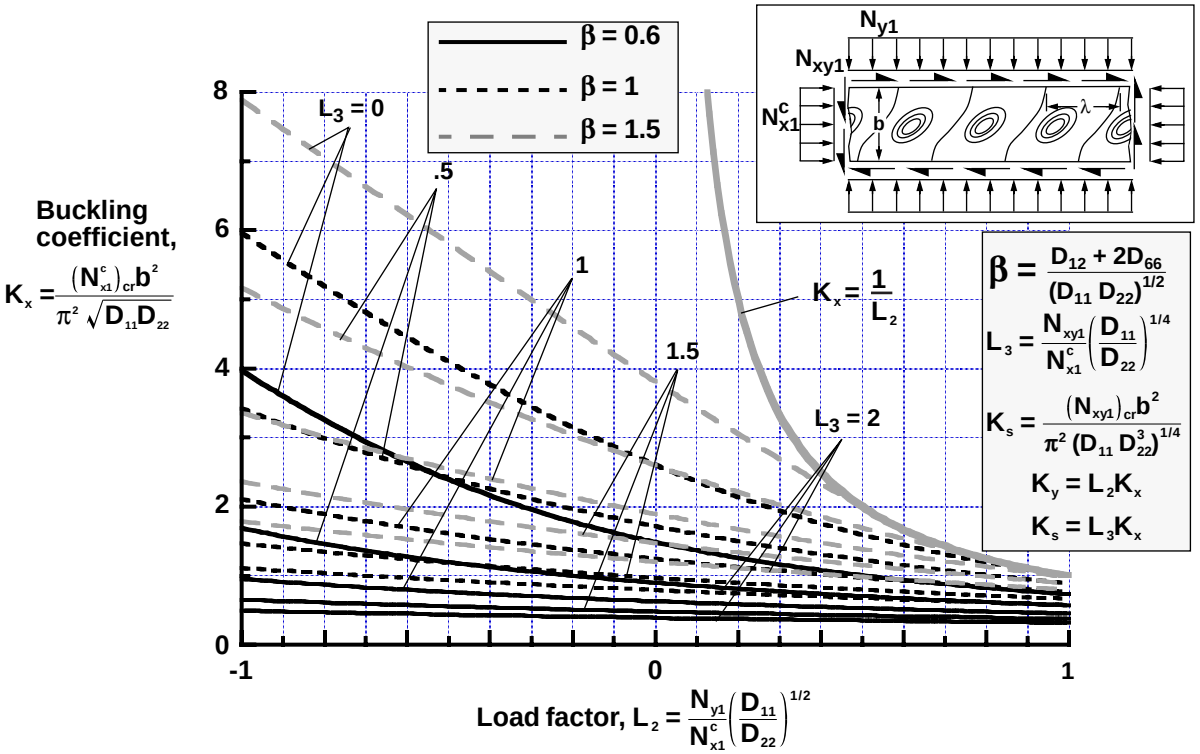

Figure 37. Effects of orthotropy parameter β and load factors on buckling coefficient for simply supported, specially orthotropic plates ($\gamma = \delta = 0.4$) subjected to axial compression, transverse tension or compression, and shear loads.

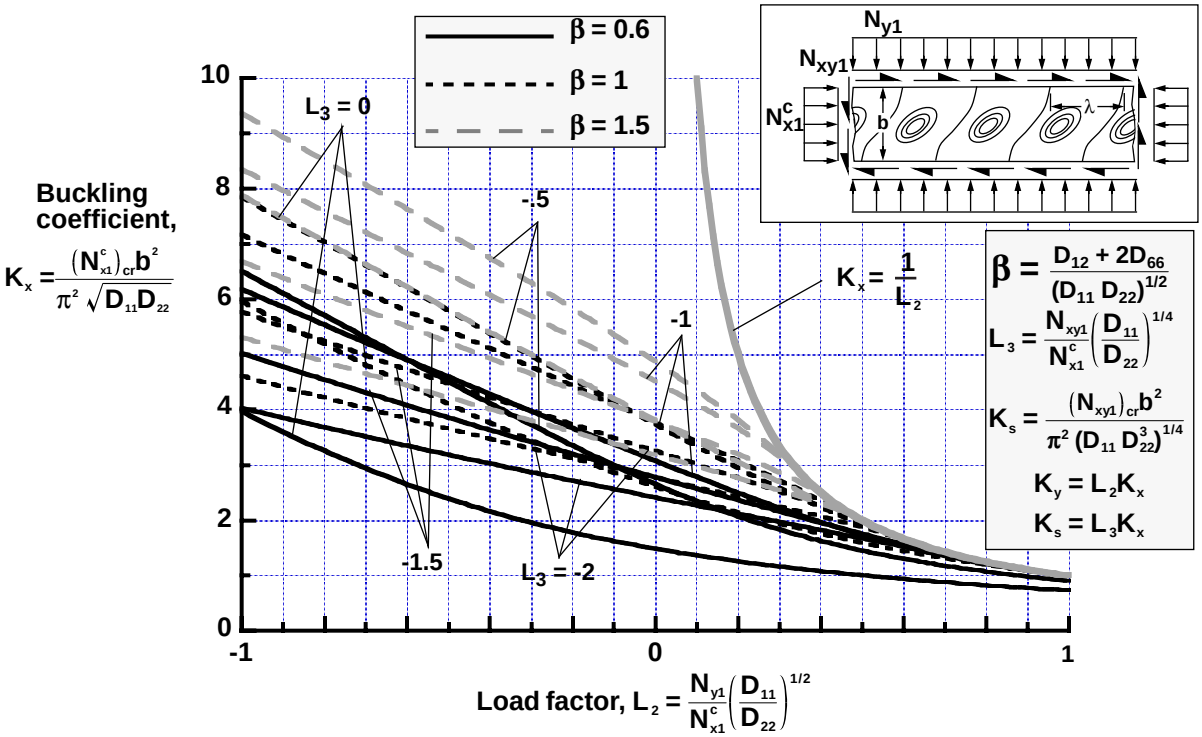

Figure 38. Effects of orthotropy parameter β and load factors on buckling coefficient for simply supported, specially orthotropic plates ($\gamma = \delta = 0.4$) subjected to axial compression, transverse tension or compression, and shear loads.

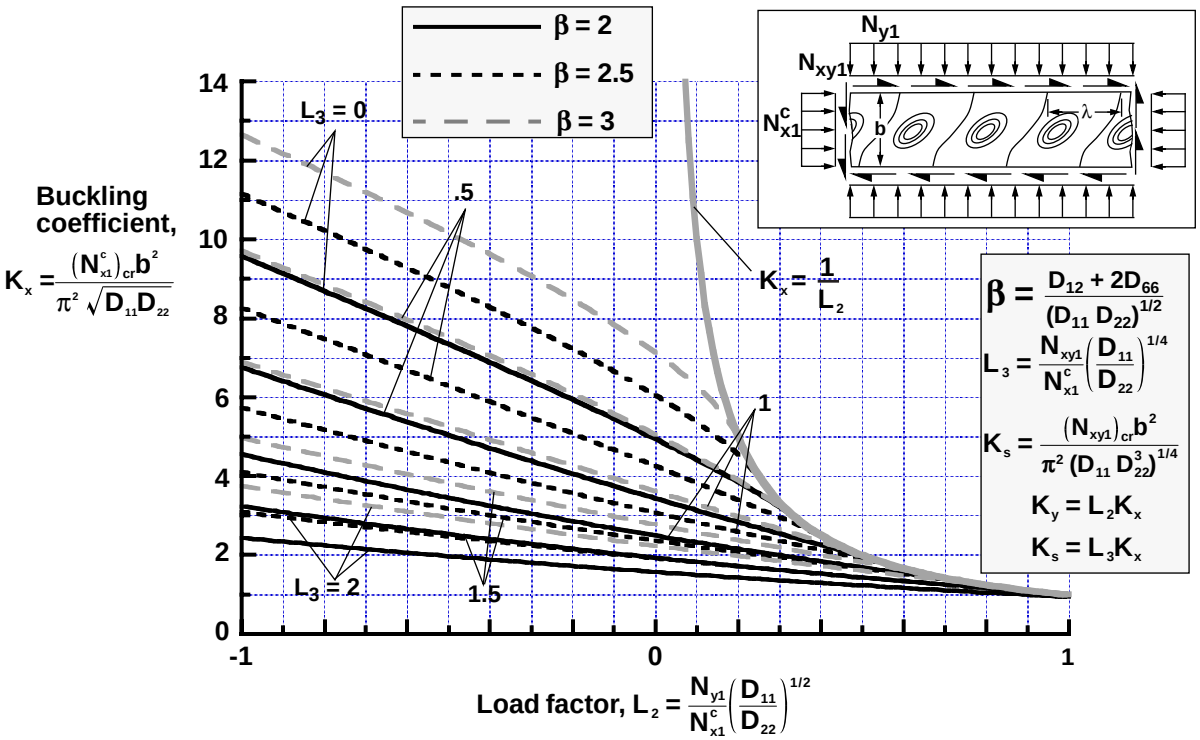

Figure 39. Effects of orthotropy parameter β and load factors on buckling coefficient for simply supported, specially orthotropic plates (γ = δ = 0.4) subjected to axial compression, transverse tension or compression, and shear loads.

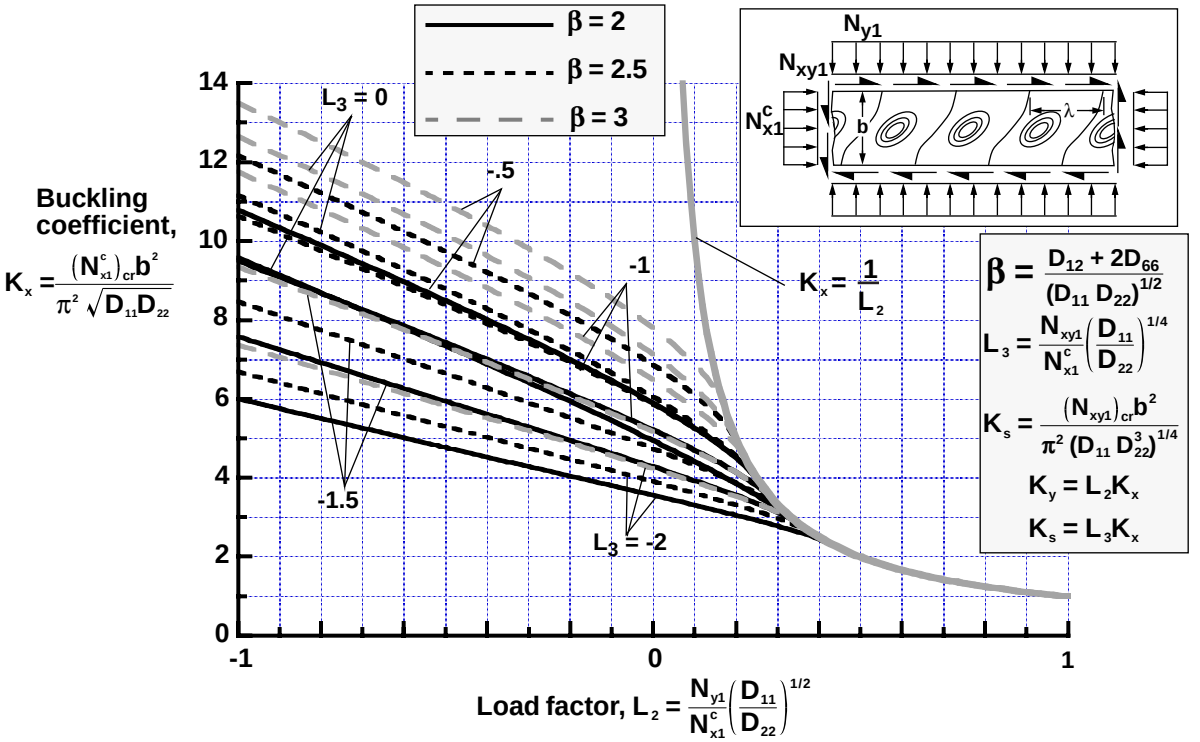

Figure 40. Effects of orthotropy parameter β and load factors on buckling coefficient for simply supported, specially orthotropic plates (γ = δ = 0.4) subjected to axial compression, transverse tension or compression, and shear loads.

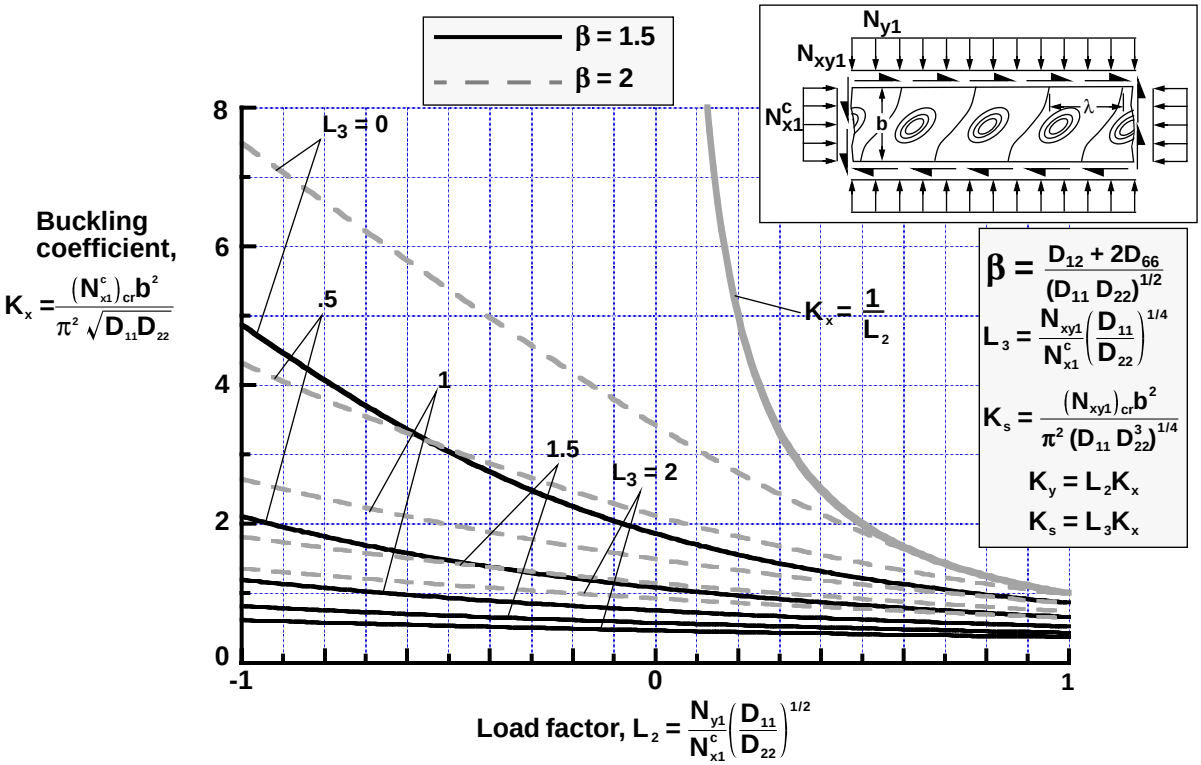

Figure 41. Effects of orthotropy parameter β and load factors on buckling coefficient for simply supported, specially orthotropic plates (γ = δ = 0.6) subjected to axial compression, transverse tension or compression, and shear loads.

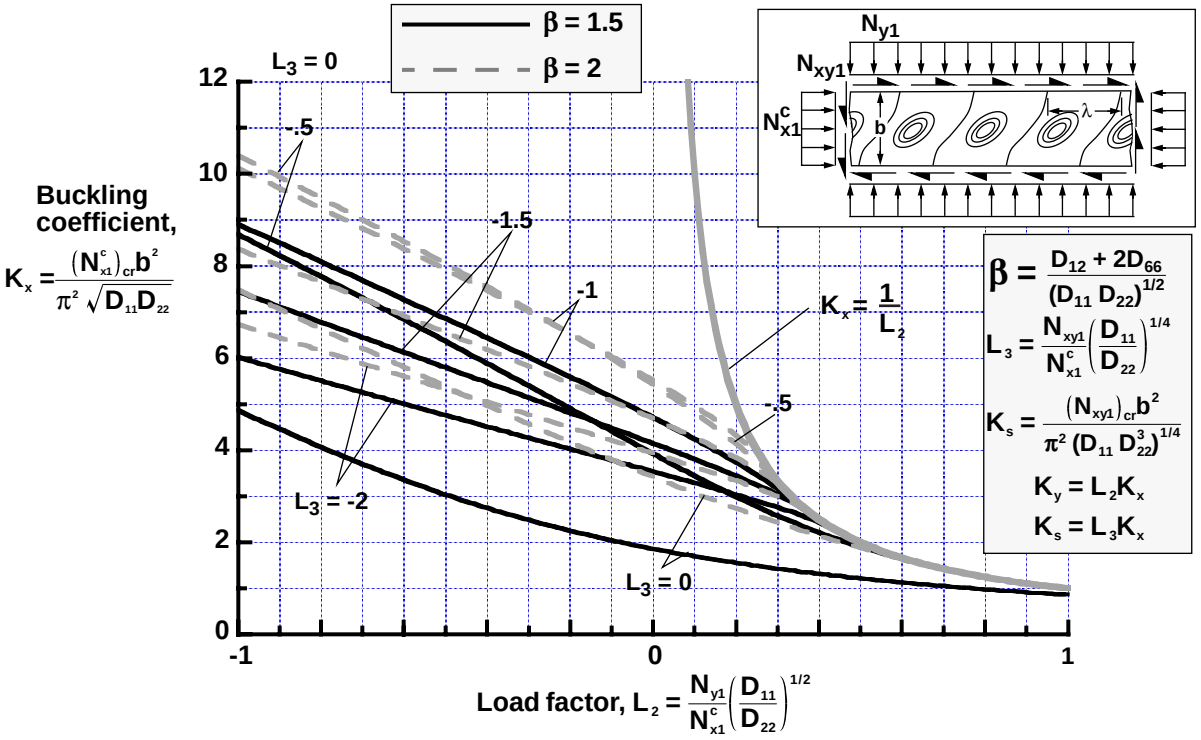

Figure 42. Effects of orthotropy parameter β and load factors on buckling coefficient for simply supported, specially orthotropic plates (γ = δ = 0.6) subjected to axial compression, transverse tension or compression, and shear loads.

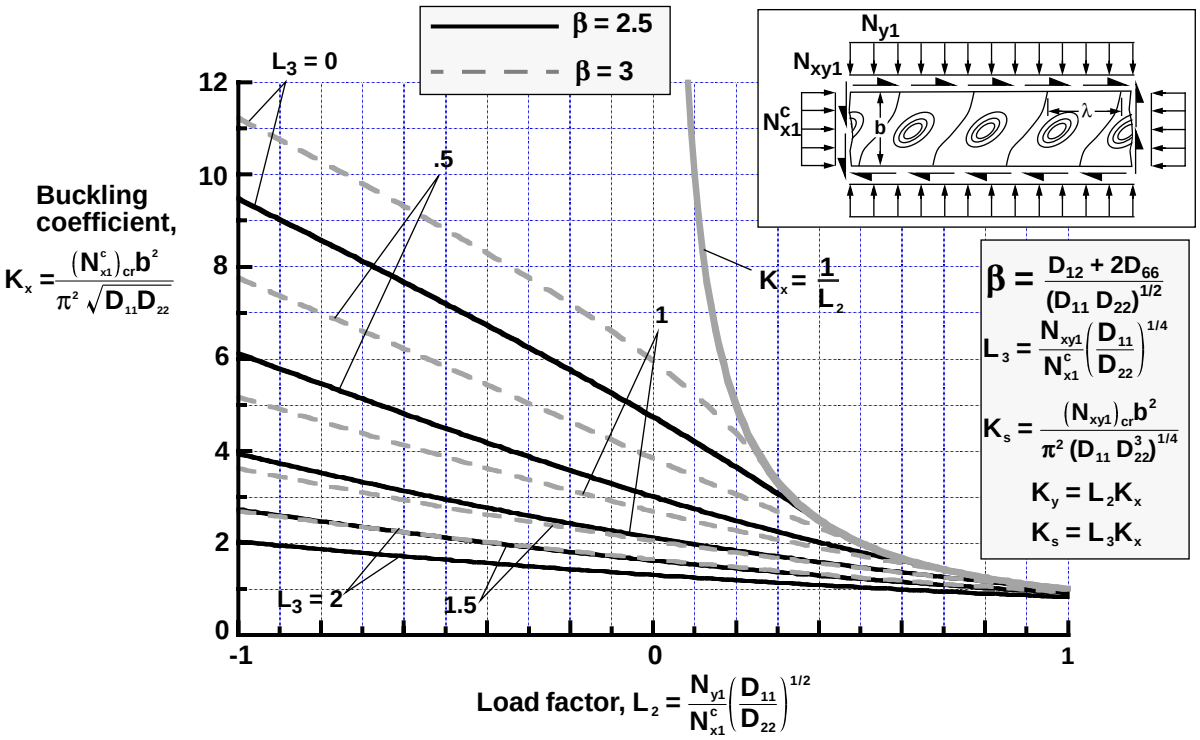

Figure 43. Effects of orthotropy parameter β and load factors on buckling coefficient for simply supported, specially orthotropic plates (γ = δ = 0.6) subjected to axial compression, transverse tension or compression, and shear loads.

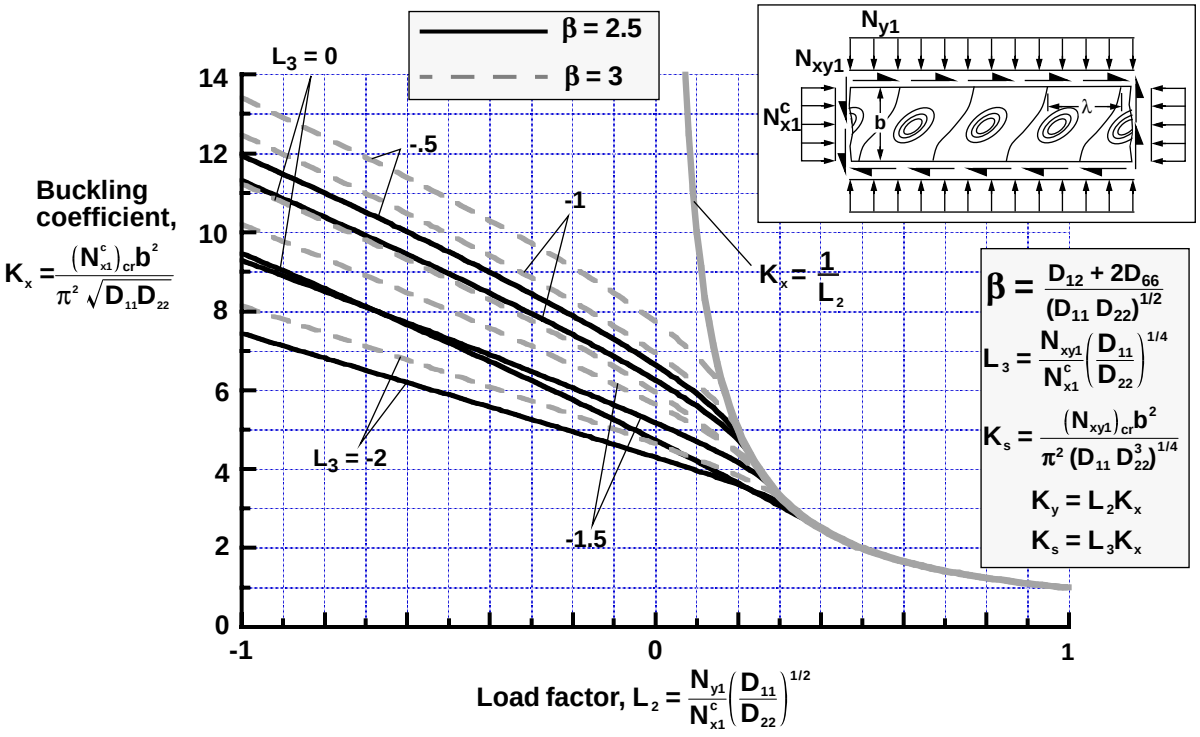

Figure 44. Effects of orthotropy parameter β and load factors on buckling coefficient for simply supported, specially orthotropic plates (γ = δ = 0.6) subjected to axial compression, transverse tension or compression, and shear loads.

REPORT DOCUMENTATION PAGE

Form Approved
OMB No. 0704-0188

1. REPORT DATE *(DD-MM-YYYY)*	2. REPORT TYPE	3. DATES COVERED *(From - To)*
01- 02 - 2003	Technical Publication	

4. TITLE AND SUBTITLE
Buckling Behavior of Long Anisotropic Plates Subjected to Fully Restrained Thermal Expansion

5a. CONTRACT NUMBER

5b. GRANT NUMBER

5c. PROGRAM ELEMENT NUMBER

6. AUTHOR(S)
Nemeth, Michael P.

5d. PROJECT NUMBER

5e. TASK NUMBER

5f. WORK UNIT NUMBER
760-21-21-04

7. PERFORMING ORGANIZATION NAME(S) AND ADDRESS(ES)
NASA Langley Research Center
Hampton, VA 23681-2199

8. PERFORMING ORGANIZATION REPORT NUMBER
L-18191

9. SPONSORING/MONITORING AGENCY NAME(S) AND ADDRESS(ES)
National Aeronautics and Space Administration
Washington, DC 20546-0001

10. SPONSOR/MONITOR'S ACRONYM(S)
NASA

11. SPONSOR/MONITOR'S REPORT NUMBER(S)
NASA/TP-2003-212131

12. DISTRIBUTION/AVAILABILITY STATEMENT
Unclassified - Unlimited
Subject Category 26
Availability: NASA CASI (301) 621-0390 Distribution: Standard

13. SUPPLEMENTARY NOTES
Nemeth, Langley Research Center
An electronic version can be found at http://techreports.larc.nasa.gov/ltrs/ or http://techreports.larc.nasa.gov/cgi-bin/NTRS

14. ABSTRACT

An approach for synthesizing buckling results and behavior for thin, balanced and unbalanced symmetric laminates that are subjected to uniform heating or cooling and which are fully restrained against thermal expansion or contraction is presented. This approach uses a nondimensional analysis for infinitely long, flexurally anisotropic plates that are subjected to combined mechanical loads and is based on useful nondimensional parameters. In addition, stiffness-weighted laminate thermal-expansion parameters are derived and used to determine critical temperature changes in terms of physically intuitive mechanical buckling coefficients. The effects of membrane orthotropy and anisotropy are included. Many results are presented for some common laminates that are intended to facilitate a structural designer's transition to the use of the generic buckling design curves that are presented in the paper. Several generic buckling design curves are presented that provide physical insight into buckling response and provide useful design data. Examples are presented that demonstrate the use of generic design curves. The analysis approach and generic results indicate the effects and characteristics of laminate thermal expansion, membrane orthotropy and anisotropy, and flexural orthotropy and anisotropy in a very general, unifying manner.

15. SUBJECT TERMS
Buckling; Anisotropy; Plates; Thermal

16. SECURITY CLASSIFICATION OF:			17. LIMITATION OF ABSTRACT	18. NUMBER OF PAGES	19a. NAME OF RESPONSIBLE PERSON
a. REPORT	b. ABSTRACT	c. THIS PAGE			STI Help Desk (email: help@sti.nasa.gov)
					19b. TELEPHONE NUMBER *(Include area code)*
U	U	U	UU	92	(301) 621-0390